NASA CR-66582

INVESTIGATION OF HEATLESS ADSORPTION TECHNOLOGY FOR CARBON DIOXIDE CONTROL FOR MANNED SPACECRAFT

By Alvin Skopp and James V. Miceli

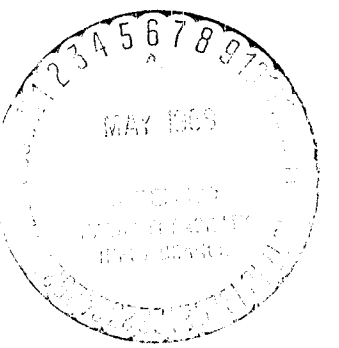

Prepared under Contract No. NAS1-6918 for

NATIONAL AERONAUTICS AND SPACE ADMINISTRATION

LANGLEY RESEARCH CENTER

HAMPTON, VA.

Esso Research and Engineering Company

Government Research Division

Linden, New Jersey

TABLE OF CONTENTS

TABLE OF CONTENTS (Cont'd)

LISTING OF TABLES

LISTING OF FIGURES

LISTING OF FIGURES (Cont'd)

FORWORD

This report describes the studies carried out by the Esso Research and Engineering Company for NASA under contract NASI-6918. The work was done during the period January 1967 to January 1968.

The authors wish to express their appreciation for the assistance provided by Rex Martin of the NASA Langley Research Center who acted as contract monitor, Howard Oakley who provided the necessary statistical support, and Specialist Thomas Coughlin and Senior Research Technician William Davis who conducted the experimental program.

ABSTRACT

This report describes the investigation for NASA (Contract NAS1-6918) to determine the applicability of "Heatless Adsorption" to carbon dioxide control in manned spacecraft.

Heatless adsorption is a low power, rapid cycling process that can remove selected components from gaseous streams. The process uses a purge gas at reduced pressure to reactivate the adsorbent. The purge can be either a portion of the product from the adsorbing bed or a portion of the depressurization gas.

The Heatless Adsorption process was evaluated in a two phase program for predrying and for carbon dioxide removal. System design parameters were evaluated using statistically designed experiments. The two most important parameters were found to be the level of purge and the space velocity. Bed length had less of an effect, while sorption temperature and cycle time were found to have no statistically important effects. A polynominal equation was derived describing the relationship between the moisture content of the product gas and these parameters. This equation may be used to equate drying capacity to fixed system weight and electrical power, and for comparing the energy required for heat assisted desorption to the energy required for heatless adsorption. This equation also provides a basis for designing a laboratory heatless drying system and for designing experiments that will describe an optimum flight prototype system design. The investigation indicated that air can be dried to a level of 2 to 30 parts per million moisture. Theoretical power requirement for a 3-man system are about 40 to 80 watts depending on the moisture level desired. The use of a purge gas to assist vacuum desorption of carbon dioxide from molecular sieves was not conclusively demonstrated to improve the net efficiency of the process. Though the cacity is improved, the material loss may be increased due to the increase in cycle rate.

1. SUMMARY

This report describes the program carried out under NASA Contract NASI-6918 to determine the applicability of Esso's Heatless Adsorption process to carbon dioxide control in manned spacecraft. As space missions grow longer, regenerative processes for removing carbon dioxide from contaminated spacecraft atmospheres will be essential. Current plans center around the use of molecular sieves for carbon dioxide removal and silica gel for predrying the contaminated gas. Predrying is required since molecular sieves will adsorb water preferrentially to carbon dioxide. Regeneration of the adsorbent would be accomplished in a vacuum type cycle (in conjunction with heat in some cases), while the desiccant would be heat desorbed. Both these methods of regeneration have shortcomings. Thermal regeneration may require a considerable amount of power to generate heat. This heat is then lost or requires heat exchange equipment to recover. Vacuum cycles are usually desorption rate and/or equilibrium limited and so require larger beds of adsorbent than are desirable.

The Heatless Adsorption process eliminates many of the problems cited above. Heatless adsorption is a low power, rapid cycling, two-bed process that can remove selected components from gaseous streams. The process uses a gas at reduced pressure as a purge for reactivating the adsorbent. The purge can be either a portion of the product from the adsorbing bed, or alternately, a portion of the depressure gas. The Heatless Adsorption method of sorbent regeneration is faster and more effective for many applications than other methods and its use usually results in savings in adsorbent weight and power requirements.

In a two phase program, the Heatless Adsorption process was evaluated for both predrying the contaminated gas and carbon dioxide removal. In the first phase, the predrying step was investigated. The effects of the different system parameters were evaluated using statistically designed experiments. The two most important parameters were found to be the level of purge and the space velocity. Bed length had less of an effect, while sorption temperature and cycle time were found to have no statistically important effects. Based on experimental data, a polynomial equation was developed describing the relationship between the moisture content of the dried gas and these parameters. This equation provides a basis for designing an optimized Heatless Drying system for spacecraft use. Examination of several possible designs show that the contaminated air can be dried to a level of 2 to 30 parts per million moisture. Theoretical power requirement for a three man system are about 40 to 80 watts depending on the moisture level desired. A prototype system should now be built so that the actual power requirements can be determined and other long term operating characteristics studied.

In the second phase of the program, the use of purge techniques was studied to improve vacuum desorption of carbon dioxide from molecular sieves. Adsorption-desorption characteristics were investigated using simulated spacecraft air with carbon dioxide partial pressures in the range of those anticipated in life support systems. Based on experimental results, relationships were developed showing air loss (during desorption) and adsorbent capacity as a function of purge, space velocity, cycle time, carbon dioxide partial pressure, bed length, and the type of molecular sieve. The data show that purge desorption may result in increased system capacities at a given rate of air loss compared to vacuum desorbed systems. Further experimentation is required to select optimum operating conditions for making best use of the purge in a spacecraft system.

2. INTRODUCTION

In order for men to survive and function in space, they must be provided with suitable gaseous environments controlled with respect to composition, temperature, and pressure. The key element in composition control involves separation of carbon dioxide from enclosed atmospheres.

Systems for carbon dioxide control in spacecraft have already been proposed based on the use of both regenerative and nonregenerative carbon dioxide adsorbents. For short space missions lasting less than two weeks, the use of nonregenerative adsorbents such as LiOH appears best for carbon dioxide removal. The weight of LiOH needed in such a life support system is directly proportional to the mission duration. As missions grow longer, therefore, regenerative carbon dioxide systems will be needed to minimize total weight.

Based on current technology, the synthetic molecular sieves are the preferred carbon dioxide adsorbents for use in such systems. These highly porous, crystalline, alumino-silicate compounds have a relatively high capacity for carbon dioxide, even at low partial pressures (1-10 mm Hg absolute). Furthermore, the adsorptive attraction is dependent on electrostatic forces rather than chemical bonding so that regeneration of the sorbent is possible. The problem with molecular sieves, however, is that their affinity for highly polar compounds such as water is even greater than that for carbon dioxide. Atmospheric humidity greatly reduces the zeolites' capacity for CO_2 by occupying adsorptive sites. Consequently, a molecular sieve based system must include provision for drying the gas before it contacts the adsorbent. This complicates the system somewhat, but on the other hand, provides flexibility in adapting it to different requirements of material conservation.

Based on these requirements, the carbon dioxide control system could be designed for three different modes of operation as shown in Table 1. Model systems have been proposed and in some cases evaluated for these operations. In general, these systems use thermally regenerated silica gel desiccant and vacuum or thermally regenerated molecular sieve. Silica gel is the preferred desiccant material since it possesses a relatively high capacity for water and yet is quite selective, having almost no affinity for carbon dioxide, oxygen and nitrogen.

Table 1

Conservation Requirements Depend on Mission Duration

Mission Length	H_2O	CO_2
12-50 days. (Fuel cell by-product water available)	Reject to space	Reject to space
50-100 days. (Isotope power source).	Recover	Reject to space
Greater than 100 days. (O_2 recovered from CO_2)	Recover	Recover

Obviously, regenerable systems which remove water and carbon dioxide independently of one another could be readily adapted to any mission, regardless of duration.

In any regenerative adsorption process, the technique used for regeneration of the adsorbent material is a key factor in establishing the overall effectiveness of the operation. Reactivation can be accomplished in several different ways. A few examples are: heating the sorbent to temperatures at which its equilibrium capacity for the adsorbate is very low; reducing system pressure, thus disturbing the solid-gas phase equilibrium of the adsorbed component; and using a displacing agent, a compound more strongly adsorbed than the component to be removed which replaces it on the adsorptive sites. Each of these methods has shortcomings. Where waste heat is not available, thermal cycles may require a considerable amount of thermoelectric power. This heat is then lost or requires heat exchange equipment for recovery. Vacuum desorption cycles are usually diffusion rate limited and so may require larger beds of adsorbent than are desirable. A cycle employing a displacing agent requires a means of separating and recovering the agent.

Heatless adsorption is a cyclic adsorption process, developed by Esso Research and Engineering Co. (1 to24) which employs a novel method for regenerating the adsorbent. This report describes the results of a study performed for the National Aeronautics and Space Administration under Contract NAS1-6918. The object of this study was to determine if the application of Heatless Adsorption technology to the control of carbon dioxide in manned spacecraft could result in weight and power saving over systems which use the other methods of adsorbent reactivation.

3. HEATLESS ADSORPTION: A NOVEL GAS SEPARATIONS TECHNIQUE

Heatless Adsorption is a cyclic, two bed, pressure-swing process which utilizes a purge to assist desorption. Figure 1 shows a typical Heatless system in which two fixed beds of solid adsorbent material are alternately cycled between adsorption and desorption.

Figure 1

BASIC HEATLESS ADSORPTION SYSTEM

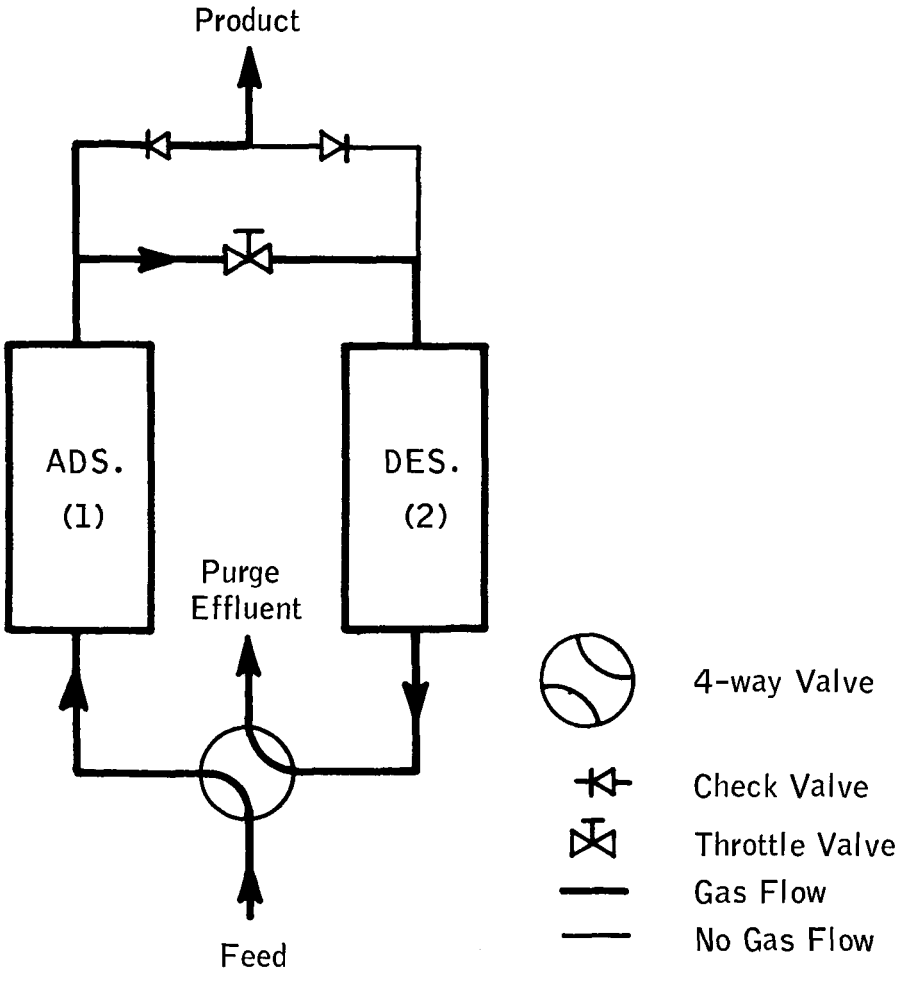

In the adsorption step (Bed 1), a feed stream is passed through the adsorption zone where specific components (e.g., H_2O and CO_2) are adsorbed. The effluent from this zone, free of these components, is split into two streams. One stream is available as product at feed pressure. The other stream is throttled to a lower pressure and used to purge the bed on desorption (Bed 2). Desorption results from the reduction in pressure and the sweeping action of the purge which leaves more concentrated with respect to the adsorbate than is the entering feed. By using two beds of adsorbent, the feed and product system can be operated continuously even though each bed operates cyclically.

3.1. Heatless Adsorption Can Offer Advantages in Weight and Power

Heatless Adsorption is characterized by several novel techniques which can make it attractive from a weight and power standpoint when compared with conventional thermal or vacuum systems. For example, unlike existing adsorption processes relying on large cyclic adsorbent capacities (and consequently relatively large adsorbent beds), Heatless Adsorption makes use of very small cyclic adsorbent capacities. These capacities are multiplied many times, however, through the use of very short cycles. Some commercial Heatless Adsorbers, for example, undergo complete cycles once every minute. The capacity of an adsorption system on a time basis is given by:

$$\frac{\text{System Capacity}}{\text{Unit Time}} = \frac{\text{Adsorbent Capacity}}{\text{Cycle}} \times \frac{\text{Number of cycles}}{\text{Unit of Time}}$$

and, experience has shown that although a smaller fraction of the ultimate capacity of the desiccant is used as the cycling rate increases, the decrease in capacity is less than the increase in the cycling rate. Thus, the system capacity, which is the product of the two, must increase. This permits the utilization of smaller, lighter weight beds of adsorbent than are possible in most other sorption processes.

Rapid cycling is made feasible by improving the desorption. This is achieved in two ways. First, with a properly selected cycle time, the heat front generated during exothermic adsorption is totally retained within the bed. Therefore, it remains available to aid in the subsequent regeneration step and the endothermic heat of desorption does not have to be externally supplied to the bed. This eliminates the need for heat exchange equipment, embedded heaters, etc. In addition, since the temperature of the adsorbent never deviates appreciably from an average value, the adsorbing bed is ready for adsorption at the start of the cycle. This eliminates the possibility of premature break-through of the adsorbate that can occur at the start of a thermally desorbed cycle if the bed has not been sufficiently cooled. Second, the use of a purge provides a sweeping action which removes the desorbed components from the adsorbent much more rapidly than with vacuum regeneration which depends entirely on a relatively slow gas diffusion mechanism.

The only specific requirement, in terms of purge, for a balanced Heatless Adsorption cycle is that the actual volume of purge at the desorption pressure be at least equal to the actual volume of feed at the higher adsorption pressure (the reasons for this are detailed in Appendix 1). In actual practice, however, a volumetric purge to feed ratio of 1:1 may not be desirable since it represents a limiting case which requires large beds to insure proper operation; the purge to feed volume ratio should be a little over 1:1. On the other hand, the use of large purge to feed ratios may also be undesirable since it requires either a large pressure differential between adsorbing and desorbing beds, or the use of a large fraction of the product as purge.

3.2. Product Loss Can be Minimized Through Proper Purge and Depressure Techniques

In the Heatless Adsorption system, product loss occurs in two ways. One way is as purge. The other occurs when depressuring the bed between the adsorption and desorption steps. This depressure loss results from gas trapped in the void spaces of the bed and from gas (O_2 and N_2 for example) which is adsorbed to some extent on the molecular sieve.

Depressure loss can be reduced by equalizing the pressure between the adsorption and desorption beds as shown in Figure 2. At the end of an adsorption cycle (Step 1, Fig. 2), the adsorbing bed at the higher pressure is connected to the desorbing bed at the lower pressure (Step 2, Fig. 2). After the pressures have equilibrated, the beds are cycled so that the functions of each are reversed (Step 3, Fig. 2). Thus, when the bed previously on adsorption is finally depressured, the amount of gas lost is reduced by the amount transferred during the equilization step. Meanwhile, the desorbed bed is partially repressured in preparation for the next adsorption cycle.

Purge losses can be eliminated using a technique called Pressure Equalization Depressuring (PED) (13). It consists of using a portion of the depressure gas (which is lost in any event) to provide the required purge. The process is shown schematically in Figure 3. After bed pressure equalization has been completed (Step 2, Fig. 3), some gas still remains in the adsorbing bed. Rather than depressuring this bed directly to the environment, it is first depressured into an evacuated cylinder until the pressures in the bed and cylinder have equilibrated (Step 3, Fig. 3). The bed is then completely depressured to its final desorption pressure, and the gas in the cylinder is used at a controlled rate to purge the bed being desorbed (Step 4, Fig. 3). The use of this gas at the low pressure provides many more volumes for purging than it would have represented during rapid depressuring. By controlling the rate at which the PED cylinder empties (i.e., with a pre-set throttle value), the purge can be used throughout all of the desorption cycle. By the end of the cycle, the cylinder has been evacuated and is once again ready to receive depressure gas from the other bed. The benefit of PED is that it provides a purge stream at no

Figure 2

BPE REDUCES DEPRESSURE LOSS

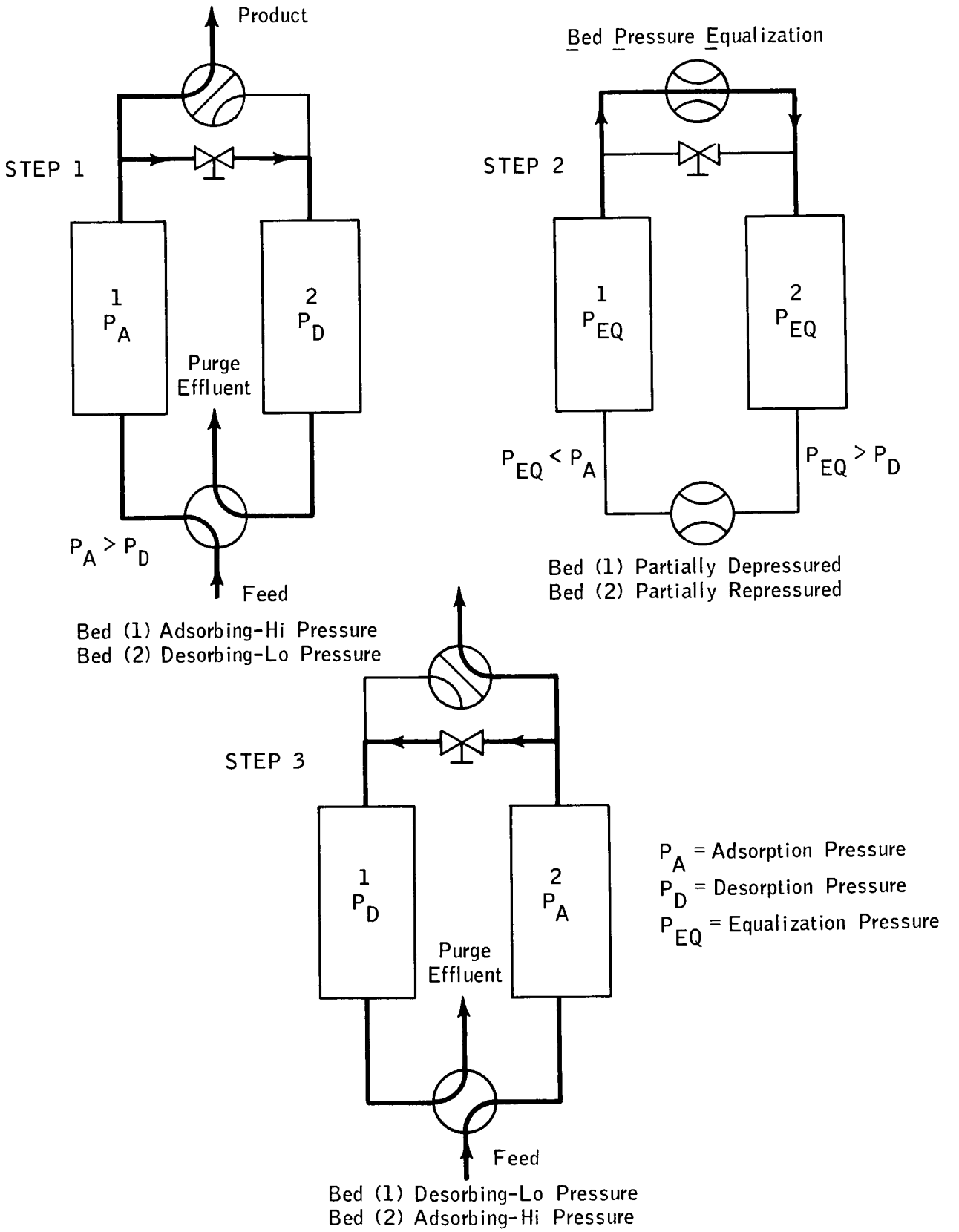

Figure 3

PED ELIMINATES PURGE LOSS

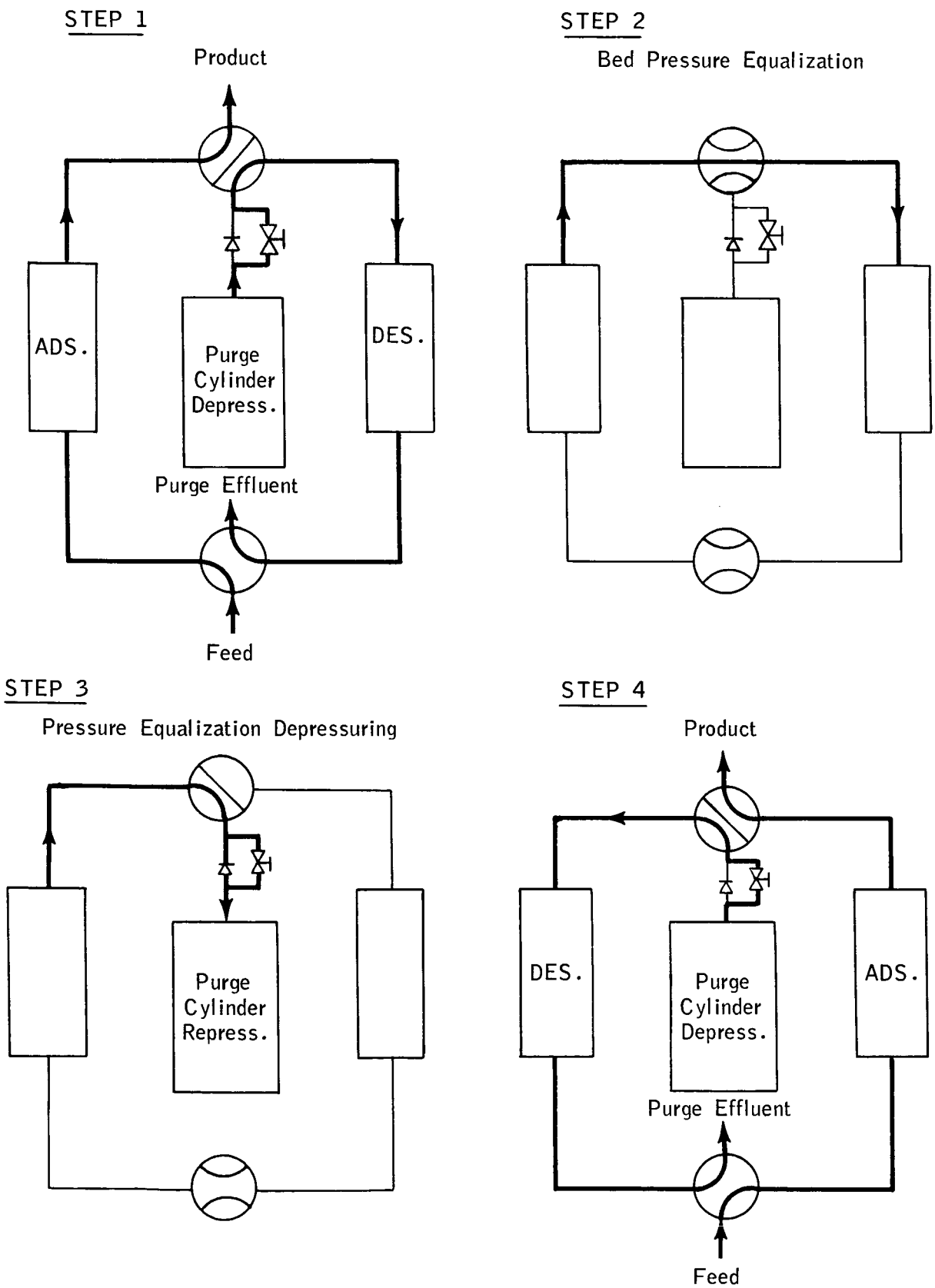

additional expense of product. In turn, the use of purge provides for more effective desorption and, hence permits the use of smaller adsorbent beds with correspondingly smaller depressure losses. On the other hand, the depressure cylinder adds a fixed amount of weight to the system, and the cycle becomes more complex. The size of the cylinder is proportional to the amount of purge desired. Thus, in a spacecraft system, for example, where overall weight is an important consideration, the reduction in the weight of the adsorbing beds and the decrease in product (air) loss derived from pressure equalization depressuring must be compared with the increase due to the added depressure cylinder. For long duration missions, the air loss rate becomes controlling and the added weight associated with PED may be acceptable. For shorter missions, however, this may not be so.

3.3. Application of Heatless Adsorption Technology to CO_2 Control in Spacecraft

Although the Heatless Adsorption technique has already been utilized in several commercial separation processes, its possible application to the removal of contaminants (such as carbon dioxide) from spacecraft atmospheres had not previously been investigated and it was the purpose of tnis study to do so. Schematic representations of the systems which were studied under NASA Contract (NAS1-6918) are shown in Figures 4A and 4B. These systems were designed for use in that particular mode of operation in which carbon dioxide is removed and rejected to space while water is conserved and returned to the cabin. The flexibility inherent in the technique however, would also make it adaptable to that mode of operation where both H_2O and CO_2 are conserved.

The process itself consists of withdrawing cabin air down stream of a temperature-humidity controller. Such a controller, needed in the life support system to maintain a habitable environment in the spacecraft, provides a partially dried stream for use in the CO_2 control system. Process air from the dehumidifier enters the adsorbing desiccant bed at a dew point of about 40 to 50°F and with an average CO_2 partial pressure of about 4 to 8 mm Hg. The "dry" product from the desiccant bed enters the adsorbing molecular sieve bed where carbon dioxide is selectively removed. If a portion of the CO_2-lean effluent is to be used as purge for regenerating the desorbing molecular sieve bed, (Figure 4A) , it is removed as a side stream. The desorbate, rich in CO_2, is rejected to space vacuum. The remainder of the CO_2-lean gas is throttled to a lower pressure and used as a purge for the desiccant before it is returned to the spacecraft cabin. In this way, none of the moisture removed during the drying step is lost. A throttle valve insures that the desired volumetric purge to feed ratio is maintained in the dryer. Figure 4B shows the same system but using the Pressure Equalization Depressuring technique for purging the desorping CO_2 bed.

The processes outlined above incorporate Heatless Adsorption techniques into both parts of the CO_2 control system. In the dryer, total product (after removal of CO_2) is used as a purge to aid the desorption of the desiccant. Since no product loss is associated with this operation, cycle times as short as 30 to 60 seconds can be employed. In the CO_2 sorption system, the use of both conventional and PED purge techniques are shown. In this part of the system, longer cycle times (e.g., 10 minutes) are necessary to limit air loss through too frequent depressurings.

Figure 4A

COMBINED HEATLESS DRYING & CO_2 REMOVAL

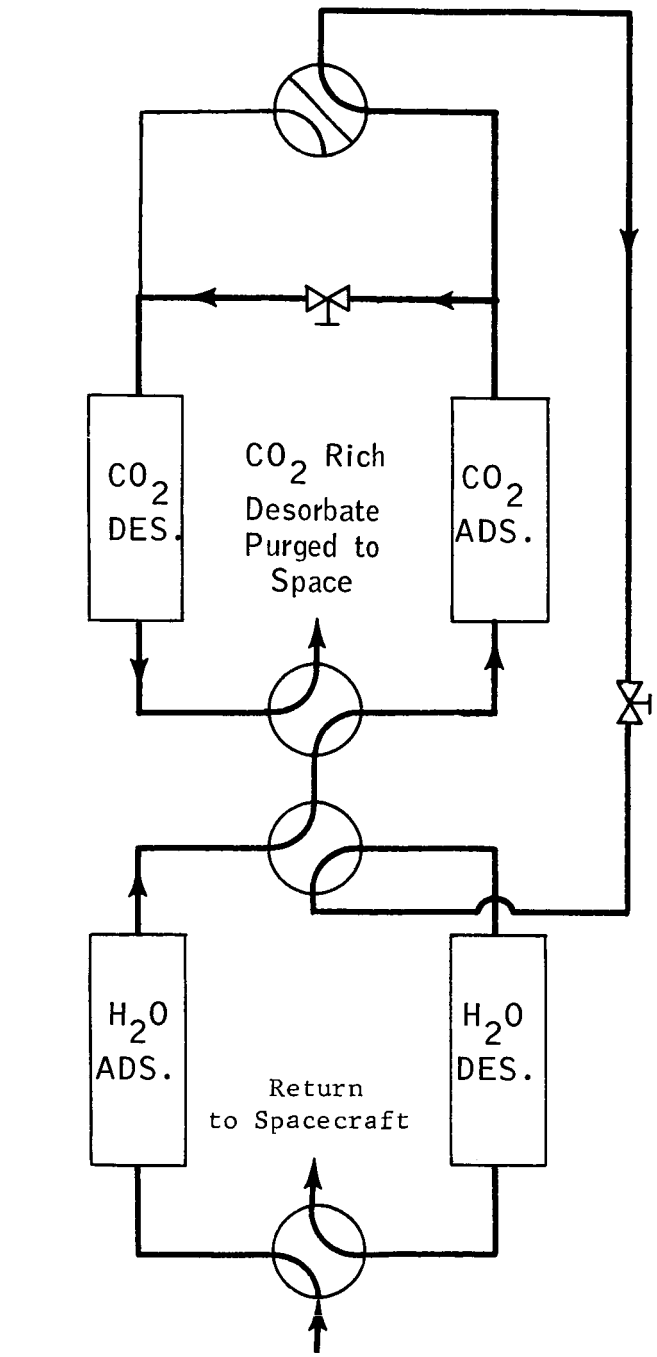

Figure 4B

COMBINED HEATLESS DRYING & CO_2 REMOVAL

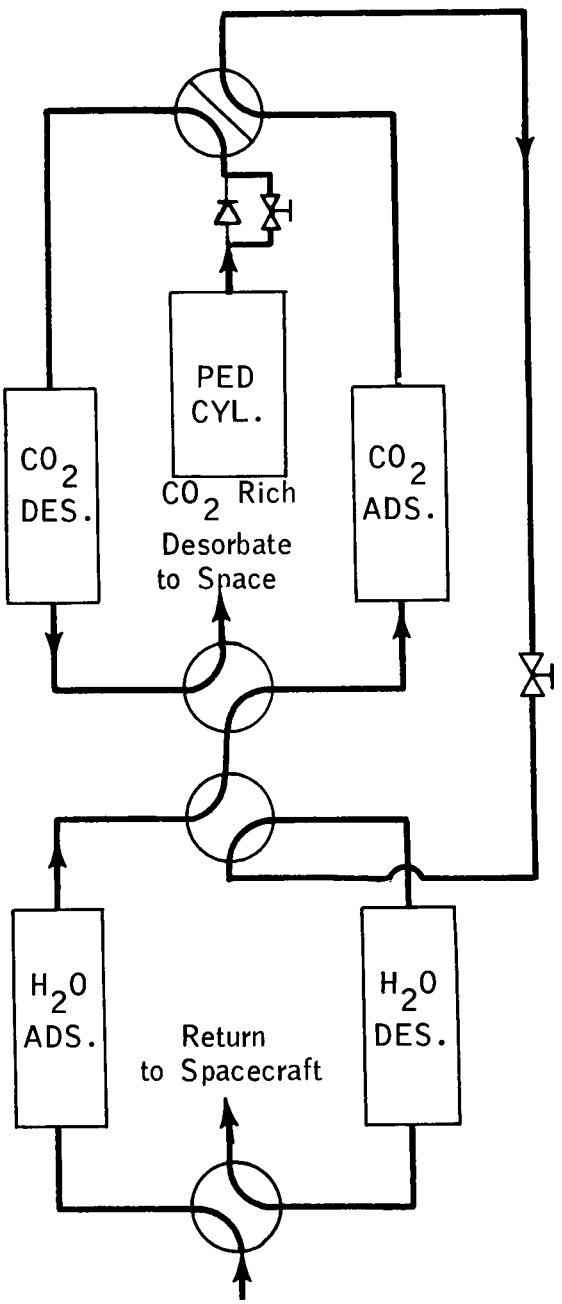

For the processes shown in Figures 4A and 4B, the only power requirements would be for the fan or blower required to make up the pressure drop through the system. There would be no need to use thermoelectric power or to circulate heating fluid for regenerating the desiccant. Interstage cooling between the silica gel and molecular sieve beds would likewise be unnecessary since the temperature of the desiccant beds would remain at the same average level during both the adsorption and desorption halves of a cycle.

The use of a four-bed system permitted a logical separation of the experimental program into two phases since the drying and CO_2 removal processes operate essentially independently of one another (e.g., a heatless drying system could be combined with an existing CO_2 process). The first phase of the program consisted of evaluating Heatless Adsorption technology for desiccant regeneration. This part of the program is discussed in Sections 4.1. to 4.9. The second phase involved an investigation of purge techniques for improving vacuum desorption of carbon dioxide from molecular sieve. This part of the research is described in Sections 5.1.2. to 5.6.

4. PHASE I: DEVELOPMENT OF DESIGN CRITERIA FOR SPACECRAFT HEATLESS DRYING SYSTEM

The objective of the experimental program was to develop a quantitative relationship which could be used to design a system for drying contaminated spacecraft air prior to CO_2 removal. This section describes the experimental program and the results that were obtained.

4.1. System Parameters

Optimum design of the drying system will involve selecting the set of operating conditions which will allow drying of the CO_2 contaminated air stream to the required dew point with a minimum expenditure of power and weight. To establish such a design, the relationship between the process variables and the effluent water concentration must be known.

Based on previous experience in Heatless Drying, it was felt that any of a total of five parameters could be important in the design of a spacecraft system: space velocity V/hr/W, volumetric purge to feed ratio, cycling rate, bed length, and adsorption temperature. In considering each of these variables, it was apparent that the level which was most beneficial from a process standpoint (i.e., the dryness of the product) would not necessarily be optimum from a weight and/or power standpoint. In general then, a compromise level had to be selected. For example, space velocity is the actual volumetric gas flow rate divided by the bed weight. Obviously, if a large enough bed is provided, almost any degree of moisture removal would be possible. However, in the interests of weight and volume, the minimum size bed is desirable. The other parameters may be looked at in the same manner. Lengthening the bed at a constant bed size or space velocity can provide improved drying but such a configuration results in large pressure drop through the bed. Once again, a compromise is required. The same is true to some extent for cycle time. As explained in Section 3.1., short cycle times are preferred from an overall capacity standpoint. In practical application, however, the design and mechanical wear of the valves will ultimately determine the shortest cycle time possible. The importance of the purge to feed ratio has already been discussed. It should be re-emphasized, however, that while a high purge to feed ratio would produce the dryest product with the smallest possible beds, such a condition would require a large pressure differential between the two beds. This would increase the power required by the blower in the system.

The parameters that were evaluated in the study are shown in Table 2 along with the values chosen for them. These values were judged to be reasonable in light of the above discussion. Except for cycle time (and purge to feed ratio of course), these values are close to those used in thermally desorbed prototype systems.

Table 2

Drying Study - Experimental Variables

Operating Variables	Level(s) Investigated
Space Velocity* (V/Hr/W)	93.8 & 156 CFH/lb. Bed
Bed Length	4.5 & 6.3 inches
Half Cycle Time	30 & 60 seconds
Purge to Feed Ratio	1.1 & 1.2
Adsorption Temperature	60° & 77°F
At Constant	
Inlet Air Dew Point	43°F - 45°F
Adsorption Pressure	570 mm Hg
CO_2 Partial Pressure	7.3 mm Hg
Desiccant - Davidson Grade 40 Silica Gel, 6-12 mesh	

*During the experimental program, changes in space velocity were accomplished by the relatively simple method of varying feed rate rather than changing bed size. Both procedures, however, are identical since changes in space velocity can be made by changing either volumetric flow rate (V/Hr) or bed weight (W) with the same overall effect.

Temperature was investigated as a variable to determine if reduced temperatures would offer significant benefits in system capacity. If so, operation at temperatures as low as 45°F would be possible without the addition of equipment since the feed enters the desiccant beds downstream of a temperature-humidity controller. This controller condenses and removes most of the moisture in the incoming stream producing a gas with a dew point of 40 to 45°F.

4.2. Description of Experimental Equipment

Experimental work was carried out using the Heatless Drying unit shown schematically in Fig. 5. The unit was designed specifically for this program and was not meant to be an optimized prototype model. This approach minimized the design and construction time and kept costs down.

All lines were of 3/8" stainless steel tubing connected by 3/8" swage-lock fittings. Gaseous feed to the system was regulated by two rotameters which metered air and CO_2 independently. The air stream was pre-dried to dew points below -90°F with a commercial Heatless Dryer (Gilbarco Model HF-200) and the CO_2 was dried by passing it through a 24 inch long silica gel bed. The required feed dew point (43-45°F) was obtained by bubbling the dry

Figure 5

EXPERIMENTAL DRYING UNIT

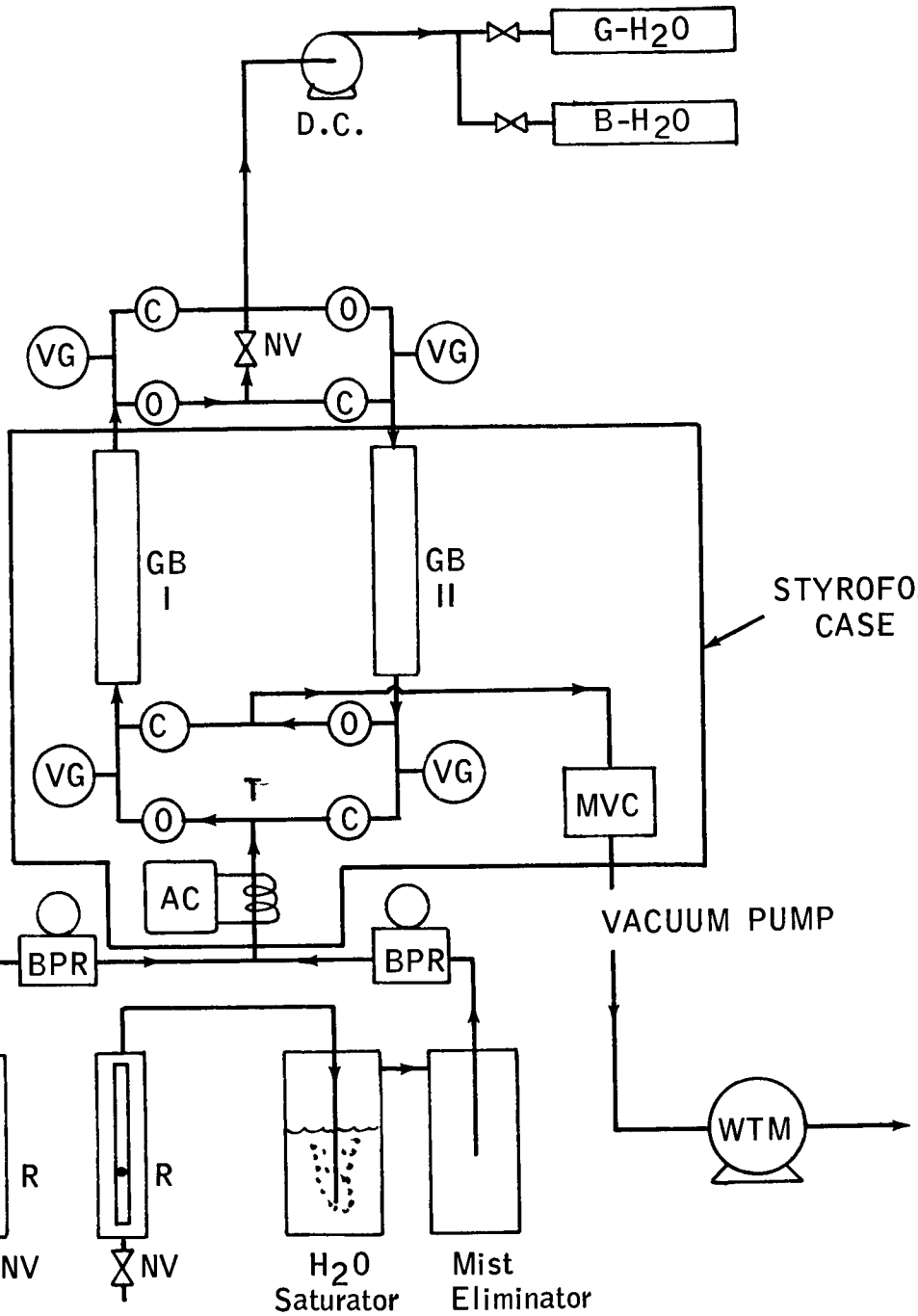

As shown,
Bed 1 is on adsorption
and Bed 2 is on purge
desorption.

Symbols:

-O- -C-	= Open, closed solenoid valves	$B\text{-}H_2O$	= Bendix Hygrometer
NV	= Needle Valve	$G\text{-}H_2O$	= Gilbarco (DuPont 510) Hygrometer
BPR	= Back pressure regulator	DC	= Diaphram Compressor
VG	= Vacuum Gauge	WTM	= Wet test meter
GB	= Glass wallbeds, 1-1/2 ID	AC	= Air conditioner
MVC	= Manostat for vacuum control	T	= Temperature point
R	= Rotameter		

air stream through water in a 4" dia. x 18" glass saturator vessel maintained at 20 psig and 74°F ± 2°F. This "wet" air then entered a knock-out drum similar in construction to the saturator in order to prevent entrained liquid water from entering the desiccant beds. The back pressure on the two separate gas streams (i.e., saturated air and dry CO_2) was maintained at 20 psig by two back pressure regulators. At the outlet of the regulators, the streams were blended and passed through a coil which could be cooled by an air conditioning unit. The same air conditioner was also used to cool the sorbing beds when operation at temperatures below ambient was required.

The desiccant containers were constructed of 1-1/2" I.D. glass pipes which could be obtained in various standard lengths. This permitted visual monitoring of the conditions of the desiccant. A more detailed picture of the bed-construction is shown in Fig. 6. The beds were packed with silica gel held in place by fine wire guaze at either end to provide a foundation for the desiccant and to prevent possible particle loss during the frequent pressure swings. The remaining unused space at both ends of the beds was filled with stainless steel mesh. In addition to acting as a low pressure-drop filler, this mesh served to distribute the feed and purge streams uniformly over the entire bed cross-section.

System vacuum was provided by a Welch Model 405 "Duo-Seal" vacuum pump rated at 1.75 CFM. A cartesian monostat (Manostat Corporation, Style No. 8) was used to control desorption pressures. Bourdon spring vacuum guages (0-30 in Hg vac) were used for pressure measurements with a rated precision of ± 0.25 in Hg (abs). A manually regulated needle valve provided the adjustable pressure drop between the adsorbing and desorbing beds needed to set the purge to feed ratio.

The dry product from the adsorbing bed was split into two streams. The larger stream, constituting 94 to 98% of the total, was used as purge for the bed being regenerated. The remaining 2 to 6% of the dry product was sampled under vacuum by a diaphram pump (Neptune Dyna Pump-4k) and analyzed for moisture content.

The principal instrument used in determining the moisture content of the dried gas stream was the Gilbarco Model SHL-100, Sorption Hygrometer (currently manufactured by DuPont as their Model 510). This instrument (originally developed by Esso Research and Engineering Company) was of considerable benefit in the present program since it operated continuously and allowed direct readings of water concentration in actual ppm by volume (See Appendix 2). The use of a Heath Servo-Chart Recorder, Model EUW-20A, in conjunction with the analyzer permitted monitoring the effluent water patterns even when the unit was unattended.

The Sorption Hygrometer detects the water concentration in a gas stream by alternately passing the wet sample gas and a dry reference gas (air or nitrogen) over two hygroscopically treated quartz crystal oscillators. The instrument compares the frequencies of the two oscillators and utilizes the difference between them to measure moisture content. Each crystal is coated with a thin film of hygroscopic material. Changes in crystal weight resulting from moisture sorption vary the oscillatory frequency. These

Figure 6

DESICCANT BED CONSTRUCTION

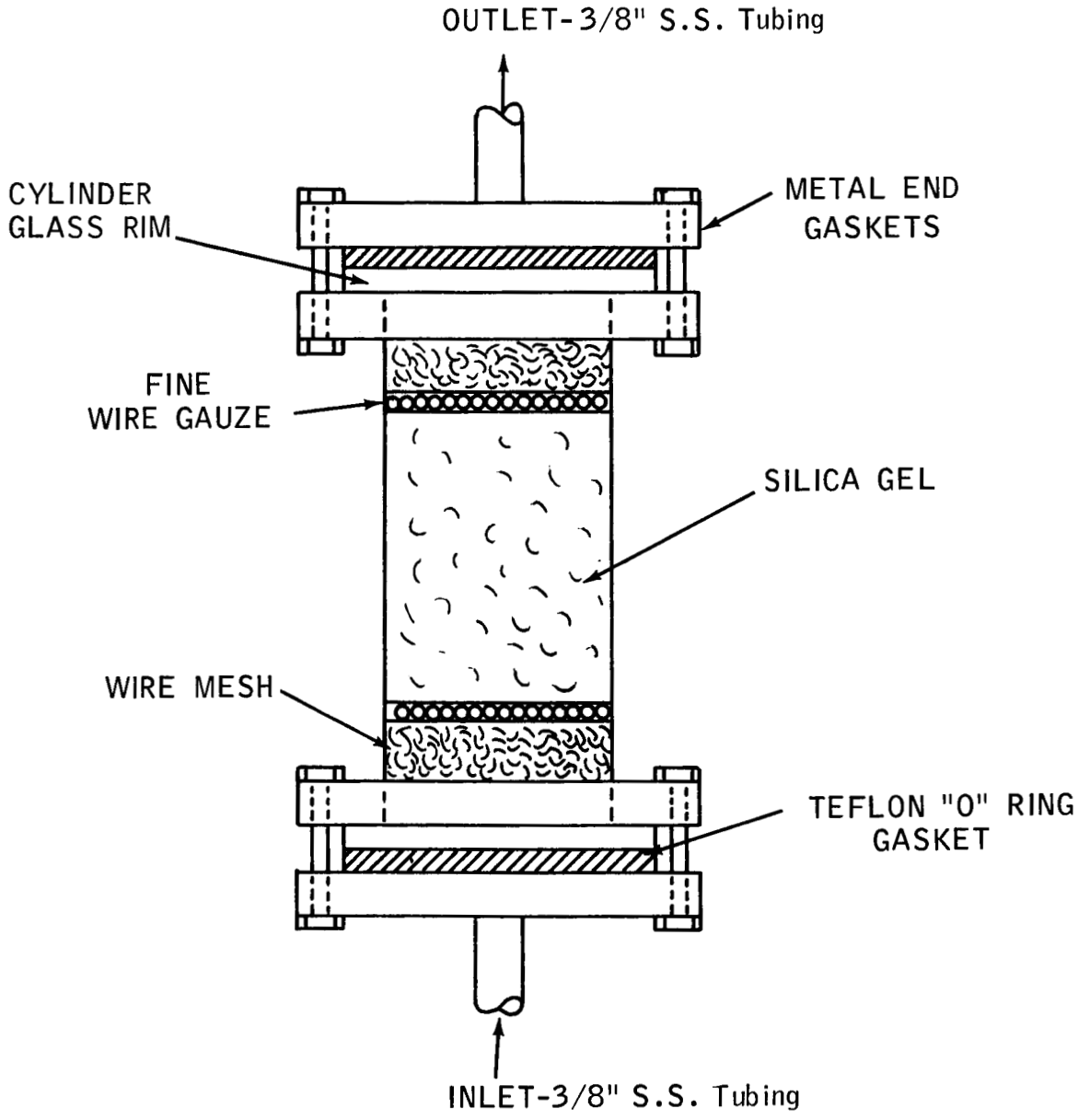

changes are compared electronically and are indicated on the hygrometer scale in ppm (v/v). A flow-switching arrangement, operating on a one-minute time cycle, is used to expose each crystal to the moist sample gas for 30 seconds and then to dry gas for 30 seconds, in order to avoid hysteresis. While one crystal is adsorbing moisture the other is drying, and vice versa. Since sorption of moisture by a coated crystal lowers its frequency, one crystal will be moving down in frequency while the other is moving up. The resulting audio frequency signal is amplified, clipped, passed through an RC circuit, and ultimately read on a meter as the moisture content of the sample.

Experience with this instrument has shown that indicated values can in general differ from actual values by about 5-10% of full scale. This means that readings in the 1-25 ppm range can vary from the true levels by $\pm$ 2.5 ppm or in the 25-250 ppm range by $\pm$ 25 ppm. In addition, the hygroscopic crystals can be contaminated by small amounts of foreign matter such as dust, fibers, and liquid water and periodically require replacement. Consequently, operation of the Gilbarco Hygrometer was periodically and independently checked by a Bendix Dew Point Hygrometer, Model DHGL-3P. The accuracy of this instrument was reported to be -1.3°F (dew point variation) at -82.3°F and +1.5°F at +18.6°F. This corresponds to .5 ppm at the 1-10 ppm level and about 300 ppm at the 3500 ppm level. A comparison between the two hygrometers showed that over an eight-month period, agreement was well within 25% even at the critical 1-5 ppm level. Some representative values are given in Table 3. On several occasions operational problems were encountered with each of the devices resulting in some avoidable experimental delay.

Table 3

Comparison of Hygrometers

Date	Gilbarco Reading (PPM)	Bendix Reading* (PPM)
4/11/67	4.2	4.7
5/3/67	3.0	3.5
6/29/67	7.5	6.5
7/6/67	92	100
9/5/67	4	5

* Dew Point Converted to PPM

4.3. Statistical Design of the Experiments

The experimental program was designed to generate data needed for developing the quantitative relationship between the remaining moisture content of the dried product and the operating parameters of the "heatless" system. The experiments were selected statistically according to a modified Box-Wilson central composite design. Basically, the Box-Wilson treatment is an efficient method of studying response surfaces. The end result of such a treatment is the development of a polynominal expression of the form:

$$y = a_o + a_1x_1 + a_2x_2 \ldots + a_{11}x_1^2 + a_{22}x_2^2 + \ldots a_{12}x_1x_2 + a_{13}x_1x_3 + \quad a_{123}x_1x_2x_3 \ldots + e$$

The y term represent the dependent variable, which in these experiments was the steady-state moisture content of the dried gas. The terms x_1, x_2, etc., represent the independent variables, i.e., space velocity, purge to feed ratio, etc. The term, e, is a measure of the experimental error, and the factors a_o, a_1, a_2, etc., are the correlating coefficients. The fitting of such a polynominal expression is treated as a particular case of a multiple linear regression.

Whereas second order factorial design requires 3^k experiments to fit a quadratic surface for k independent variables, the central composite design reduces this to $2^k + 2k + 1$ experiments. A geometric representation of the central composite design is shown in Figure 7 for three x factors ($k = 3$). The corner points of the figure represent the 2^k design, the points marked by the open circles represent the additional 2k treatment combinations, and the center point represents the singular design. All the points are located symmetrically around the center. The primary levels, high and low, of each of the x-variables are noted in a coded form as +1 and -1, respectively. The level at the origin is represented as 0 and at the external points as $\pm \alpha$.

For fitting the response surface to the five variables of this drying study, the central composite design called for $2^5 + 2 \cdot 5 + 1$ or 43 experiments not including replication. It was on this basis that the experimental program was originally designed. An analysis of the data, however, after only partially completing this design showed that temperature had no effect on the steady state moisture level of the dried product, although it did effect transient behavior as explained in Section 4.8. Elimination of temperature reduced the number of system variables to four and the number of experiments to $2^4 + 2 \cdot 4 + 1$ or 25 excluding replication. Part A of Table 4 shows the revised design that was followed for the remainder of the experimental program. Because each of the individual drying experiments required from eight to twelve days to complete, (i.e., to reach a steady state moisture level in the product characteristics of that drying run), only twelve of the twenty-five experiments in Table 4A could be completed. Those that were made are indicated by an asterisk in the table. This number does not include a total of five replications that were made, or four experiments shown in part B of the table that were made as part of the original five factor design before eliminating temperature as a variable. Counting all these runs, a total of twenty-one experiments was completed for this study.

Figure 7

BOX WILSON CENTRAL COMPOSITE DESIGN

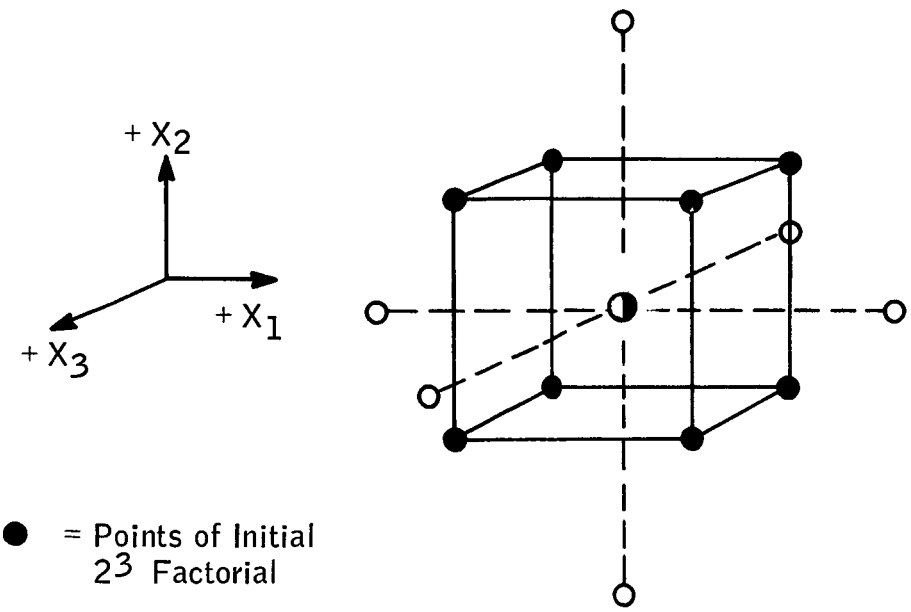

● = Points of Initial 2^3 Factorial

○ = Additional points for composite design

◐ = Center point

Table 4A

Four Factor Design @ 77°F Sorption Temperature

Coded Form x_1	x_2	x_3	x_4	Purge/Feed Vol/Vol	Space Velocity CFH/lb Silica Gel	Half Cycle Time Sec	Bed Length Inches
-1	-1	-1	-1	1.1	93.8	60 (1)	4.5*
1	-1	-1	-1	1.2	93.8	60	4.5*
-1	1	-1	-1	1.1	156.0	60	4.5*(2)
1	1	-1	-1	1.2	156.0	60	4.5*(3)
-1	-1	1	-1	1.1	93.8	30 (1)	4.5*
1	-1	1	-1	1.2	93.8	30	4.5*
-1	1	1	-1	1.1	156.0	30	4.5*
1	1	1	-1	1.2	156.0	30	4.5*
-1	-1	-1	1	1.1	93.8	60	6.3*
1	-1	-1	1	1.2	93.8	60	6.3
-1	1	-1	1	1.1	156.0	60	6.3*
1	1	-1	1	1.2	156.0	60	6.3
-1	-1	1	1	1.1	93.8	30	6.3
1	-1	1	1	1.2	93.8	30	6.3*
-1	1	1	1	1.1	156.0	30	6.3
1	1	1	1	1.2	156.0	30	6.3*
				$\pm \alpha$ Points			
-2	0	0	0	1.05	124.9	45	5.4
2(4)	0	0	0	1.25	124.9	45	5.4
0	-2	0	0	1.15	62.7	45	5.4
0	2	0	0	1.15	187.1	45	5.4
0	0	-2	0	1.15	124.9	75	5.4
0	0	2	0	1.15	124.9	15	5.4
0	0	0	-2	1.15	124.9	45	3.6
0	0	0	2	1.15	124.9	45	7.2
				Center Point			
0	0	0	0	1.15	124.9	45	5.4

Table 4B

Additional Experiments Made at 60°F

1.1	93.8	60	4.5 *(2)
1.2	156.0	60	4.5 *
1.1	156.0	30	4.5 *
1.2	93.8	30	4.5 *

* Runs Completed

(1) Since the design is symmetrical, 60 sec can be taken as -1 and 30 sec as +1

(2) Replicated once

(3) Replicated three times

(4) $\alpha = \pm 2$ for a four factor design

4.4. Outline of Experimental Procedures

The experiments required monitoring the water concentration in the dried effluent until a steady state condition had been achieved. This steady state level then represented the system response to the particular combination of variables used. The parameters were varied according to the statistical experimental design discussed in the previous section and within limits determined to be representative of those which might exist in future spacecraft.

The unit was designed to operate continuously once the process variables had been set. For each run, this involved setting the CO_2 and air flow rates, adjusting the automatic timer which activated the cycling valves, then fixing the purge to feed ratio by setting the pressures on the two beds. For the experiments below ambient temperature, the air conditioner was set to maintain 60°F.

Although the drying unit ran continuously around the clock, its operation was attended only during normal work day hours (less than 1/3 total operating time) and this involved only periodic adjustments in flow rates and bed pressures. In general, overnight variations for the former were less than 10% while the latter varied by no more than $\pm$ 0.5 in Hg. During the day, hourly readings were taken of effluent water concentration, inlet and outlet bed pressures, inlet gas temperature, saturator temperature, and ambient temperature. In addition, the moisture content of the feed gas was monitored periodically. This was done to provide a check on the operation of the saturator system.

Periodic shut-down of the unit became necessary as a result of system leaks, valve failures, and required mechanical changes (e.g., replacing beds). Actual time spent in diagnosing problems and subsequently eliminating them may have cost as much as 10% of the total available experimental time. This is not considered to be excessive, however, since the unit operated almost continuously for over 5,000 hours.

4.5. Data Summary

Figure 8 shows the typical response that was obtained in the drying experiments. Each complete drying experiment took anywhere from one week to ten days to complete, and an additional day or two to dry the desiccant between runs. Figure 8 shows a plot of the moisture content, in both parts per million and dew point, versus the number of completed drying cycles for Run 15. As used in this report, parts per million or ppm for short, is defined as $(P_{H_2O}/P \text{ atm}) \cdot 10^6$, where P_{H_2O} is the partial pressure of H_2O in the gas, and P atm is atmospheric pressure. Reference to Appendix 2 will show that this is the most convenient way of representing the results.

The shape of the drying response curve is characteristic of a Heatless Drying process. Since the cycles are short, change between alternate cycles are small. As cycling proceeds, the moisture content of the product increases from its initial level (Point A) to some final or steady state level (Point C) determined

Figure 8

Typical Response for Drying Experiments

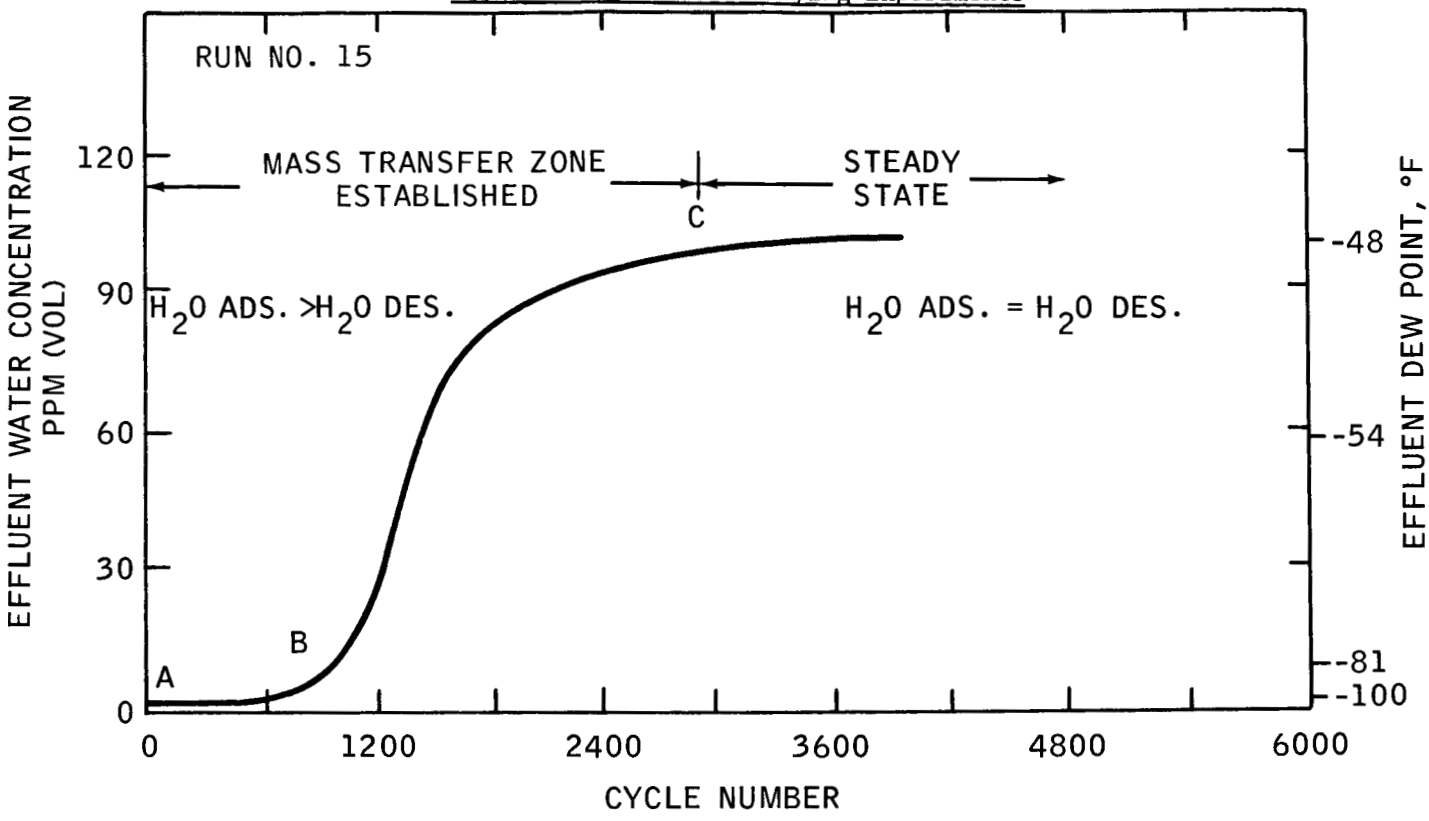

by the operating condition of that run. This steady state situation is reached when the mass transfer zone in the bed is sufficiently developed to saturate the purge to that level required for removing an amount of water equal to that brought into the bed during adsorption. In those cycles before the steady state is reached (Point B to Point C), the mass transfer zone in the bed is continually increasing since the amount of water desorbed is less than the amount adsorbed.

The drying curves for the other runs are shown in Figures 9 to 23. Individual data points have been omitted from these figures but are available in Appendix 3. Referring to Figures 4, 16, 17, and 22, it can be seen that four of the drying runs were made in a different manner from the others. These four runs were made starting with beds that contained more moisture than they should have had based on their operating conditions. Consequently, the initial moisture contents were higher than the steady state levels reached after many cycles of operation.

Replications were made of Runs 6, 7, and 8 (Figures 14, 15, and 16, respectively). Run 6 was replicated to obtain an estimate of experimental error. Run 7 was replicated because it was made at that combination of operating conditions (i.e., low purge to feed ratio, high space velocity, long cycle time, and short beds) which produced a relatively high moisture level that was very sensitive to small changes in operating conditions. Figure 15 shows just how sensitive it was. Variation of only $\pm$ .02 in the purge to feed ratio changed the moisture content by more than 150 ppm.

A summary of all the results of the drying experiments is given in Table 5. A total of twenty-one runs were completed at sixteen different conditions.

Table 5

Summary of Drying Results

Experiment Number	Purge/Feed Vol/Vol	Space Velocity CFH/lb	Half Cycle Time Sec	Bed Length In	Sorption Temp °F	Steady State Moisture Level In Dried Gas, PPM	
1	1.1	156.0	30	4.5	77	67	
2	1.2	156.0	30	4.5	77	7.5	
3	1.1	93.8	30	4.5	77	30	
4	1.1	93.8	60	4.5	77	34	
5	1.2	93.8	60	4.5	77	1.5	
6	1.2	156.0	60	4.5	77	9	(1)
6R1	1.2	156.0	60	4.5	77	13	
6R2	1.2	156.0	60	4.5	77	20	
6R3	1.2	156.0	60	4.5	77	11	
7	1.1	156.0	60	4.5	77	165	*(2)
7R1	1.1	156.0	60	4.5	77	450	
8	1.1	93.8	60	4.5	60	>30	(3)
8R1	1.1	93.8	60	4.5	60	<52	
9	1.2	93.8	30	4.5	60	3	
10	1.2	93.8	30	4.5	77	2	
11	1.1	156.0	30	4.5	60	67	
12	1.2	156.0	60	4.5	77	9	
13	1.1	93.8	60	6.3	77	18	
14	1.2	93.8	30	6.3	77	1	
15	1.1	156.0	60	6.3	77	100	
16	1.2	156.0	30	6.3	77	6	

* See Figure 15.

(1) Taken as 9 for analysis of variance and regression

(2) Taken as 307 for analysis of variance and regression

(3) Taken as 41 for analysis of variance and regression

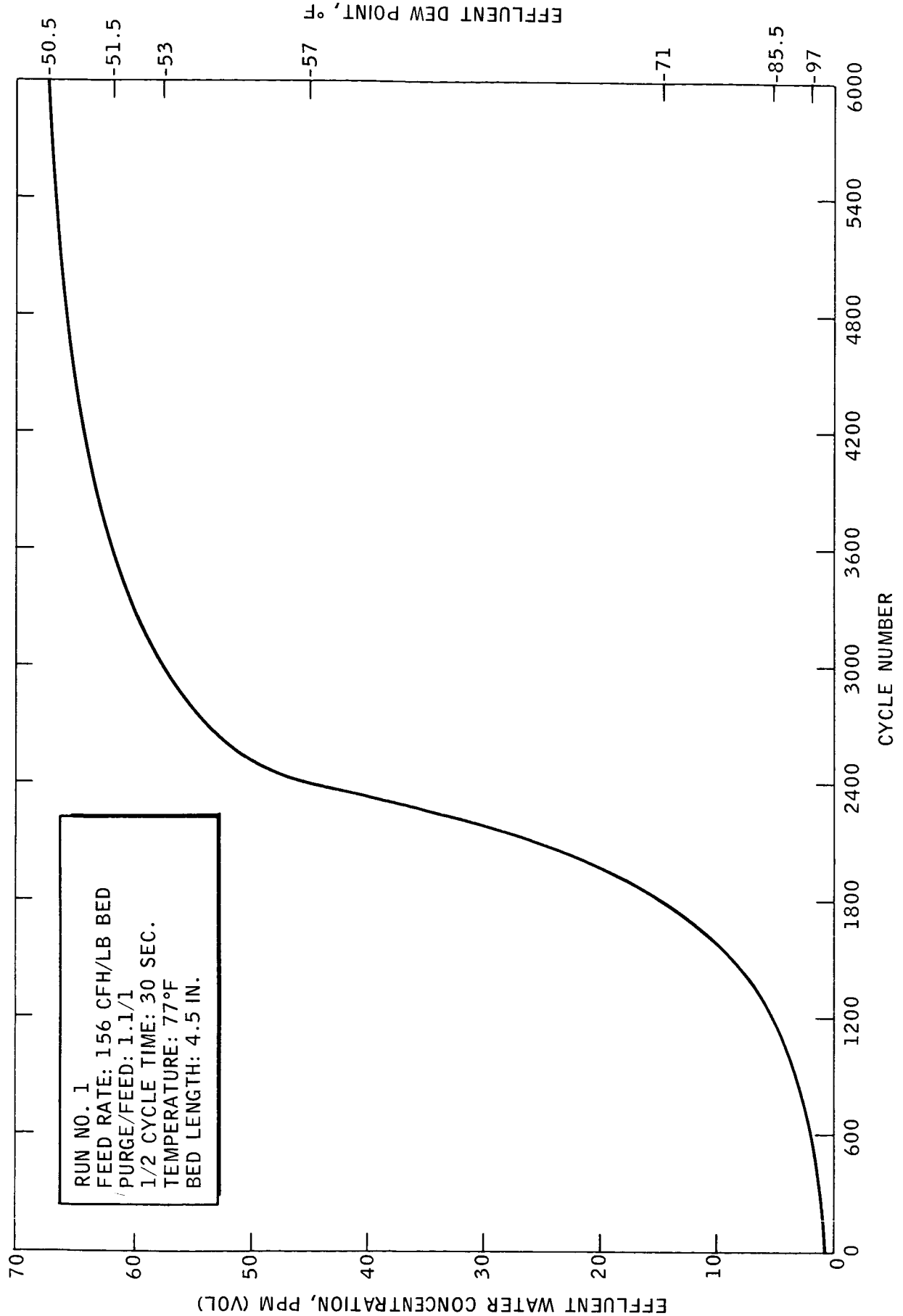
EFFLUENT DEW POINT, °F
-50.5
-51.5
-53
-57
-71
-85.5
-97
EFFLUENT WATER CONCENTRATION, PPM (VOL)
70
60
50
40
30
20
10
0
0
600
1200
1800
2400
3000
3600
4200
4800
5400
6000
CYCLE NUMBER
RUN NO. 1
FEED RATE: 156 CFH/LB BED
PURGE/FEED: 1.1/1
1/2 CYCLE TIME: 30 SEC.
TEMPERATURE: 77°F
BED LENGTH: 4.5 IN.

Figure 9

Figure 10

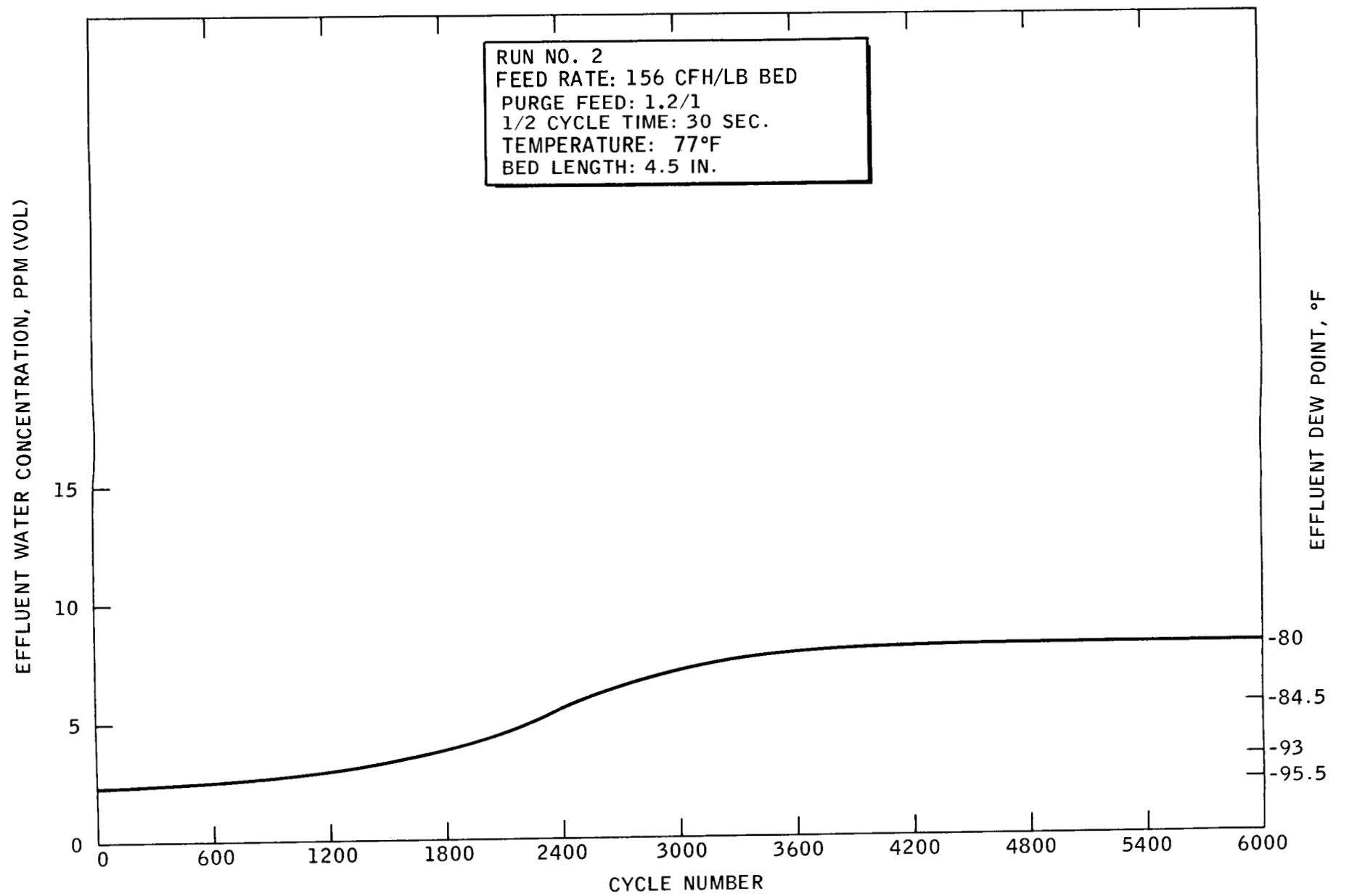
RUN NO. 2
FEED RATE: 156 CFH/LB BED
PURGE FEED: 1.2/1
1/2 CYCLE TIME: 30 SEC.
TEMPERATURE: 77°F
BED LENGTH: 4.5 IN.
EFFLUENT WATER CONCENTRATION, PPM (VOL)
EFFLUENT DEW POINT, °F
15
10
5
0
-80
-84.5
-93
-95.5
0
600
1200
1800
2400
3000
3600
4200
4800
5400
6000
CYCLE NUMBER

Figure 11

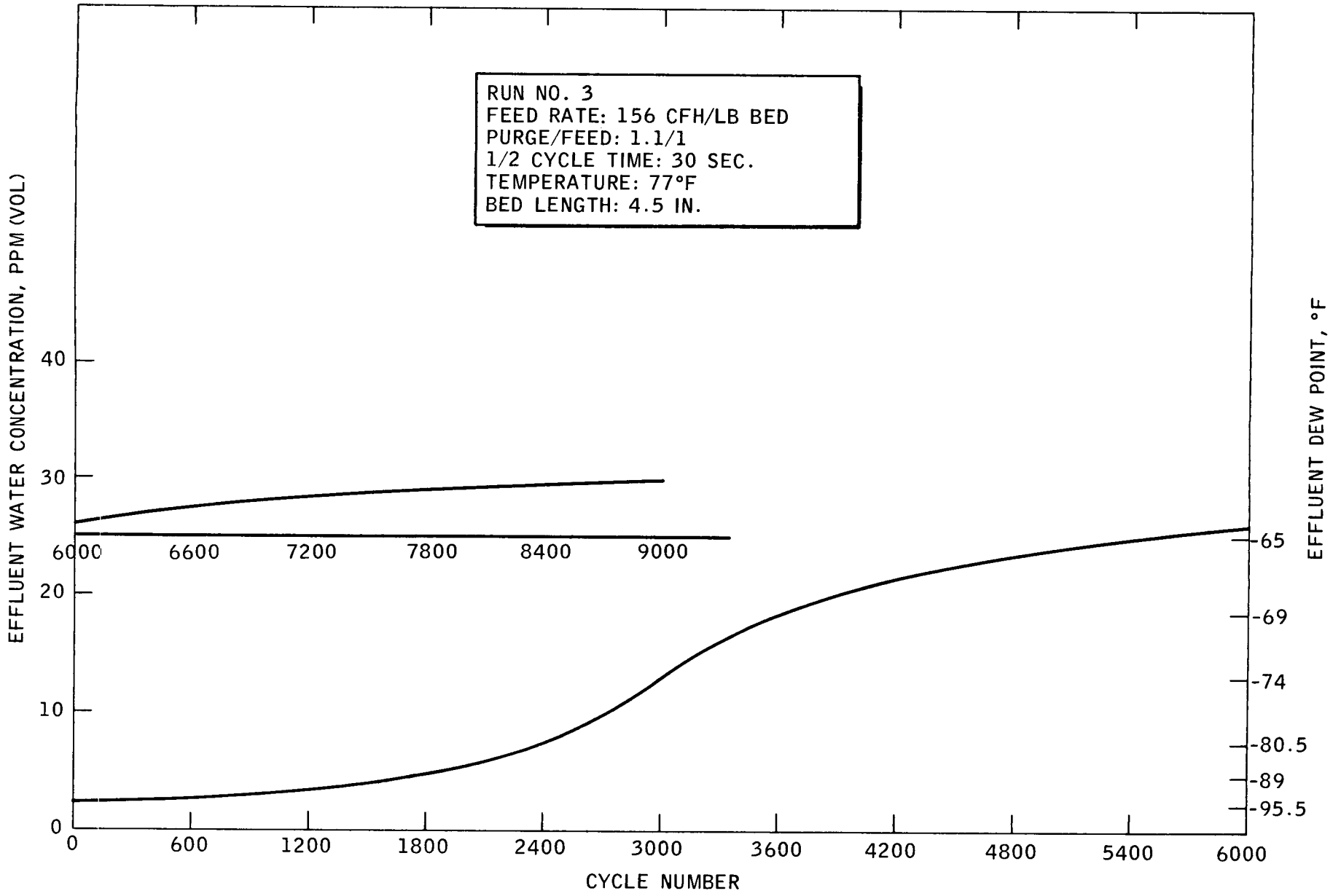
RUN NO. 3
FEED RATE: 156 CFH/LB BED
PURGE/FEED: 1.1/1
1/2 CYCLE TIME: 30 SEC.
TEMPERATURE: 77°F
BED LENGTH: 4.5 IN.
EFFLUENT WATER CONCENTRATION, PPM (VOL)
EFFLUENT DEW POINT, °F
CYCLE NUMBER
0
10
20
30
40
600
1200
1800
2400
3000
3600
4200
4800
5400
6000
6600
7200
7800
8400
9000
-65
-69
-74
-80.5
-89
-95.5

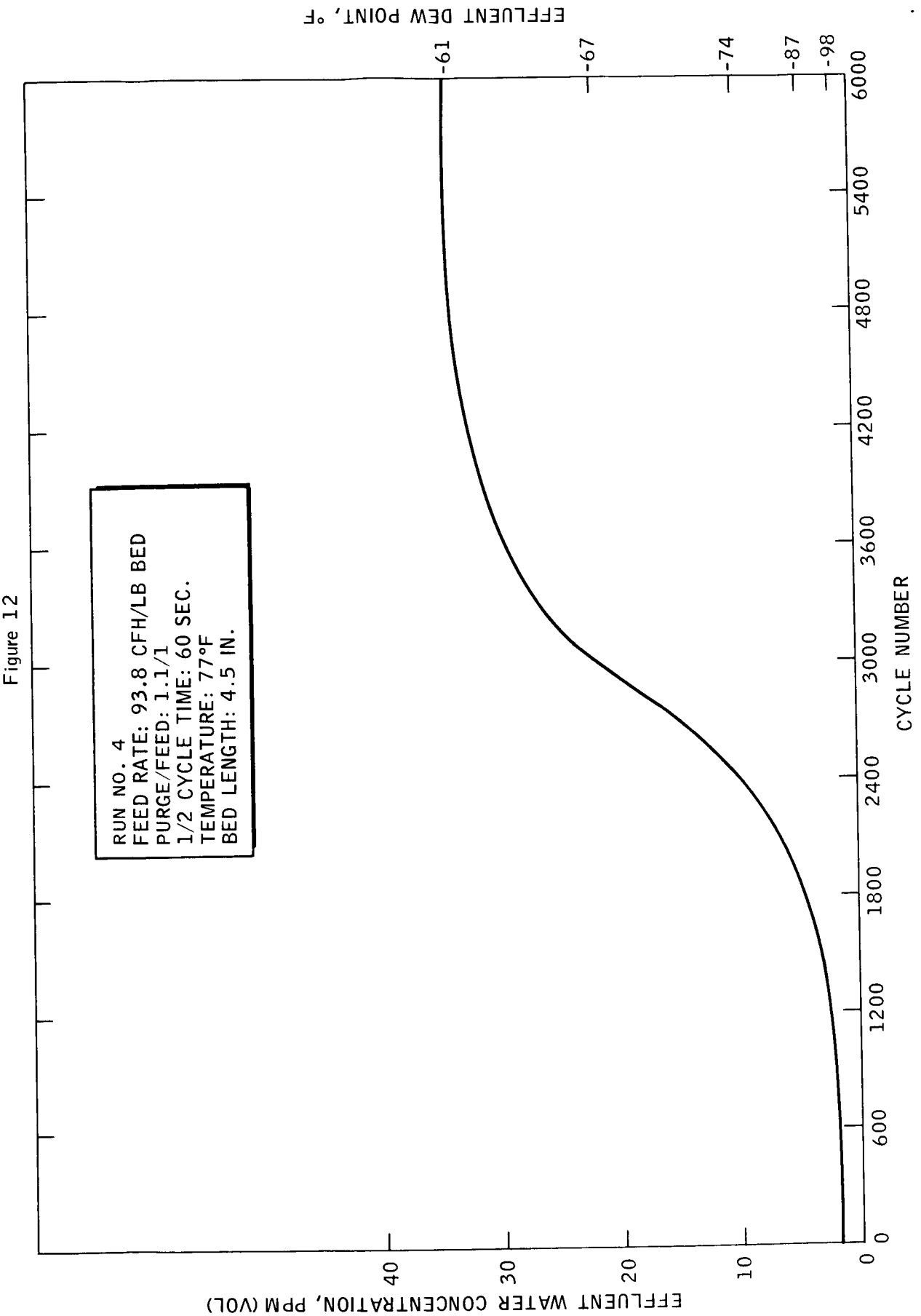
RUN NO. 4
FEED RATE: 93.8 CFH/LB BED
PURGE/FEED: 1.1/1
1/2 CYCLE TIME: 60 SEC.
TEMPERATURE: 77°F
BED LENGTH: 4.5 IN.
EFFLUENT WATER CONCENTRATION, PPM (VOL)
0
10
20
30
40
EFFLUENT DEW POINT, °F
-61
-67
-74
-87
-98
0
600
1200
1800
2400
3000
3600
4200
4800
5400
6000
CYCLE NUMBER

Figure 12

Figure 13

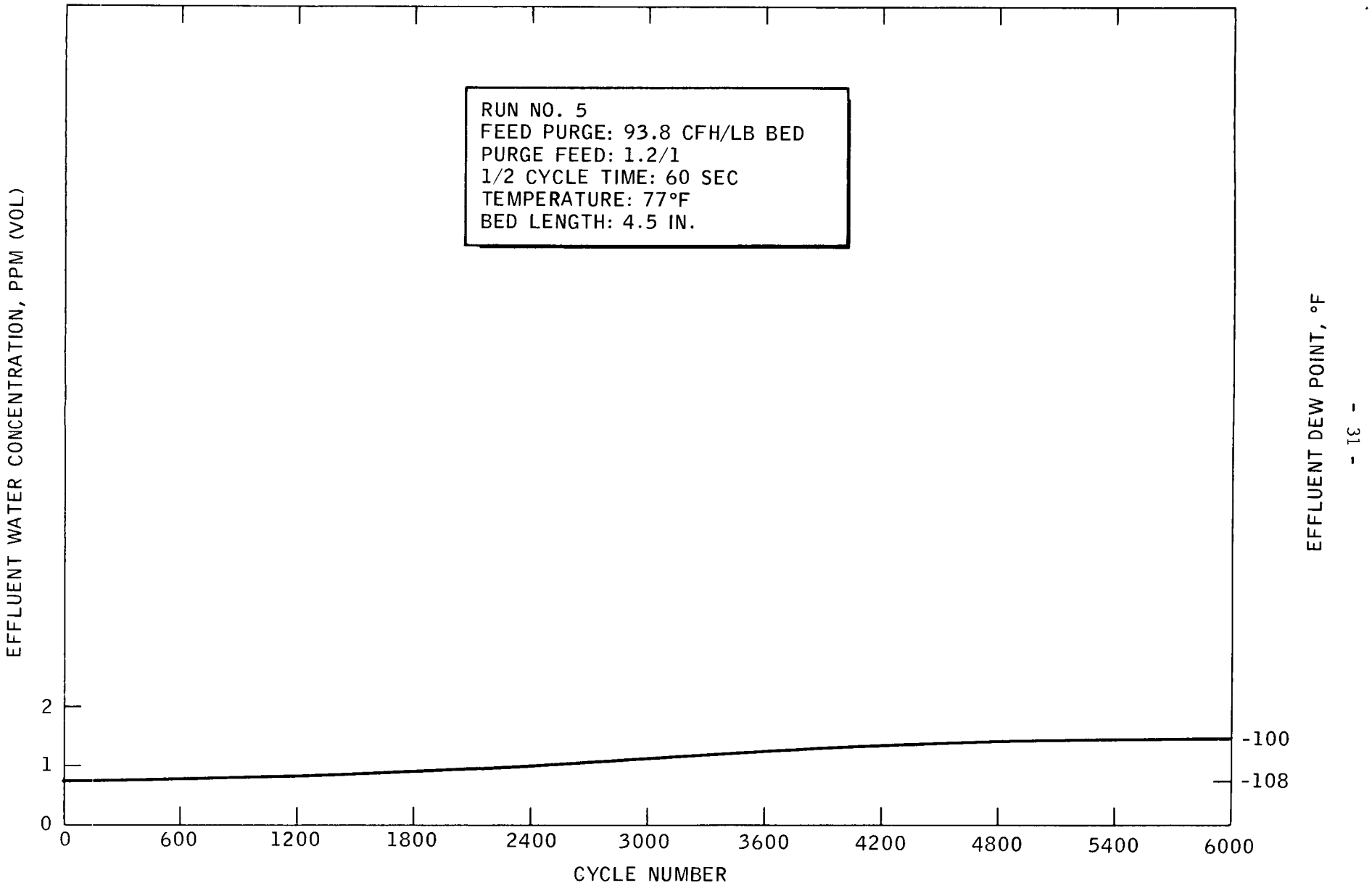
RUN NO. 5
FEED PURGE: 93.8 CFH/LB BED
PURGE FEED: 1.2/1
1/2 CYCLE TIME: 60 SEC
TEMPERATURE: 77°F
BED LENGTH: 4.5 IN.
EFFLUENT WATER CONCENTRATION, PPM (VOL)
EFFLUENT DEW POINT, °F
2
1
0
-100
-108
0
600
1200
1800
2400
3000
3600
4200
4800
5400
6000
CYCLE NUMBER

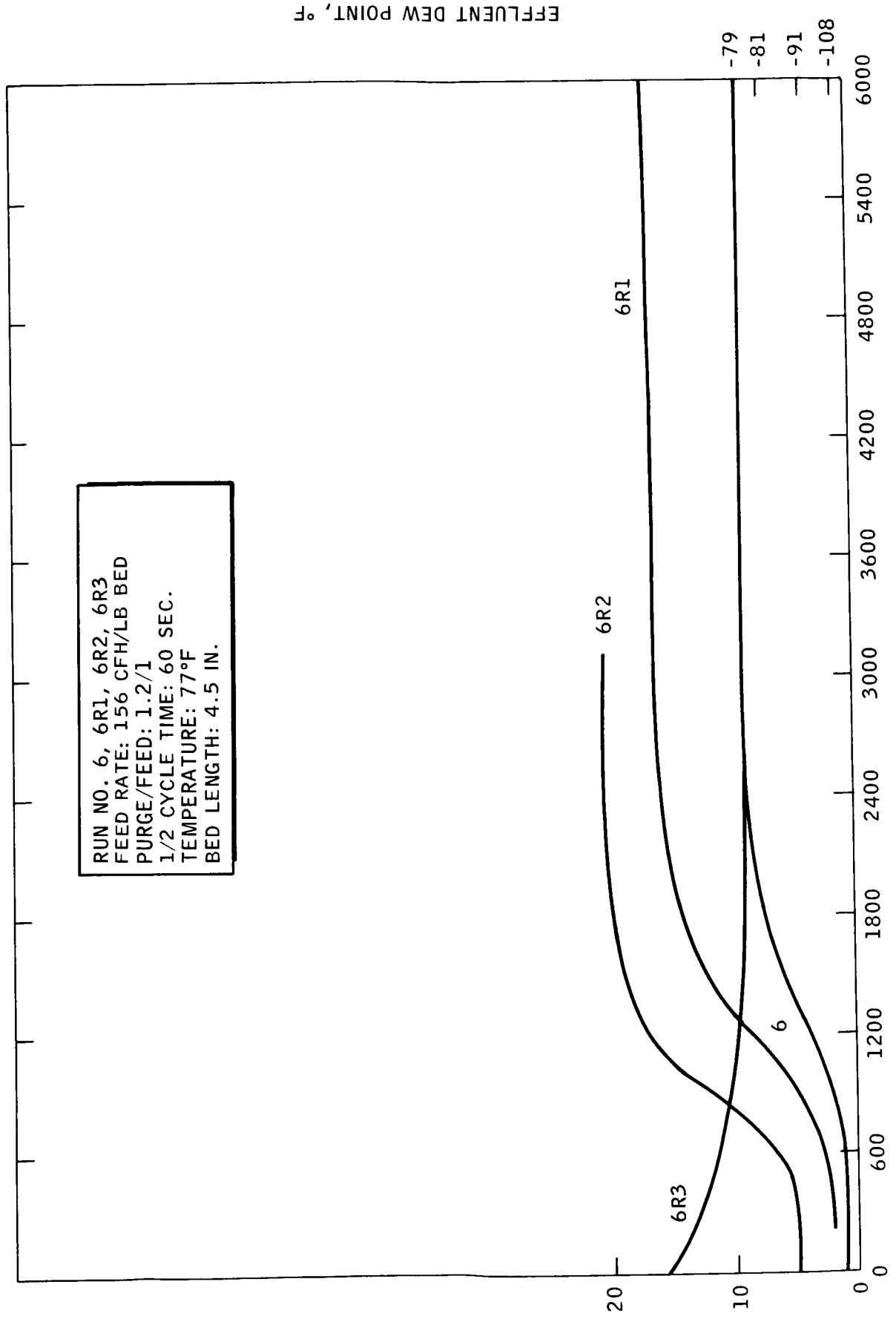
EFFLUENT DEW POINT, °F
-79
-81
-91
-108
RUN NO. 6, 6R1, 6R2, 6R3
FEED RATE: 156 CFH/LB BED
PURGE/FEED: 1.2/1
1/2 CYCLE TIME: 60 SEC.
TEMPERATURE: 77°F
BED LENGTH: 4.5 IN.
6R1
6R2
6
6R3
EFFLUENT WATER CONCENTRATION, PPM (VOL)
20
10
0
0
600
1200
1800
2400
3000
3600
4200
4800
5400
6000
CYCLE NUMBER

Figure 14

Figure 15

LARGE EFFLUENT RESPONSE TO CHANGES IN P/F OBSERVED

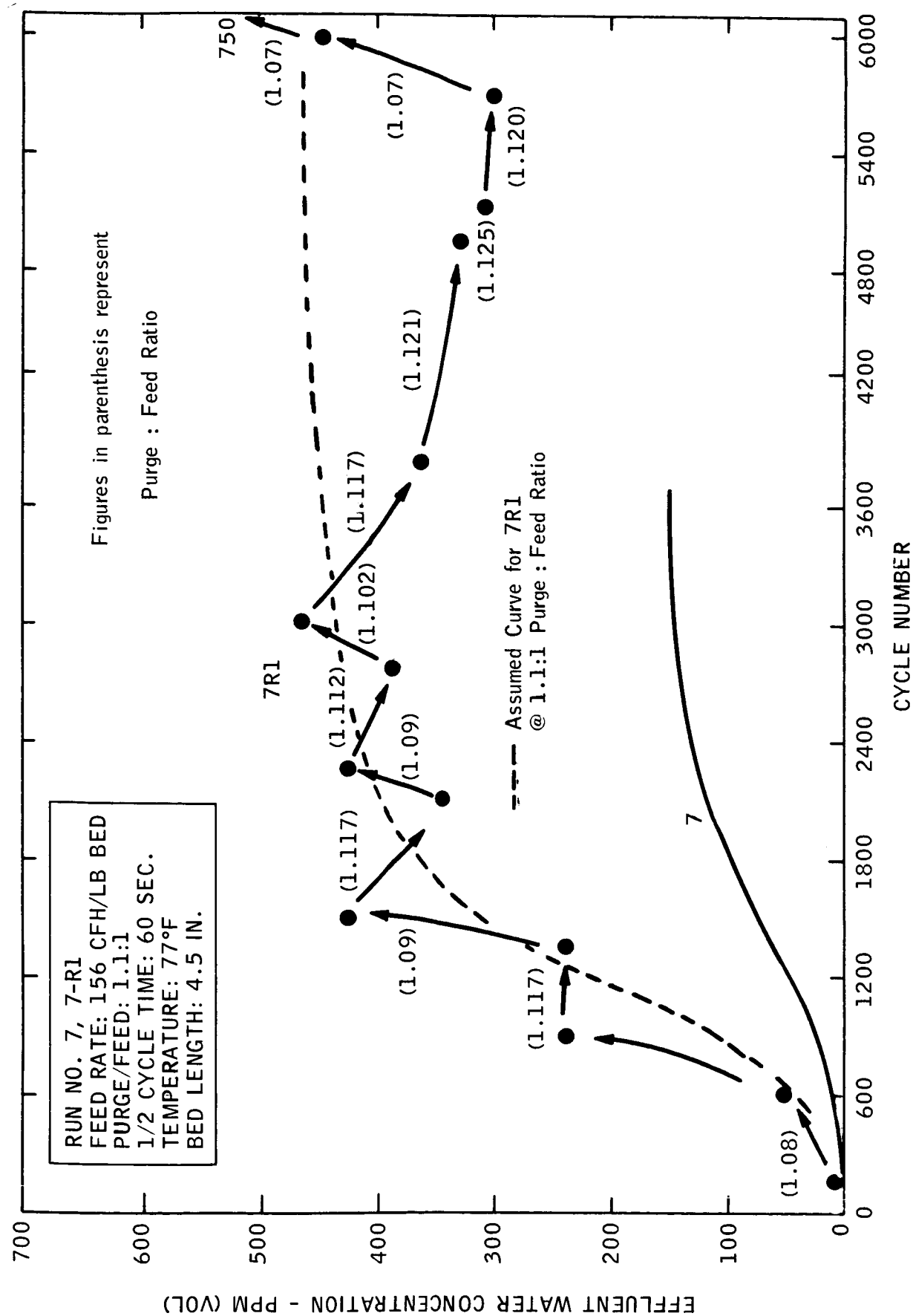

Figure 16

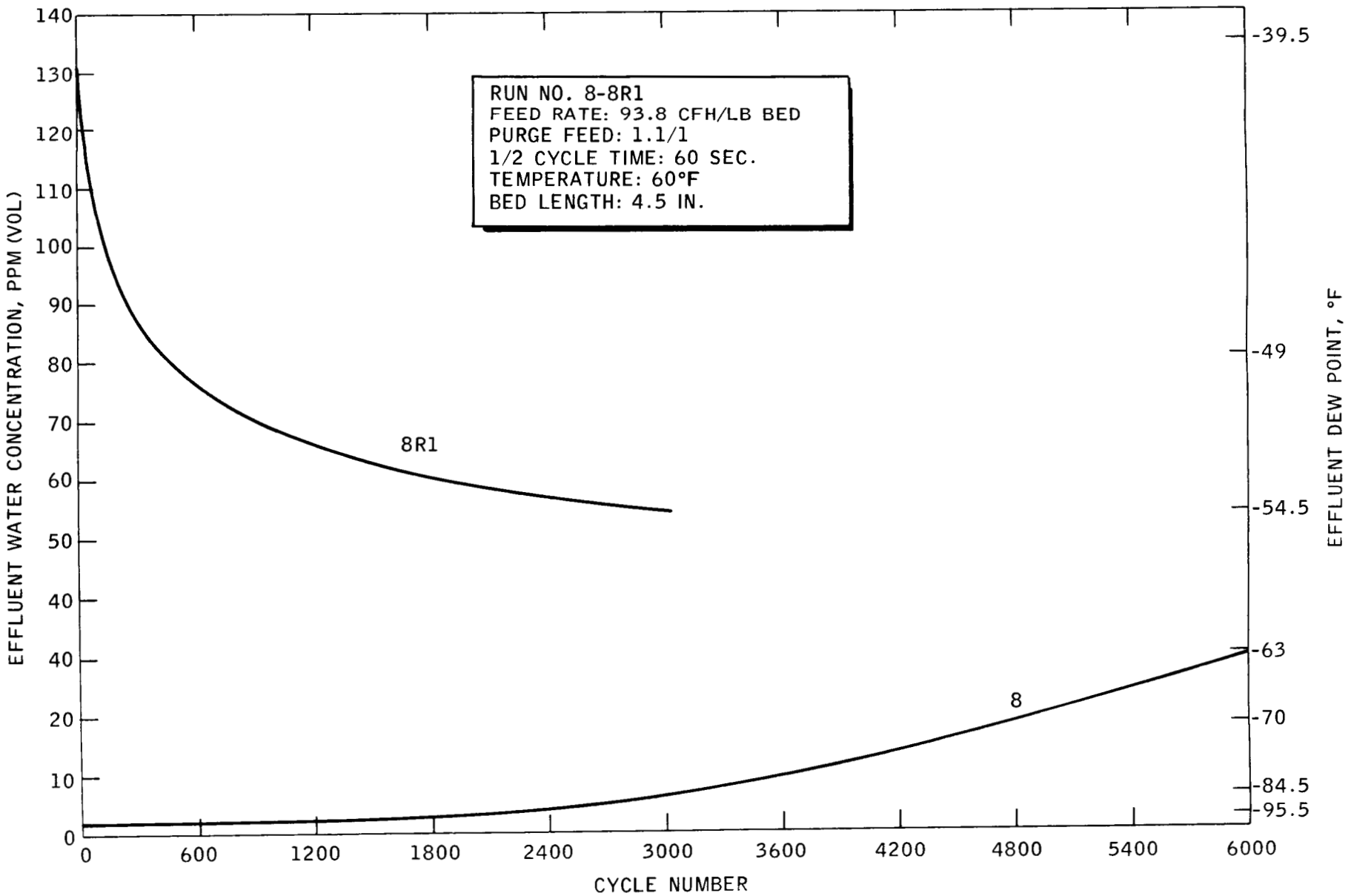
RUN NO. 8-8R1
FEED RATE: 93.8 CFH/LB BED
PURGE FEED: 1.1/1
1/2 CYCLE TIME: 60 SEC.
TEMPERATURE: 60°F
BED LENGTH: 4.5 IN.
8R1
8
EFFLUENT WATER CONCENTRATION, PPM (VOL)
EFFLUENT DEW POINT, °F
CYCLE NUMBER
0
10
20
40
50
60
70
80
90
100
110
120
130
140
0
600
1200
1800
2400
3000
3600
4200
4800
5400
6000
-39.5
-49
-54.5
-63
-70
-84.5
-95.5

Figure 17

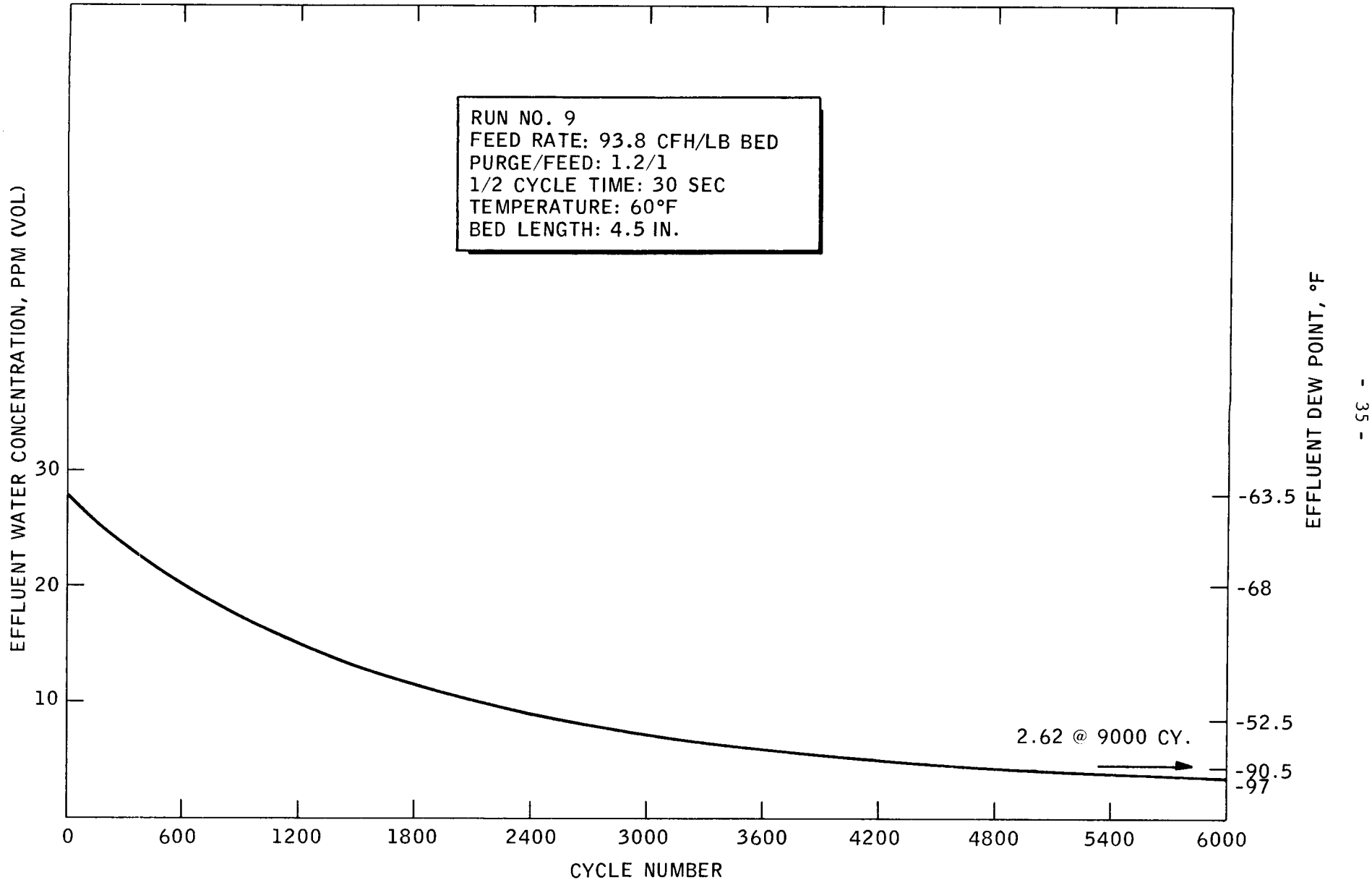
RUN NO. 9
FEED RATE: 93.8 CFH/LB BED
PURGE/FEED: 1.2/1
1/2 CYCLE TIME: 30 SEC
TEMPERATURE: 60°F
BED LENGTH: 4.5 IN.
EFFLUENT WATER CONCENTRATION, PPM (VOL)
30
20
10
EFFLUENT DEW POINT, °F
-63.5
-68
-52.5
-90.5
-97
2.62 @ 9000 CY.
0
600
1200
1800
2400
3000
3600
4200
4800
5400
6000
CYCLE NUMBER

Figure 18

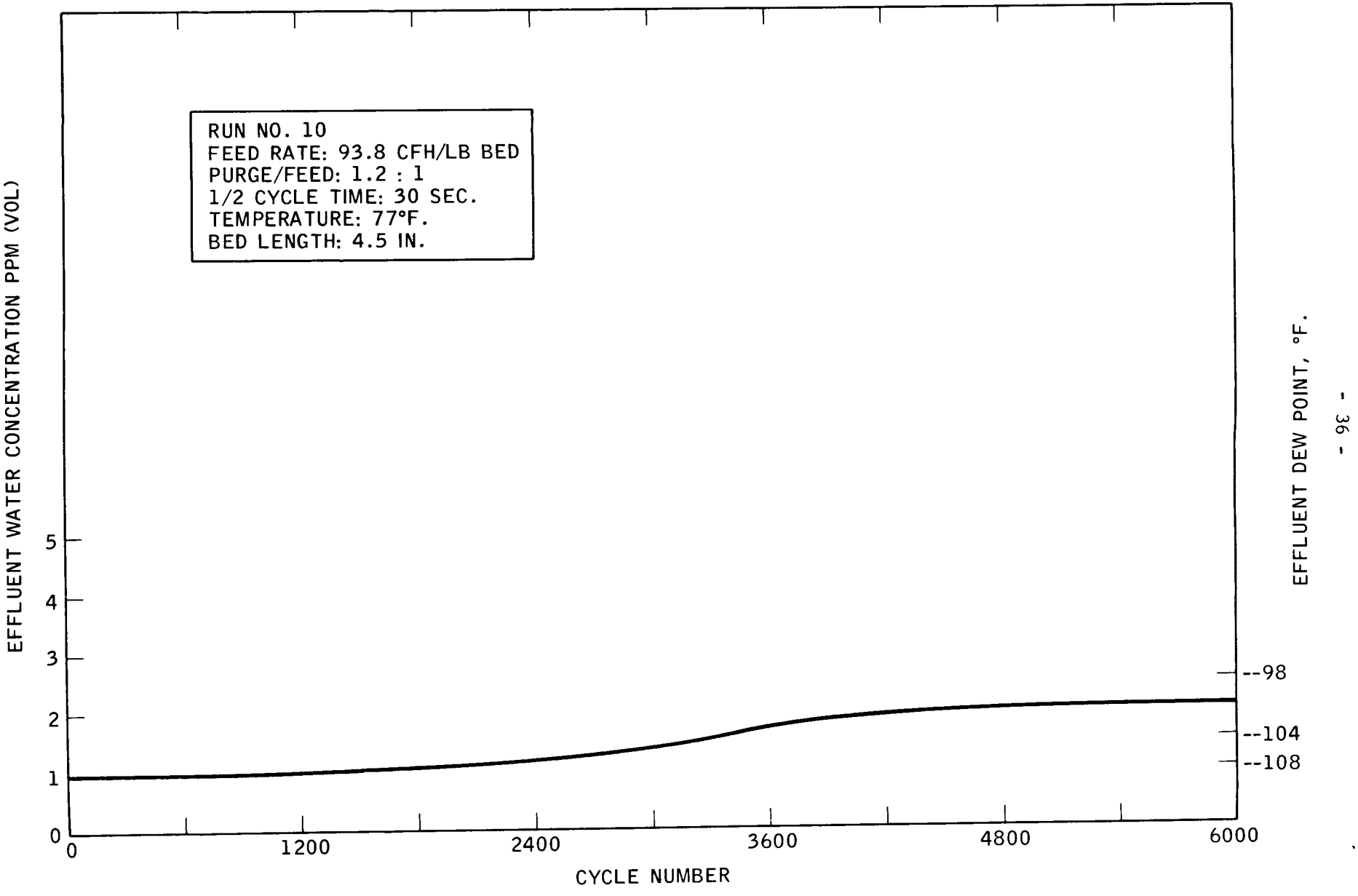
RUN NO. 10
FEED RATE: 93.8 CFH/LB BED
PURGE/FEED: 1.2 : 1
1/2 CYCLE TIME: 30 SEC.
TEMPERATURE: 77°F.
BED LENGTH: 4.5 IN.
EFFLUENT WATER CONCENTRATION PPM (VOL)
0
1
2
3
4
5
0
1200
2400
3600
4800
6000
CYCLE NUMBER
EFFLUENT DEW POINT, °F.
--98
--104
--108

Figure 19

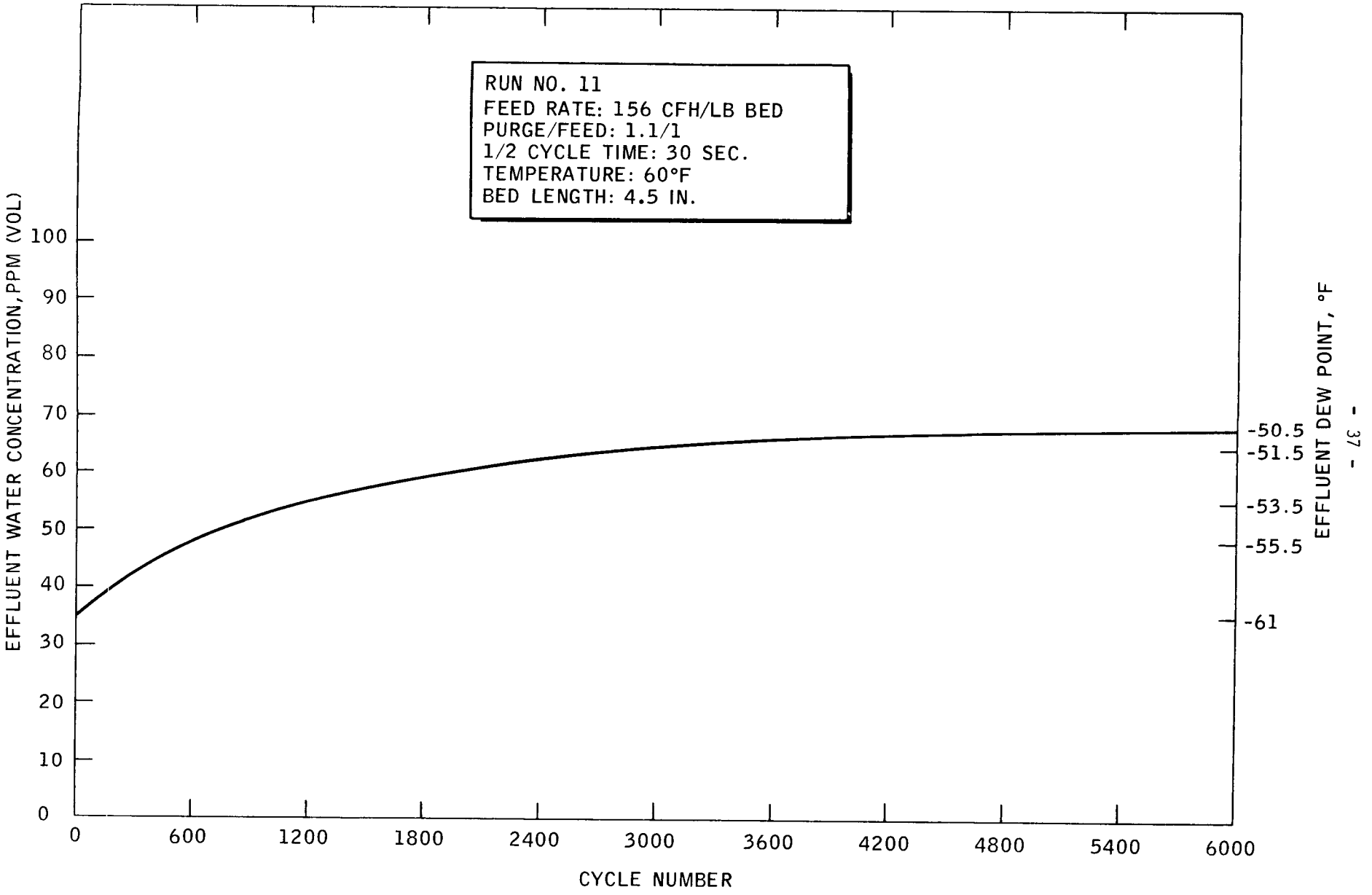
RUN NO. 11
FEED RATE: 156 CFH/LB BED
PURGE/FEED: 1.1/1
1/2 CYCLE TIME: 30 SEC.
TEMPERATURE: 60°F
BED LENGTH: 4.5 IN.
EFFLUENT WATER CONCENTRATION, PPM (VOL)
100
90
80
70
60
50
40
30
20
10
0
0
600
1200
1800
2400
3000
3600
4200
4800
5400
6000
CYCLE NUMBER
-50.5
-51.5
-53.5
-55.5
-61
EFFLUENT DEW POINT, °F

Figure 20

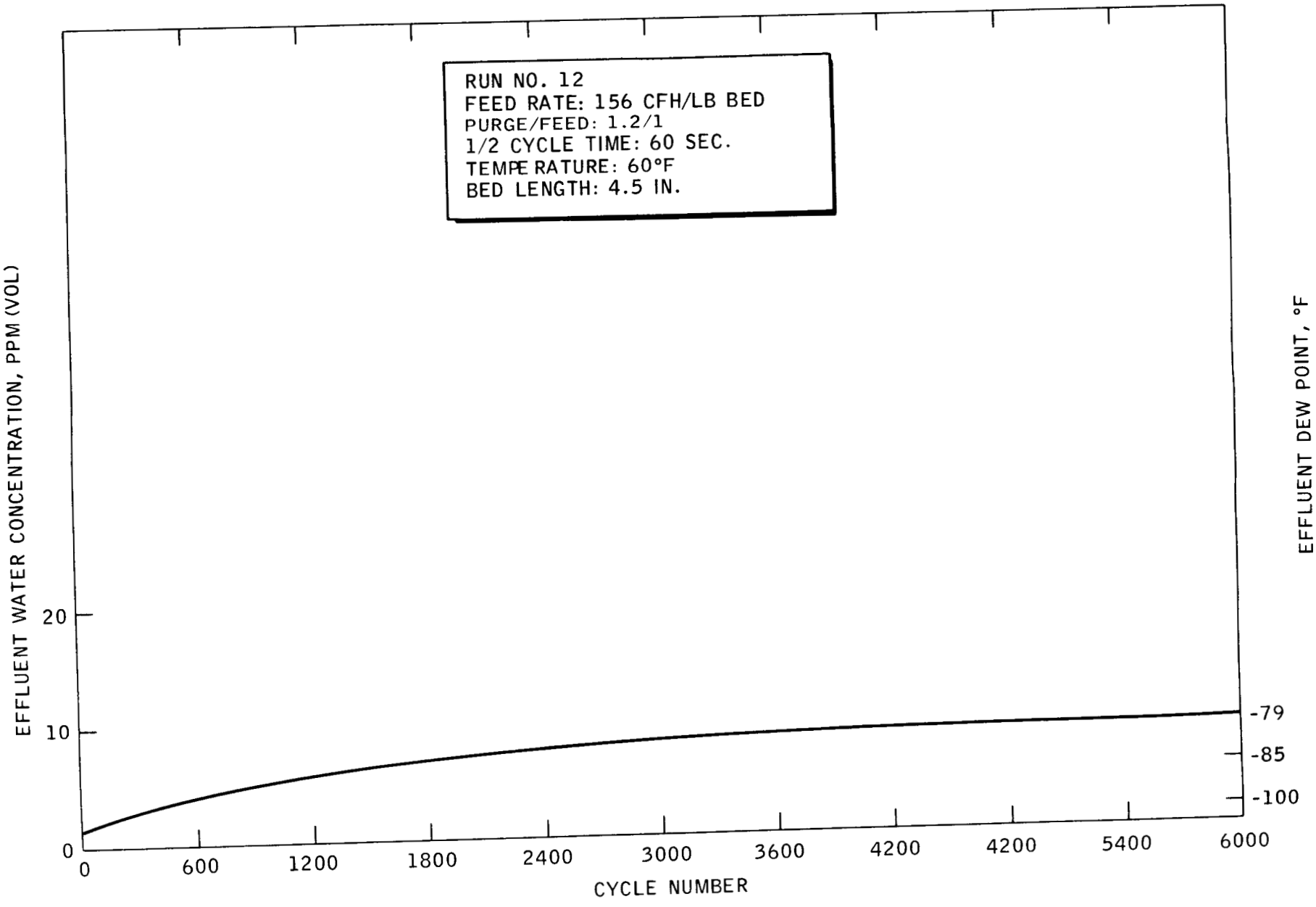
RUN NO. 12
FEED RATE: 156 CFH/LB BED
PURGE/FEED: 1.2/1
1/2 CYCLE TIME: 60 SEC.
TEMPERATURE: 60°F
BED LENGTH: 4.5 IN.
EFFLUENT WATER CONCENTRATION, PPM (VOL)
20
10
0
0
600
1200
1800
2400
3000
3600
4200
4200
5400
6000
CYCLE NUMBER
EFFLUENT DEW POINT, °F
-79
-85
-100

Figure 21

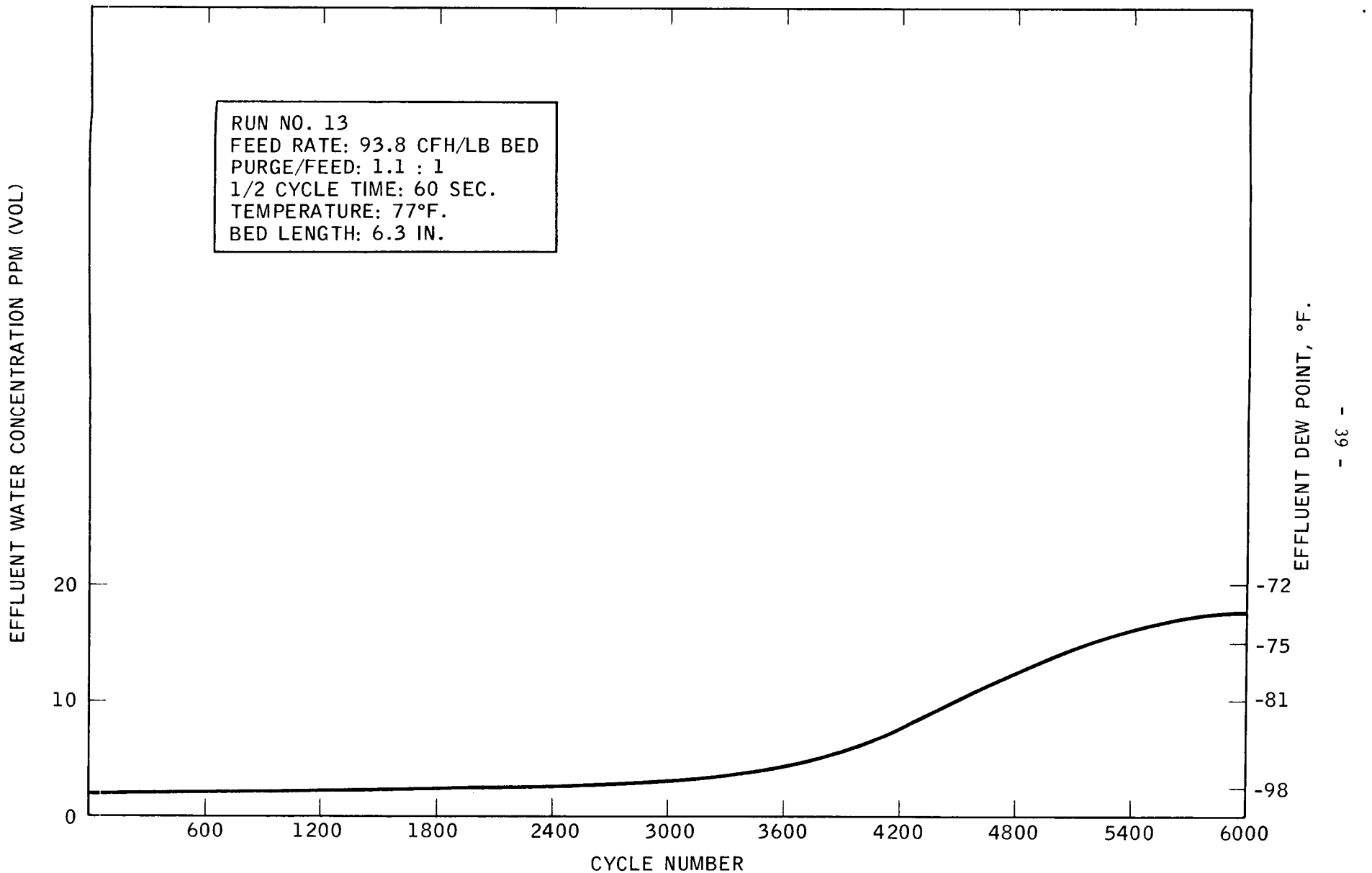
RUN NO. 13
FEED RATE: 93.8 CFH/LB BED
PURGE/FEED: 1.1 : 1
1/2 CYCLE TIME: 60 SEC.
TEMPERATURE: 77°F.
BED LENGTH: 6.3 IN.
EFFLUENT WATER CONCENTRATION PPM (VOL)
EFFLUENT DEW POINT, °F.
0
10
20
-98
-81
-75
-72
600
1200
1800
2400
3000
3600
4200
4800
5400
6000
CYCLE NUMBER

Figure 22

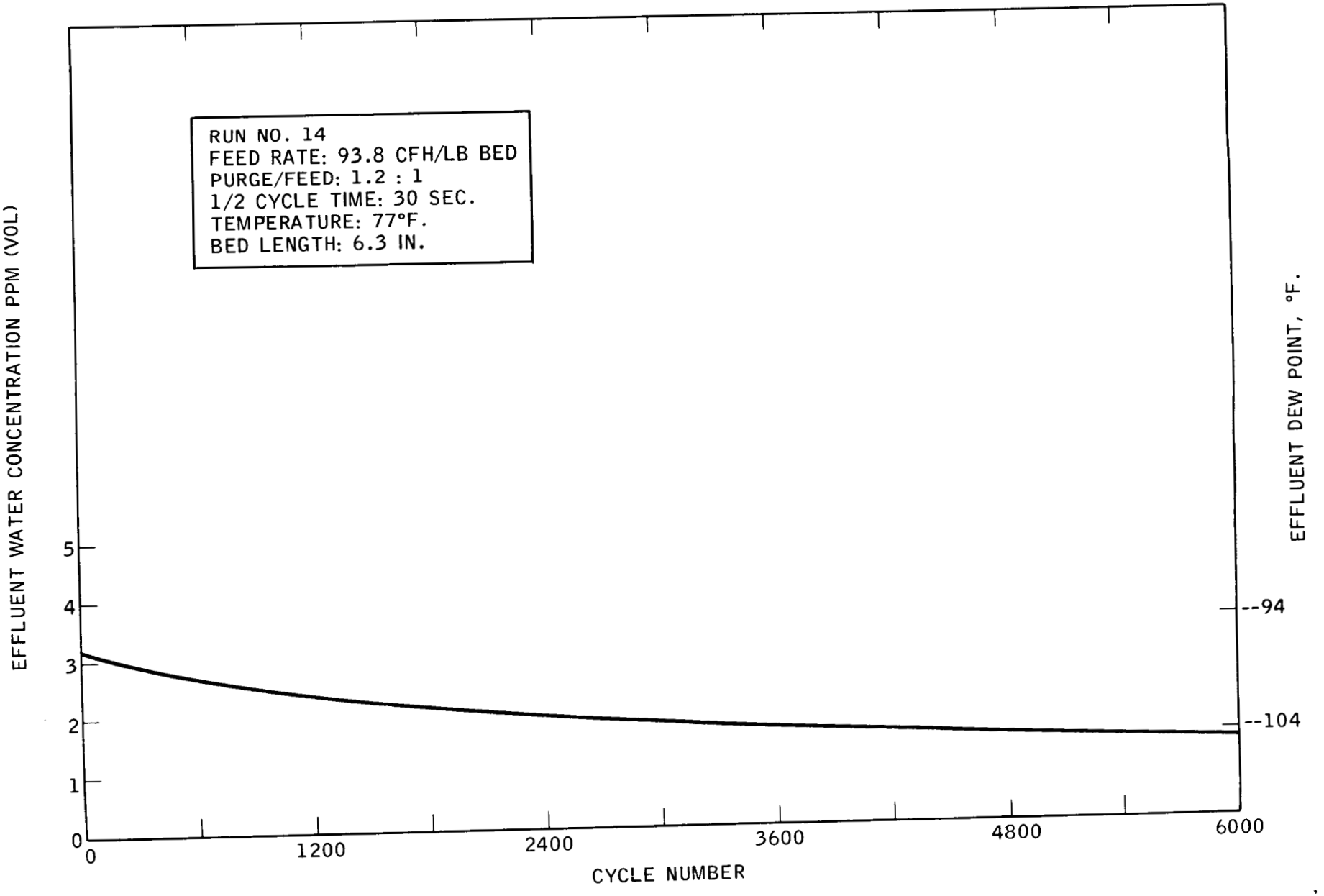
RUN NO. 14
FEED RATE: 93.8 CFH/LB BED
PURGE/FEED: 1.2 : 1
1/2 CYCLE TIME: 30 SEC.
TEMPERATURE: 77°F.
BED LENGTH: 6.3 IN.
EFFLUENT WATER CONCENTRATION PPM (VOL)
EFFLUENT DEW POINT, °F.
5
4
3
2
1
0
--94
--104
0
1200
2400
3600
4800
6000
CYCLE NUMBER

Figure 23

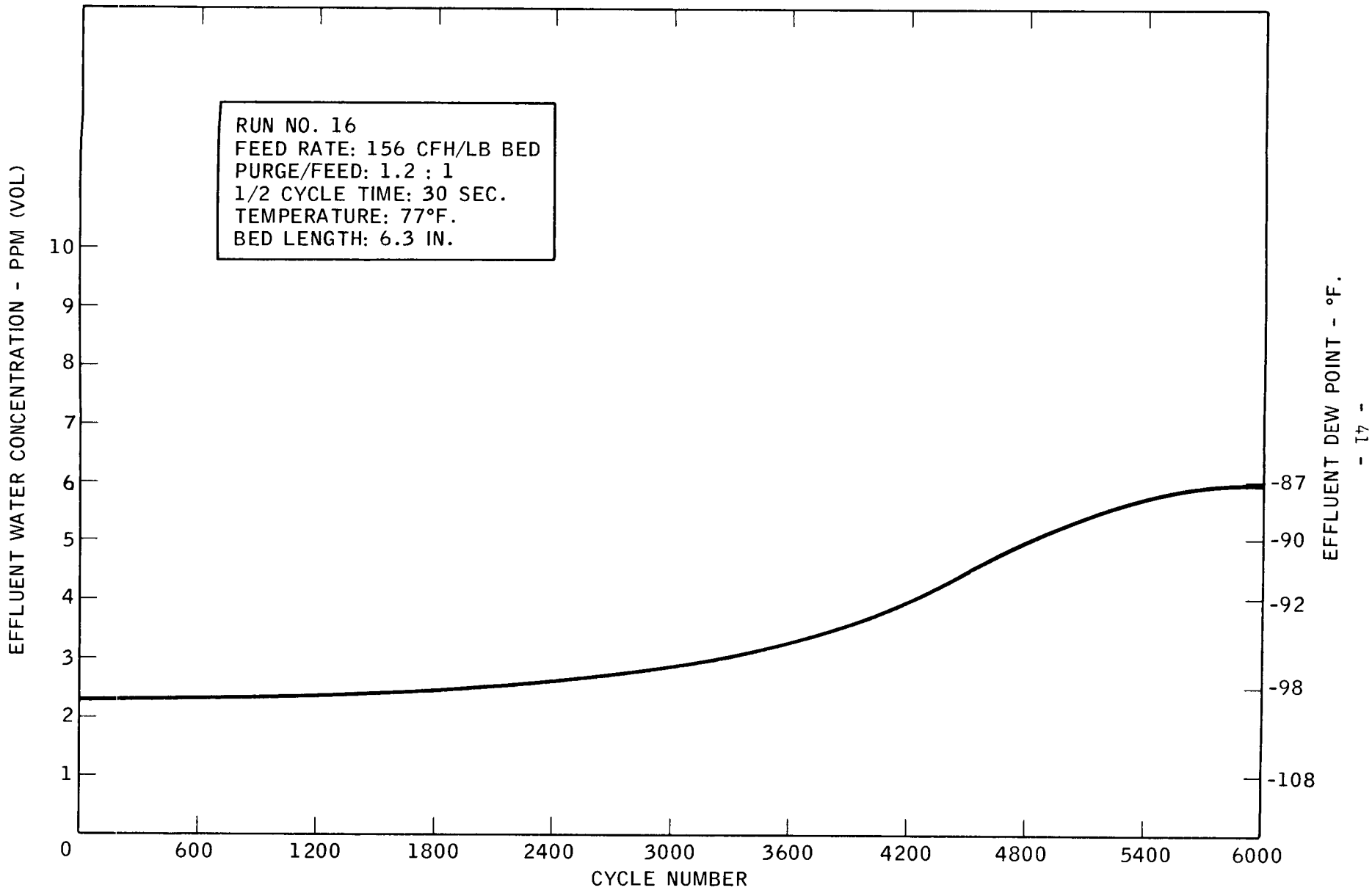
RUN NO. 16
FEED RATE: 156 CFH/LB BED
PURGE/FEED: 1.2 : 1
1/2 CYCLE TIME: 30 SEC.
TEMPERATURE: 77°F.
BED LENGTH: 6.3 IN.
EFFLUENT WATER CONCENTRATION - PPM (VOL)
EFFLUENT DEW POINT - °F.
0
1
2
3
4
5
6
7
8
9
10
-87
-90
-92
-98
-108
600
1200
1800
2400
3000
3600
4200
4800
5400
6000
CYCLE NUMBER

4.6. Data Analysis and Correlation

The experimental program was originally designed to study the effects of five operating parameters: purge to feed ratio, space velocity, cycle time, bed length, and sorption temperature. This number was reduced to four when it was found that temperature had no effect on the steady state moisture content of the dried gas. Reference to Table 6 will show that the corresponding runs at 60 and 77°F produced results which on average checked as closely as those in replicate runs.

Table 6

Comparison of Results at 66° and 77°F

Experiment	Purge to Feed Ratio	Space Velocity, CFH/lb Sorbent	Half Cycle Time Sec.	Temp, °F	Steady State Moisture Level, PPM
1	1.1	156	30	77	67
11	1.1	156	30	60	67
10	1.2	93.8	30	77	2
9	1.2	93.8	30	60	3
4	1.1	93.8	60	77	34
8	1.1	93.8	60	60	>30
8R1	1.1	93.8	60	60	<52
6	1.2	156	60	77	9
6R1	1.2	156	60	77	13
6R2	1.2	156	60	77	20
6R3	1.2	156	60	77	11
12	1.2	156	60	60	9

Note: Bed Length = 4.5" for all these experiments

Of the four remaining variables, it was apparent that purge to feed ratio and space velocity were important parameters. The effects of cycle time and bed length, however, were less obvious. Consequently, an analysis of variance (ANOVA) was made of the data to determine their importance. For this analysis, the data were divided into two groups shown as A and B in Tables 7 and 8, respectively. In Group A, the effect of cycle time was studied in conjunction with the purge to feed ratio and the space velocity. In Group B, the effect of bed length was considered with the other two variables.

Table 7

Group A ANOVA

Temperature = 77°F

Bed Length = 4.5"

Run No.	Treatment Combination	Steady State PPM H_2O	Log PPM
3	(1)	30	1.477
10	a	2	0.301
1	b	67	1.826
2	ab	7.5	0.875
4	c	34	1.531
5	ac	1.5	0.176
7	bc	307	2.487
6	abc	9	0.954

Source	Effect	Sum of Squares	Degree of Freedom	Mean Square
A	-1.254	3.144	1	3.144 (1)
B	.664	0.882	1	0.882 (1)
C	.167	0.056	1	0.056
AB	.012	0.0003	1	0.003
AC	-.190	0.0724	1	0.0724
BC	.203	.082	1	0.082
ABC	-.101	.020	1	0.020
Error**		0.0858	3	0.0286 (2)
Total		4.5156	10	
Grand Mean		1.212		
F0.05, 1, 3		10.13		
MS Crit.		0.290		

A = Purge to feed ratio
B = Space velocity, CFH/lb bed
C = Half cycle time, Sec.

(1) Significant at the 95% confidence level
(2) See Table 9

Table 8

Group B ANOVA

Temperature = 77°F

Bed Length = 4.5"

Run No.	Treatment Combination	Steady State PPM H_2O	Log PPM
4	(1)	34	1.531
10	a	2	0.301
7	b	307	2.487
2	ab	7.5	0.875
13	c	18	1.255
14	ac	1	0.000
15	bc	100	2.000
16	abc	6	0.778

Source	Effect	Sum of Squares	Degree of Freedom	Mean Square
A	-1.330	3.537	1	3.537 (1)
B	.763	1.165	1	1.165 (1)
C	-.290	0.169	1	0.169 (2)
AB	-.087	0.015	1	0.015
AC	.091	0.017	1	0.017
BC	-.002	0.000006	1	0.000006
ABC	.104	0.0215	1	0.0215
Error		0.0585	3	0.0286 (3)
Total		5.1884	10	
Grand Mean		1.162		
F0.05, 1, 3		10.13		
MS Crit.		0.290		

A = Purge to feed ratio
B = Space velocity, CFH/lb bed
C = Bed length, inches

(1) Significant at the 95% confidence level
(2) Significant at the 90% confidence level
(3) See Table 9

The source terms A, B, C, AB, AC, etc., in Tables 7 and 8 refer to the linear and interaction terms in the linear models.

$$\log \text{PPM} = f\ (P/F,\ SV,\ CT/2)$$

and

$$\log \text{PPM} = f'\ (P/F,\ SV,\ BL)$$

In these models, the logarithm of the moisture content was used as the dependent variable rather than the moisture content per se. The logarithm form was chosen for two reasons. The first is that adsorption breakthrough data are often correlated[a] by a function of the form:

$$\log \frac{\text{PPM component in effluent}}{\text{PPM component in feed}} = g\ (\text{space velocity, time on adsorption, etc.})$$

Although this equation describes transient behavior for long adsorption cycles, there are similarities between it and the slow but steady buildup of moisture in a rapidly cycling heatless process. The second reason is simply that the use of the logarithm function resulted in a better empirical fit to the data than did the linear form. This is best understood by realizing that it was necessary to correlate large variations in the independent variable (i.e., 1 to 310 PPM H_2O) with relatively small changes in the values of the dependent variables. The data were correlated using a multiple linear regression technique. If the linear response had been assumed, an error in the moisture content at some low level would have been given as much weight in the regression as the same absolute error at some higher level. For example, a 1 PPM error at the 10 PPM moisture level would have been considered as important as the same error at 100 or 1000 PPM. In contrast, the logarithm transformation provided a constant relative error which was far more realistic for these experiments.

In the analysis of variance, a factor is assumed to be significant if its mean square value is large compared to the mean square experimental error. Based on replications of Run 9, the mean square error was calculated to be 0.0286 for these experiments.

Table 9

Estimates of Experimental Error Mean Square

Run No.	PPM H_2O	log (PPM H_2O)
6	9	0.954
6R1	13	1.114
6R2	20	1.301
6R3	11	1.041
Range, W	11	0.347
$S_{error} = W/2.059$	5.3	0.169
MS_{error}	28.1	0.0286

degrees of freedom = 3

(a) Derived for constant pattern, isothermal adsorption with external diffusion controlling. See: (25).

For any of the factors to be significant at the 95% confidence level, their mean square value should be ten or more times this value. Reference to Tables 7 and 8 will show that the mean squares for only purge to feed and space velocity satisfy this requirement. Bed length is significant at only the 90% confidence level, while cycle time becomes important only below the 80% level.

Based on a 90% confidence level, the data were correlated by an equation of the form: $\log PPM = a_o + a_1 (P/F) + a_2 (SV) + a_3 (BL)$ using standard regression techniques to determine the three constants. The final equation which was obtained is:

$$\log PPM\ H_2O = 14.8612 - 12.5875\ (P/F) + 0.01113\ (CFH/lb\ bed) - 0.1218\ (BL, inches)$$

Using this equation, all the experimental results were subjected to prediction with the results shown in Table 10.

Table 10

Correlation Does Good Job in Predicting Data

Run No.	Moisture Level of Dried Gas	
	Actual	Predicted
1	67	160
2	7.5	8.8
3	30	32
4	34	32
5	1.5	1.8
6	9,13,20,11	9
7	165,450	160
8	30, 52	32
9	3	1.8
10	2	1.8
11	67	160
12	9	8.8
13	18	20
14	1	1.1
15	100	96
16	6	5.3

Most of the data are predicted very well by the equation. Nevertheless, in using this equation for design purposes, it is important to realize its limitations as well as its value. The prime value of the equation is that it provides the tool needed to optimize the drying sub-system within the framework of an overall life support system. In the range of moisture levels that is of most interest (i.e., 0 to 100 PPM), the equation does an excellent job of predicting the results at different drying conditions. The two cases for which there is the largest discrepancy between actual and predicted values are Runs 1 and 7. Both these runs were made at the low purge to feed ratio and high space velocity. Run 1 was made with a thirty-second half cycle time and Run 7 was made with a sixty-second half cycle time. The results of these

runs indicate that there is some form of variable interaction among the purge to feed, space velocity and cycle time. The combination of high purge to feed, high space velocity and long cycle time appears to be right at the edge of operability for the Heatless Drying system. Evidence of this is shown in Figure 15 for Run 7. In this run, small variations in the low purge to feed ratio produced very large fluctuations in the product moisture content. Thus, although no significant interaction was found in the statistical analysis of the data, there is little doubt of its existence.

4.7. Heatless System Designs

The data summarized in Table 5, and the equation derived from these data in Section 4.6., can be used to design Heatless Driers for use in the CO_2 control system of manned spacecraft. Table 11 gives examples of Heatless Drying systems, the desiccant weight and the power shown are based on a 3-man system.

The desiccant requirements were determined directly from the space velocities of Table 5 and the required gas flow rates. Gas flow rate is set by the CO_2 removal rate and the removal efficiency of the molecular sieve beds. A value of about 4 CFM/man appears to be typical for maintaining CO_2 partial pressure in the range of 4 to 8 mm Hg.

Table 11

Drier Design for 3-Man CO_2 Control System

System Pressure	∽10 psia
Gas Temp, °F	60 - 75°
Gas Dew Point, °F	∽45°
Gas Flow Rate CFM/Man	4
Half Cycle Time	30 to 60 seconds
Bed Length	4.5"
Desiccant	6 - 12 mesh Grade 40 Silica Gel

Steady State Moisture Content of Dried Gas, PPM		Lbs Silica Gel Per Bed	Purge to Feed Ratio	Compression Ratio of Blower	Theoretical Power for Blower, Watts
From Exp.	From Design Eqn.				
30-34	32	7.7	1.1	1.12	41.3
67	160	4.6	1.1	1.12	
2-3	1.8	7.7	1.2	1.22	79.6
7.5-9	8.8	4.6	1.2	1.22	

The compression ratio was determined from the purge to feed ratio. The purge to feed ratio was defined in Section 3.1 as the ratio of the volumetric flow through the desorbing bed divided by the volumetric flow through the adsorbing bed. For the four-bed carbon dioxide control system (see Figure 4A and 4B), 98 to 99% of the dried gas would be typically returned to the desorbing desiccant bed after carbon dioxide removal. Consequently, the ratio of the volumetric flows in the drying beds would be approximately equal to the ratio of the pressures in these beds. In turn, the compression ratio required by the blower to push gas through the four bed system would just about equal this pressure ratio. Having established the necessary compression ratio, the theoretical power requirements could then be calculated for the system blower.

It should be emphasized that since neither heating nor cooling of the desiccant or the gas is required for heatless systems, the power shown in Table 11 represents the total requirements of the entire CO_2 control system with the exception of the small additional amount of power needed for cycle control (e.g., timer, operating the valves, etc.). Furthermore, elimination of heating and cooling results in the saving of that weight associated with heat exchange or heat generating equipment and significantly reduced system complexity.

It is important to recognize that the water concentrations shown in the table are the steady state values that would be reached after many hours of cyclic operation. As Figures 9 to 23 indicate, the moisture buildup is gradual so that the average water level of the dried gas, over a fixed period of time, is lower than the steady state level. Since it is the total amount of water entering the CO_2 system that determines the decrease in capacity, the drying system can be designed to operate at less severe conditions than would be calculated, based on steady state operation.

4.8. Additional Design Considerations: Effect of Temperature Fluctuations and Cycle Disruptions

In addition to the principal effects described in the preceding sections, two other characteristics of the process were observed which are important.

The possibility exists, for example, that during operation of a Heatless Drying system in a space vehicle, some mechanical malfunction may cause interruption in normal cycling. The question obviously arises as to how long a time would be available for repairs in the event of such an occurrence.

This problem was studied experimentally by discontinuing cycling at the end of several runs and observing the buildup of moisture in the product. As might be expected, this buildup depended strongly on the space velocity, and on the purge to feed ratio that had been used prior to the upset. Figure 24 illustrates this effect. When operating at the high space velocity and the low purge to feed ratio, the water level of the product exceeded 200 ppm in about 10 minutes. Increasing the purge to feed ratio from 1.1 to 1.2 for such a system reduced the amount of saturated bed which existed at steady state and thereby provided an additional 20 to 30 minutes before the moisture content reached this same level. Finally, when low

space velocities were used in conjunction with high purge to feed ratios as much as an hour and a half was available before the 200 ppm level was exceeded. These times can undoubtedly be extended by cycling the valves manually on some regular basis. Nevertheless, the time available to complete corrective actions will in general vary with conditions -- more severe operating conditions providing less time than the less severe ones.

Figure 24

BREAKTHROUGH TIME VARIES WITH PROCESS CONDITIONS

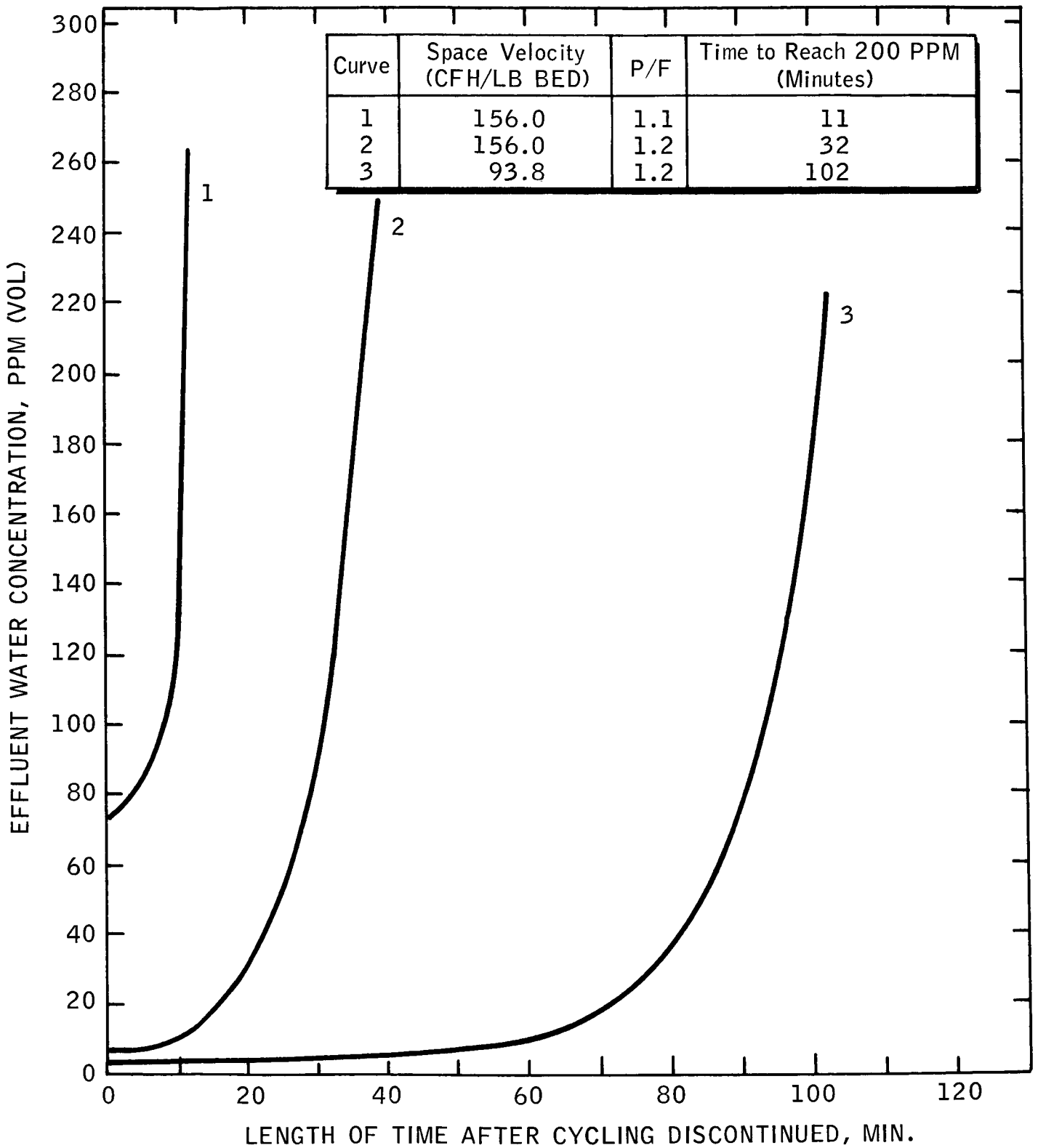

The other observation made in these studies, that would have bearing on system design and integration, was that changes in sorption temperature could produce transient changes in the product moisture content even though they produced no long lasting effects. An example of this is shown in Figure 25. In this case, an initially wet bed was cycled at 60°F for 24 hours, during which period the product moisture content dropped from 200 to 25 PPM. At this point, the system temperature was raised to 77°F. The response to this change was an immediate rise in the effluent concentration. However, within twenty-four hours, the level had passed through a maximum and was back to 25 PPM once more. Continued cycling drove the water level even lower as indeed it would have done at the lower temperature. The importance of these results is that, at worse, any effect due to temperature fluctuations will be short lived and therefore need not merit undue concern in the design or a system.

Figure 25

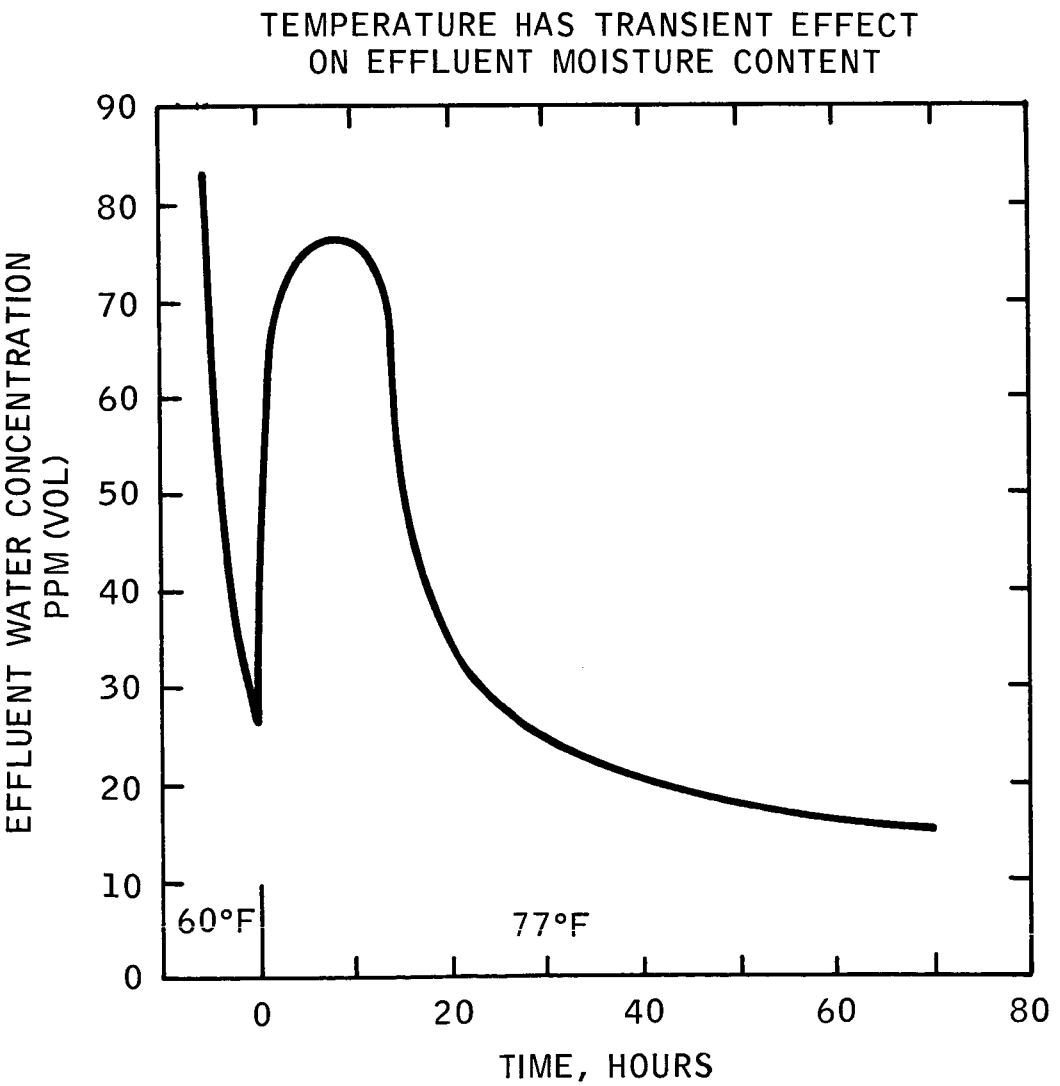

4.9. CONCLUSIONS AND RECOMMENDATIONS

It is apparent from the results obtained in this study that the Heatless Drying process could provide an effective means of producing the ultra-dry air needed by the molecular sieve-based carbon dioxide control systems of future manned spacecraft. The Heatless Drying technique would eliminate much of the complexity inherent in the thermal swing cycle. With a heatless system, there would be no need for interbed heating or cooling of process streams, or for direct heating or cooling of the sorbent. Elimination of heat generating and heat exchange equipment should result in direct reduction of overall system weight.

Adsorbent requirements for a heatless system would be competitive with those of thermally desorbed systems (26). Furthermore, electric power requirements would be much lower than for those systems that are solely dependent on thermo-electric power for desiccant reactivation. Whether or not this would also be true for systems that propose to use waste heat in conjunction with electric power would depend largely on what fraction of the total power requirements could be supplied by the former method.

This study has also shown that a Heatless Drying system would be relatively temperature insensitive. Any upsets due to temperature fluctuations would be transistory. Operating temperature could thus be selected to meet the requirements of the carbon dioxide sorbing beds or of the temperature-humidity controller. Spare drying capacity would be available in the event of a failure in the cycling process but the amount of spare capacity would depend on the operating conditions prior to the upset.

In summary, this work has shown that the Heatless Drying process has excellent potential for improving the carbon dioxide control system of future manned spacecraft. Nevertheless, there are still problems to consider before designing an actual system. For one thing, the effect of rapid cycling on valve wear and operability must be determined. Another important factor is the effect of long term cycling on the capacity and physical integrity of the sorbent. Finally, although theoretical power requirements for the system are low, data are needed to determine the actual power needed by the air blower operating in a heatless system. Information such as this can best be obtained in a full scale prototype system. It is therefore recommended that a prototype Heatless Drier be built based on the design equation developed and then tested as part of full scale carbon dioxide control systems.

5. PHASE II: INVESTIGATION OF PURGE DESORPTION TECHNIQUES FOR A SPACECRAFT CO_2 SORPTION SYSTEM

The objective of Phase II of the program was to investigate the use of purge techniques for improving vacuum desorption of CO_2 from molecular sieve. This section describes the experimental program and results obtained therein.

5.1. System Parameters

In designing the CO_2-molecular sieve sorption system, three factors will have to be considered: system weight*, air loss during desorption, and gas flow rate. System weight will depend to a large extent on the amount of molecular sieve required and therefore the sorbent's cyclic capacity. The gas flow rate will be set by the CO_2 removal efficiency (i.e., fraction of CO_2 in the gas that is adsorbed), and the CO_2 concentration in the gas. Gas flow rate, together with system pressure drop, will determine the power required by the fan to move the gas through the system. Finally, air loss during desorption will depend on the purity of the CO_2 that is rejected to space during desorption of the molecular sieve. Such loss comes from air trapped in the void spaces of the bed and from oxygen and nitrogen which is adsorbed by the molecular sieve. The maximum air loss which can be tolerated will depend on several factors but the duration of the mission is the primary one since all air lost from the space capsule must be made up from a reserve supply carried on board.

Based on previous experience, it was known that the reduction which purge desorption could make in sorbent requirement and desorption air loss would depend on the cycle itself and its particular set of operating parameters. Consequently, it was necessary to evaluate the effectiveness of purge desorption at a variety of different operating conditions. The system parameters that were considered important and varied in this study were cycle time, space velocity, bed length, CO_2 partial pressure in the gas, and CO_2 sorbent. Table 12 shows the values that were investigated for each of these parameters.

Table 12

System Parameters Investigated

Operating Variables	Levels Investigated
Purge	0.3 and 0.6 $\frac{SCFH}{LB\ Bed}$, plus one level PED purge (Purge cylinder vol. = .065 $ft.^3$/lb sieve
Space Velocity	104, 139 and 173 $\frac{CFH}{LB\ Bed}$
Bed Length	5 and 9 inches (3.3:1 and 6:1 L:D)
Cycle Time	10, 20, 30, 60 Minutes
CO_2 Feed Partial Pressure	4 and 7.5 mm Hg abs.
Molecular Sieve	Linde 5A and 4A, 1/16" Extruded pellets

* System weight in this section refers only to that associated directly with CO_2 removal, i.e., molecular sieve, containers, cycling valves, etc. It does not include any weight associated with the dessicant system that is needed to pre-dry the gas.

Two types of purge were studied: conventional product purge where a very small portion of the CO_2 lean product was used to purge the vacuum desorbed bed, and PED purge where a portion of the depressure gas (see Section 3.2) was used as the purging medium. The need to study both types of purge, in relation to the five other parameters listed above, required that the experimental unit built be easily adaptable to different conditions and modes of operation.

5.2. Description of Experimental Equipment

A schematic diagram of the pilot unit used for the CO_2 removal studies is shown in Figure 26. As in the drying unit, all lines were made of 3/8" SS tubing connected by swage-lock fittings, and the beds were constructed of 1-1/2" glass pipe. The molecular sieve was held in these beds with stainless steel wire mesh packed firmly on both side of the adsorbent (See Figure 6).

The system gas was a mixture of CO_2 and air metered independently through two rotameters. The air stream was pre-dried to dew points below -90°F with a commercial Heatless Dryer (Gilbarco Model HF-200) and the CO_2 was dried by passing it through a 24-inch long silica gel bed. Back pressure was maintained at 20 psig with two back pressure regulators. The separate streams were blended in proper proportions to yield the desired flow rates and CO_2 partial pressures. The mixed stream was then fed to the bottom of the adsorbing bed. This bed was maintained at the adsorbing pressure (about 21.9 in Hg abs.) by means of a CENCO, Megavac, vacuum pump, Model 92003 (rated at 2 CFM free air capacity) and an Emil Greiner, Model 5, cartesian manostat.

Desorption vacuum was provided by a Cenco Model 91506, Hyvac 7, vacuum pump (rated at 2.79 CFM free air capacity and 1.24 CFM at 1 millitorr pressure). The pump was connected to the beds through approximately 5 feet of 3/8" line. Desorption pressure was measured at a point in this line located about 15" from the outlet of the beds with a Barocel 511 Pressure Transducer. The amount of desorbate was measured by a wet test meter connected to the discharge of the Cenco Hyvac Vacuum pump.

For conventional purging, a portion of the CO_2 lean product was withdrawn, passed through a flow measuring rotameter and a flow control valve and then through the desorbing bed. For the pressure Equalization Depressuring technique of purging, a 42.5 in^3 cylinder was provided. This gave the equivalent of .065 ft^3 of volume/lb sieve. After bed pressure equalization, the adsorbing bed would be depressured into this evacuated cylinder through an Asco model 803041VM solenoid valve. After completing the PED step, this valve would be automatically closed and the gas in this cylinder used at a controlled rate (flow control valve) to purge the desorbing bed.

Automatic cycling was achieved throughout every step of the process using the same type of solenoid valves. These were activated sequentially by a cycle programmer manufactured by the Automatic Timer Corporation. This programmer was capable of independently activating any of ten solenoid valves in any part of the cycle. This allowed for maximum flexibility in operation. Figure 27 shows the valve sequence used for those runs utilizing the Pressure Equalization Depressuring purge technique.

Figure 26

CO_2 SORPTION UNIT

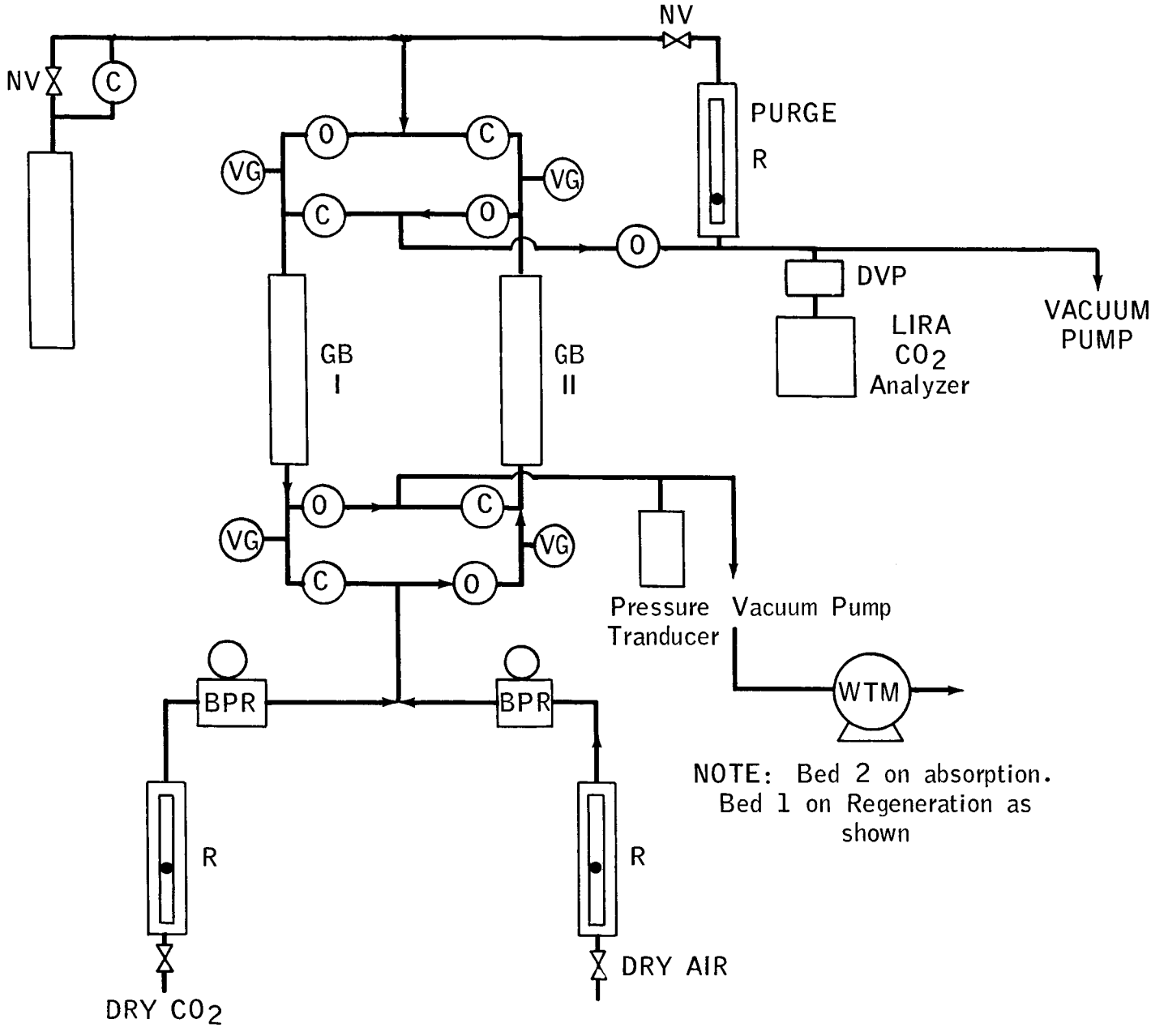

R = Rotameter
NV = Needle valve
BPR = Back pressure regulator
VG = Bourdon vacuum gauges

DVP = Diaphragm vacuum pump
WTM = Wet test meter
Ⓒ, Ⓞ - Closed, open solenoid valves

Figure 27

PROGRAM CONTROLLED PROCESS SEQUENCE - CO_2 UNIT

10 MINUTE HALF CYCLE

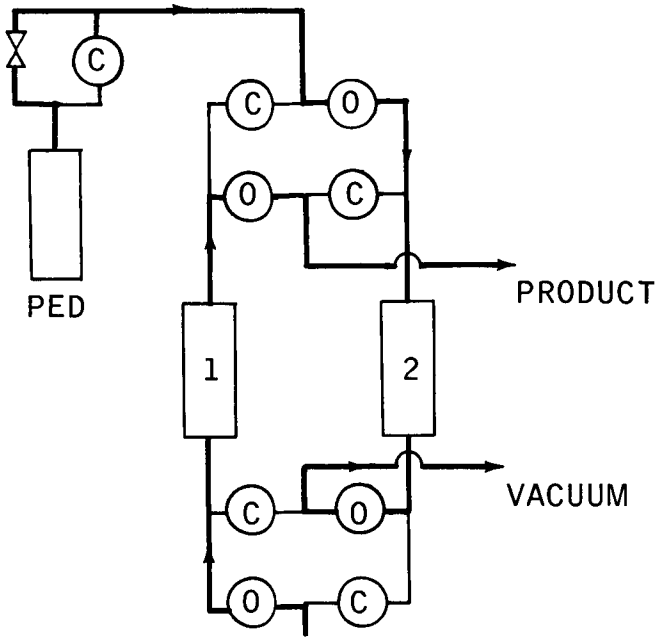

(a) BED 1 ON ADSORPTION (10 MIN.)
BED 2 ON PED PURGE (10 MIN.)

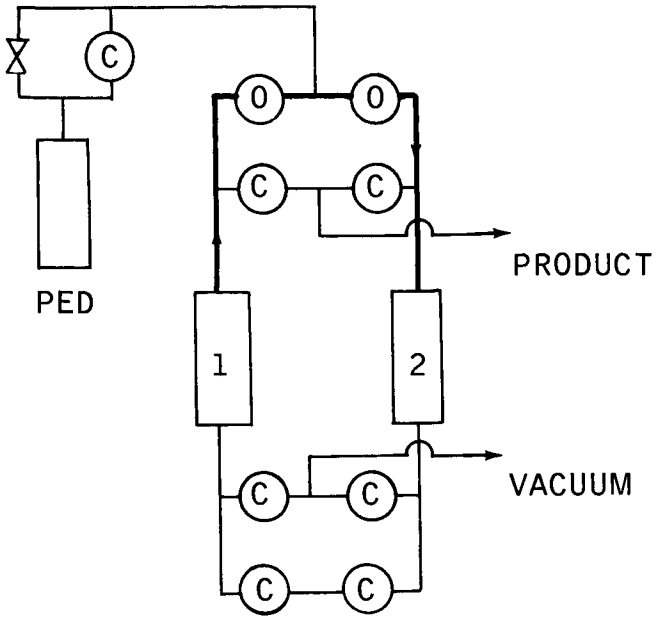

(b) BPE (10 SEC.)

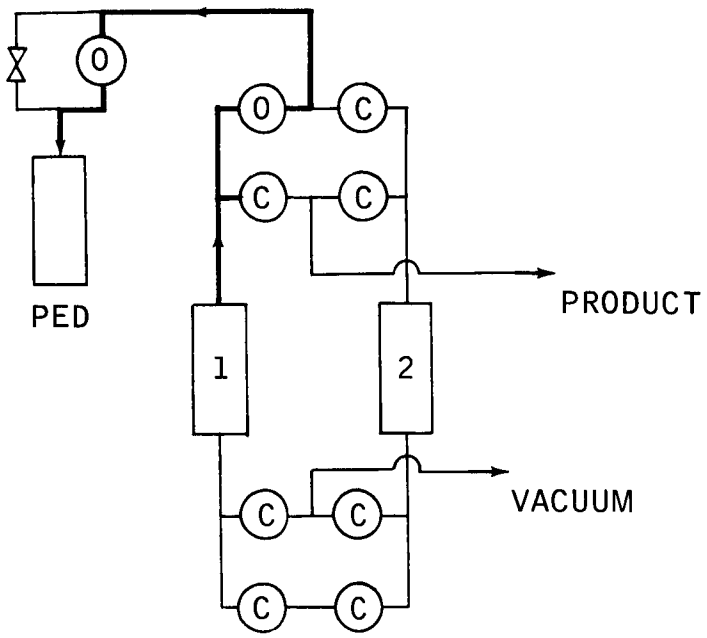

(c) PED (10 SEC.)

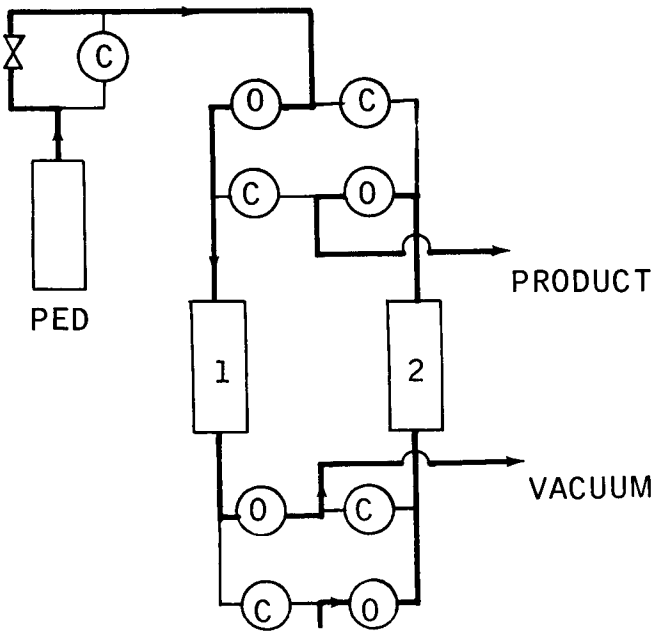

(d) BED 1 ON PED PURGE (10 MIN.)
BED 2 ON ADSORPTION (10 MIN.)

(O) = OPEN SOLENOID VALVE

(C) = CLOSED SOLENOID VALVE

Continuous sampling of the CO_2-lean product was carried out with a Neptune Dyna Diaphragn Pump (Model #3), and analysis of this sample was made by an infra-red CO_2 analyzer (Mine Safety Appliance, Model Lira 200). The same analyzer was also used for monitoring the feed CO_2 content. The signal from the CO_2 analyzer was continuously recorded on a Sargent Model 72150 Recorder. A typical recorded output is shown in Figure 28. The "saw-tooth" effect was obtained in all experiments and represents the breakthrough pattern of the system (i.e., the CO_2 concentration in the effluent from the adsorbing bed) while the upper solid horizontal line represents the CO_2 concentration of the feed. The area between the feed line and the product concentration curve indicates the amount of carbon dioxide removed per cycle. This was calculated for each run by graphical integration. A sample calculation is given in Appendix 4.

The CO_2 analyzer was calibrated daily since there was some tendency for the output signal to drift with time. Electronic problems with the analyzer were normally easy to detect and correct. On occassion, however, other malfunctions such as a faulty detecting cell were not as readily apparent, and these resulted in some loss of experimental time.

The sorbing beds were charged with 1/16" extruded molecular sieve obtained from the Linde Co. Activation of the bed consisted of removing adsorbed moisture and other contaminents by purging under vacuum with large volumes of dry air for a period of about twenty hours. The adsorbent was changed only three times during the course of the study, when the bed became inadvertently contaminated with vacuum pump oil, when the bed length was changed, and finally when the 4A adsorbent was substituted for the 5A molecular sieve.

Having selected the set of operating conditions to be used in a particular run (i.e., space velocity, purge rate, cycle time, adsorption pressure, and CO_2 feed concentration), the system was allowed to operate for three to four complete cycles prior to recording any data. In contrast to the drying experiments which required thousands of cycles, a few cycles were all that were needed for the CO_2 system to reach a steady state operation.

Figure 28
LIRA OUTPUT-RUN PED 1

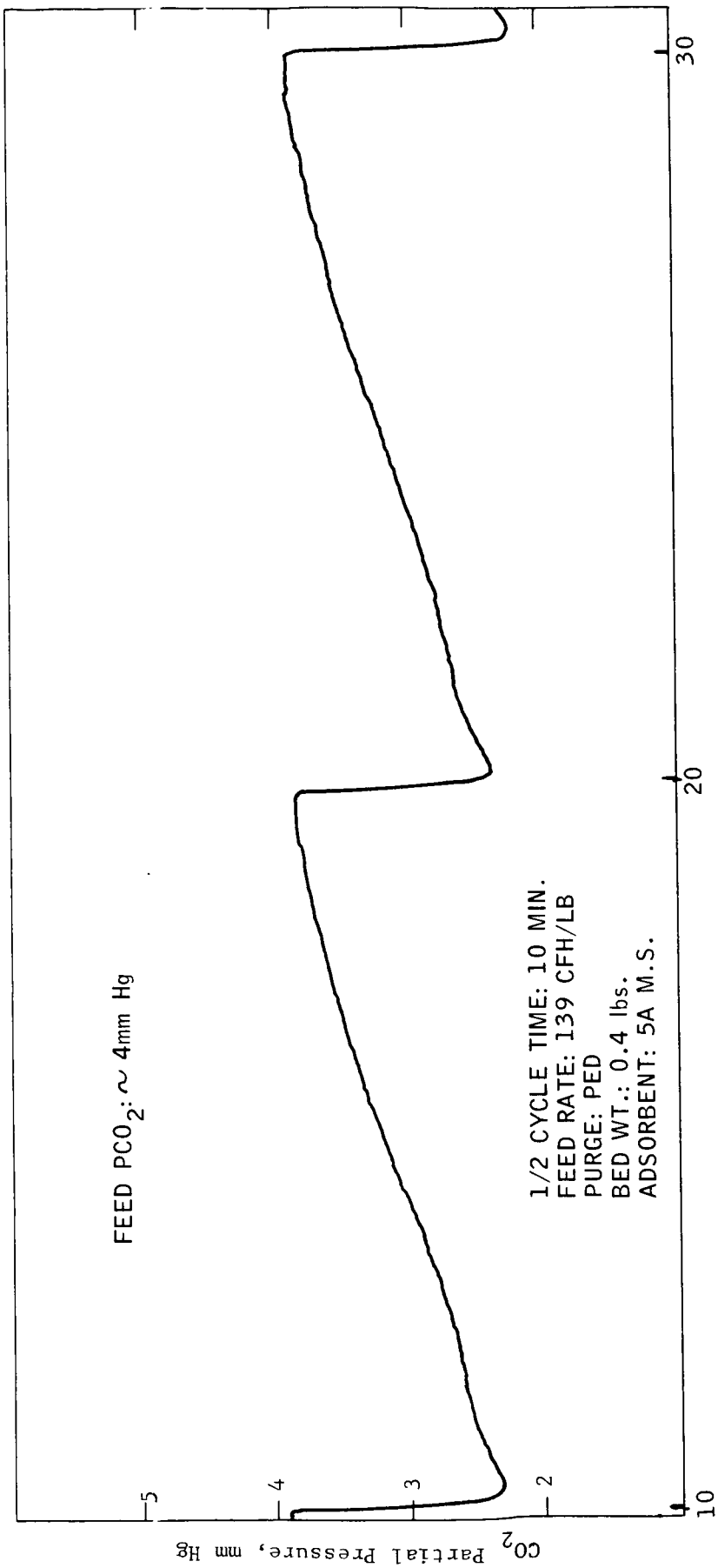

5.3. Experimental Design

The experimental unit built for the CO_2 sorption studies was designed to allow maximum flexibility in experimentation. Although this made changing all operating variables a simple and rapid procedure, it necessarily resulted in a unit which was not optimally designed from the standpoint of weight, size, power requirements, etc. In particular, the vacuum provided for desorption was far less than would be obtained in a system where the beds are desorbed to space. In our studies, desorption pressures below 0.5 mm Hg (abs) could not be obtained; this pressure being measured downstream of the desorbing bed. This comparatively high desorption pressure resulted in less effective CO_2 desorption, and consequently, lower operating capacities than would be obtained in systems with better vacuum. Recognizing this operating problem, it was decided to run conventional vacuum desorbed cycles in our equipment in order to provide base cases with which to compare the purge desorbed runs. Any differences noted between conventional and purge aided vacuum desorption in these experiments therefore reflect real differences that would exist in an actual system.

A very large experimental effort would have been required if the CO_2 system were to be evaluated by a statistically designed program as complete as the one employed in the experimental drying studies. In the CO_2 system, six process variables were studied at as many as four different levels. In contrast, the desiccant studies involved only five variables at two different levels. Furthermore, the development of an equation relating capacity (or air loss) to these independent variables would not be directly applicable to a CO_2 system design because of the limitations discussed in the preceding paragraph. Consequently, it was decided to design an experimental program based on a modified central composite plan which would permit satisfactory interpretation of the effects of each of the process variables. Basically, this involved eight distinct areas of investigation which covered the four variables: CO_2 partial pressure, feed rate, bed weight and adsorbent type. Different levels of purge rate and cycle time were carried as additional parameters common to each of these areas. The experimental design is described in Tables 13 and 13A. Table 13 lists each of the variables with the different levels investigated for each. A numerical symbol has been assigned to each of these levels in order to simplify the tabulation of runs presented in Table 13A. Reference to Table 13A shows that in the first set of experiments, the combined effects of purge rate and cycle time were studied thoroughly to form a basis of comparison with each of the other runs. This was repeated partially in the second set at a higher CO_2 partial pressure. Sets 3 and 4 were used to obtain the effect of feed rate at each of the two CO_2 pressures. Columns 5 and 6 represent the experimental runs performed to observe the effects of changing bed length to diameter ratio and columns 7 and 8 represent those runs used to compare 5A and 4A sieve. In all, this plan called for 70 separate runs but in fact the total number made amounted to many more since most of the runs were replicated several times.

Table 13

CO_2 Experimental Design

Variable	Levels Investigated	Symbol
Purge Rate	0 SCFH/Lb Bed	1
	0.3 "	2
	0.6 "	3
	PED Purge cylinder volume = .065 ft^3/lb bed	4
1/2 Cycle Time	10 Min	1
	20 "	2
	30 "	3
	60 "	4
CO_2 Partial Pressure	4.0 mm Hg	1
	7.5 "	2
Space Velocity	104 CFH/Lb Bed	1
	139 "	2
	173 "	3
Bed Length (Weight)	5 Inches (.22 Lbs)	1
	9 Inches (.397 Lbs)	2
Adsorbent	5A M.S.	1
	4A M.S.	2

Table 13A

Variable	Levels Investigated							
	1	2	3	4	5	6	7	8
Purge Rate	1,2,3,4	1,3,4	1,3,4	1,3,4	1,3,4	1,3,4	1,3,4	1,3,4
Half Cycle Time	1,2,3,4	1,2	1,2	1,2	1,2	1,2	1,2	1,2
CO_2 Partial Pressure	1	2	1	2	1	2	1	2
Space Velocity	2	2	1,3	1,3	2	2	2	2
Bed Length	2	2	2	2	1	1	2	2
Adsorbent	1	1	1	1	1	1	2	2
Total Runs	16	6	12	12	6	6	6	6
	Effect of Purge, Cycle Time and PCO_2		Effect of Feed Rate		Effect of Bed Length		Effect of Sieve Type	

5.4. EXPERIMENTAL RESULTS

The results of the carbon dioxide sorption program are presented in Sections 5.4.1. through 5.4.5. A tabulation of all the experimental data is given in Appendix 5.

The objective of this part of the program was to determine under what conditions, if any, purge aided vacuum desorption provided an improved method of regenerating the adsorbent vis à vis conventional vacuum desorption. In Section 5.4.1., the results of using product purge are compared to those obtained using vacuum desorption. In Section 5.4.2., this comparison is extended to PED purge. In Sections 5.4.3. and 5.4.4., the changes that bed length and space velocity make in purge effectiveness are considered. Finally, in Section 5.4.5., a comparison is made between the use of 4A and 5A molecular sieves in purge desorbed systems. In all five of these sections, the experimental data are presented in figures showing the relationship between the adsorbent's capacity (lbs CO_2 adsorbed/Hr/lb sieve) and the amount of air lost when desorbing the carbon dioxide to space vacuum. In most cases, the points shown in these figures are averages obtained from replicated experiments.

Representing the data as plots of air loss versus sorbent capacity offers two advantages. First, such a plot contains all the information needed to generate a system design. This can be seen by refering to section 5.5 where some examples of design calculations are given. Secondly, presenting the data in this graphical form permits direct determination of whether the purge has helped or not in any particular case. This can be appreciated more fully by reference to Figure 29. Here, the data curves are shown for two hypothetical modes of operation (e.g., purge desorption, mode 2, versus vacuum desorption, mode 1) labelled 1 and 2. On the basis of system capacity and the air loss ratio, that mode of operation represented by Curve 2 is preferred to that represented by Curve 1. At equivalent capacities (Point B

Figure 29

EXAMPLE OF DATA PRESENTATION
FOR THE CO_2 SORPTION EXPERIMENTS

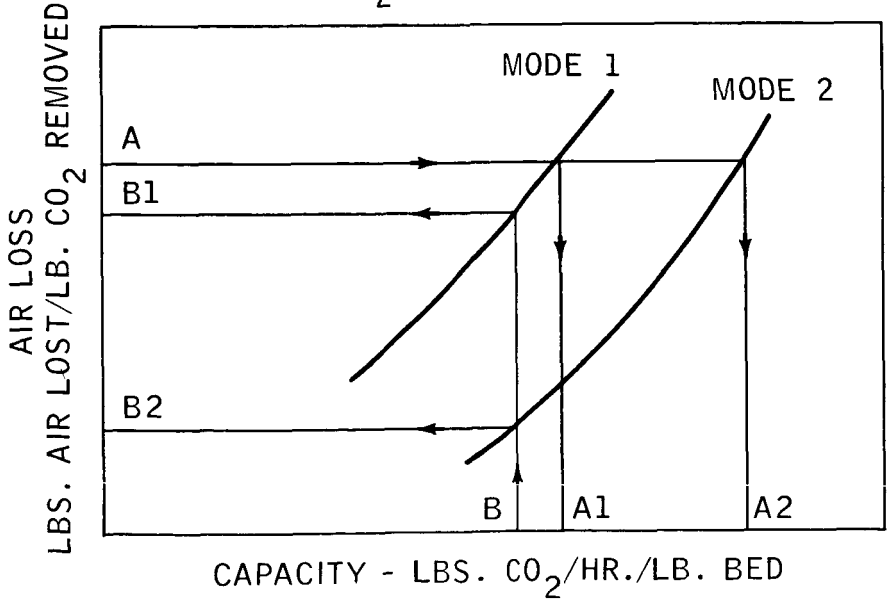

for example), less air will be lost when operating at the former set of process conditions (Point B2) than with the latter (Point B1). Alternately, at the same rate of air loss (Point A for example), the capacity obtained with Operation 2 (Point A2) is greater than that for Operation 1 (Point A1). Obviously, compromise conditions which partially reduce both bed size and air loss are also possible. The important point to emphasize in analyzing such curves is that, other factors being equal, a more favorable condition exists whenever a given set of data fall below a second set of data.

In reviewing the data presented in Sections 5.4.1 through 5.4.5., it should also be kept in mind that the capacities shown are lower, and the air losses higher than would be obtained in an actual spacecraft system (or a prototype of one) designed with a minimum of void space and operating under space vacuum conditions. As Figure 30 shows, the best desorption vacuum that could be obtained in these experiments was only 500 microns measured at the outlet of the bed. In contrast, CO_2 prototype systems that have been evaluated have used vacuums of 200 microns or less (26) This large difference in vacuum biases any comparison in favor of the prototype system.

One final point should be made concerning the presentation of the data in this part of the report. In all cases, the product purge is shown as SCFH/lb molecular sieve rather than as the actual volumetric flow ratios (i.e., purge CFH /Feed CFH) used for the drying experiments. The reason for this is the desorption pressure was not constant in the CO_2 sorption studies but decreased continually through the desorption as shown in Figure 30. Consequently, the actual volumetric flow rate of the purge increased throughout the desorption and no one value could be assigned to it.

5.4.1. Effect of Conventional Purge

The first series of experiments was made to determine what relative system improvements could result if conventional product-purge were used to aid vacuum desorption of carbon dioxide from molecular sieve. The results obtained are shown in Figures 31 and 32. The data are shown at different cycle times for two carbon dioxide partial pressures. At all conditions, experiments were also made using vacuum desorption without purge. This provided base cases to which the results obtained with purge-aided desorption could be compared.

It is apparent from the data that the use of purge is beneficial over a wide range of operation. All purge curves fall below the vacuum data for air loss ratios in excess of 0.15 lbs air/lb CO_2. For any design air loss ratio above this value, some combination of purge level and cycle time can therefore be selected which will result in greater system capacity than that corresponding to conventional vacuum desorption. At air loss ratios below this, the results obtained with purge showed no difference from those obtained without it. For the long space missions, for which these regenerative systems are being considered, it is these low air loss rates that are of most interest. Therefore, product purging appears to offer no advantage for these long missions compared to vacuum desorption although it could have application for shorter missions.

Figure 30

EFFECT OF CYCLE LENGTH ON
DESORPTION VACUUM

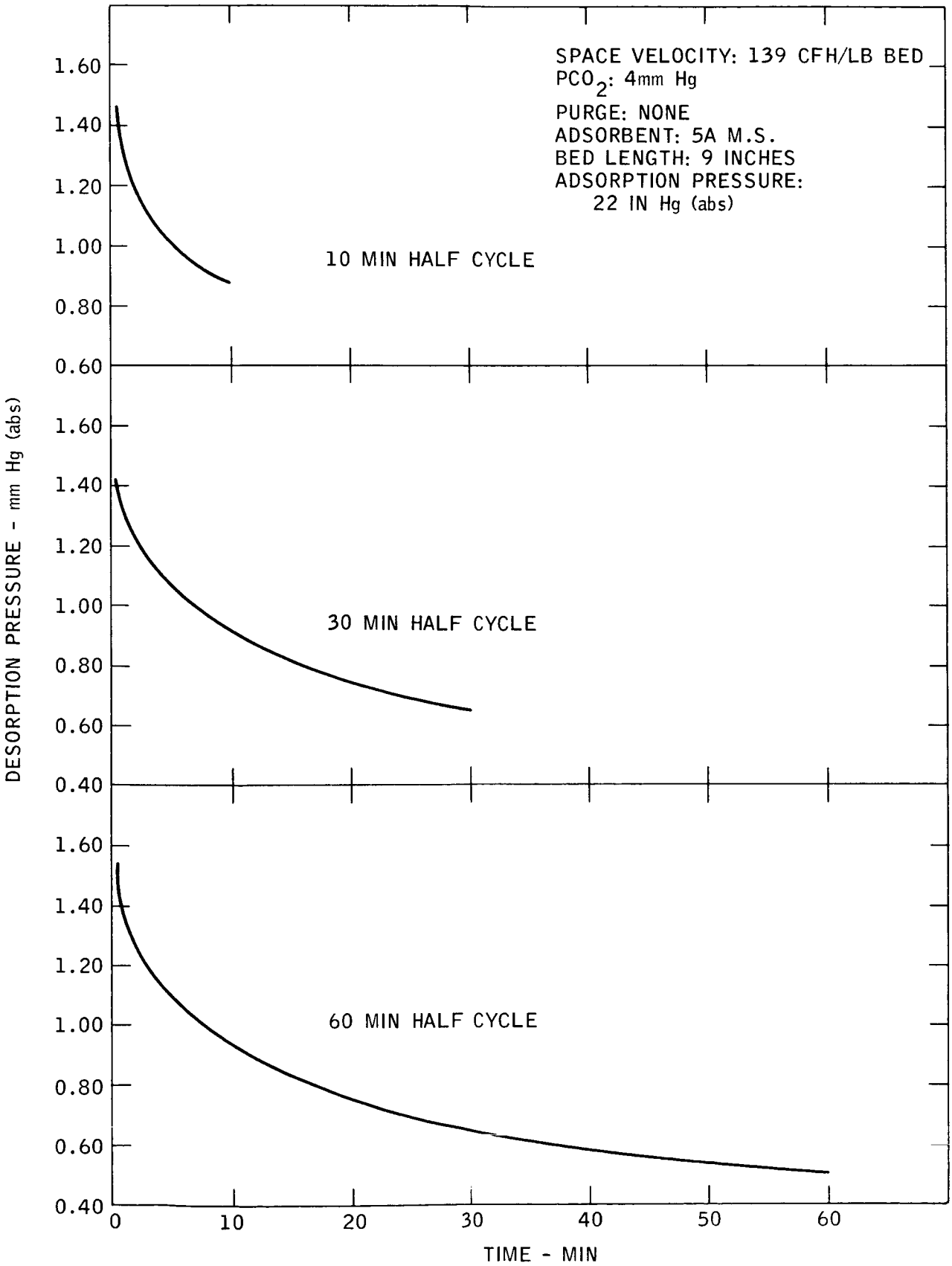

Figure 31

CO_2 SORPTION - EFFECTS OF CYCLE TIME & PURGE

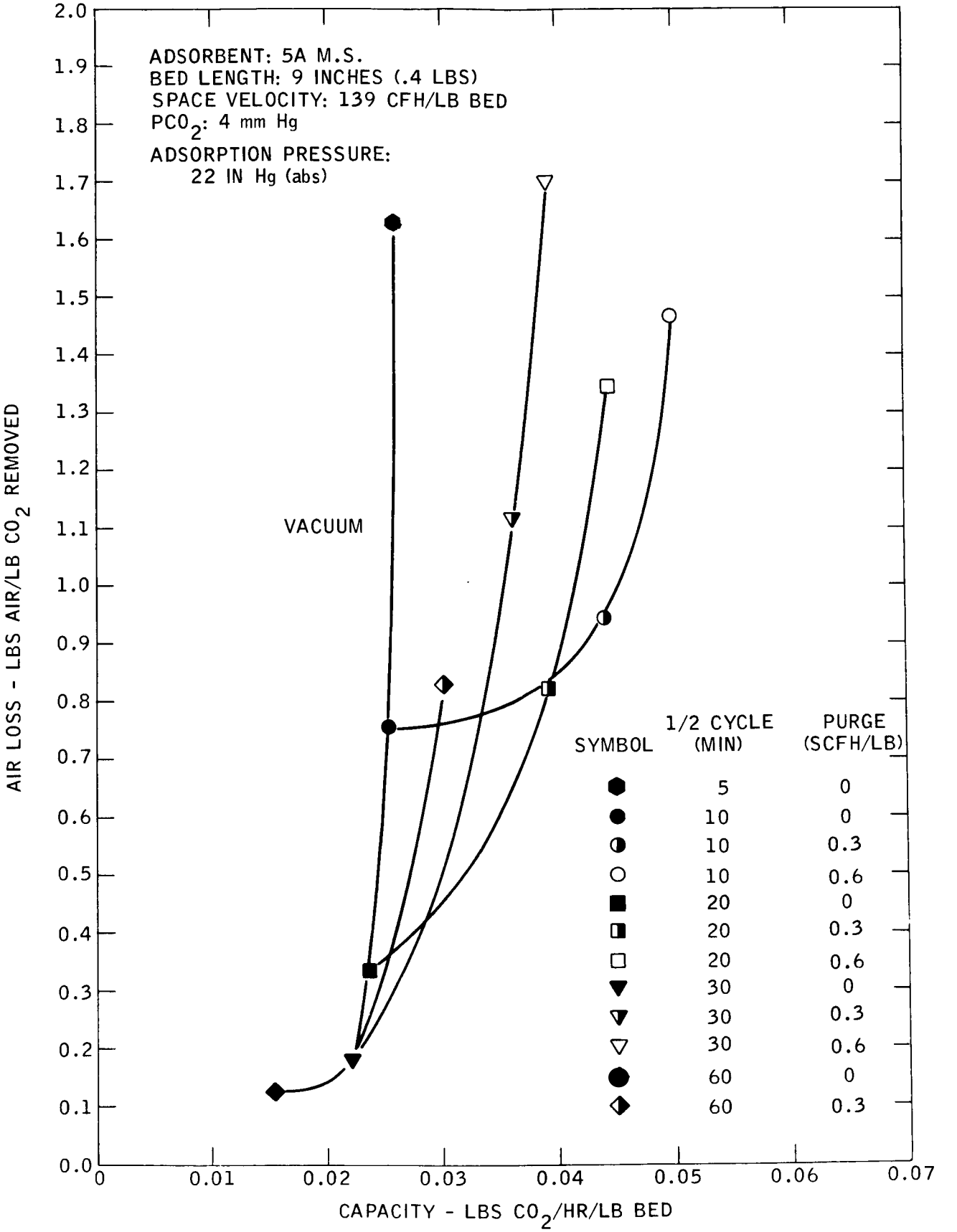

Figure 32

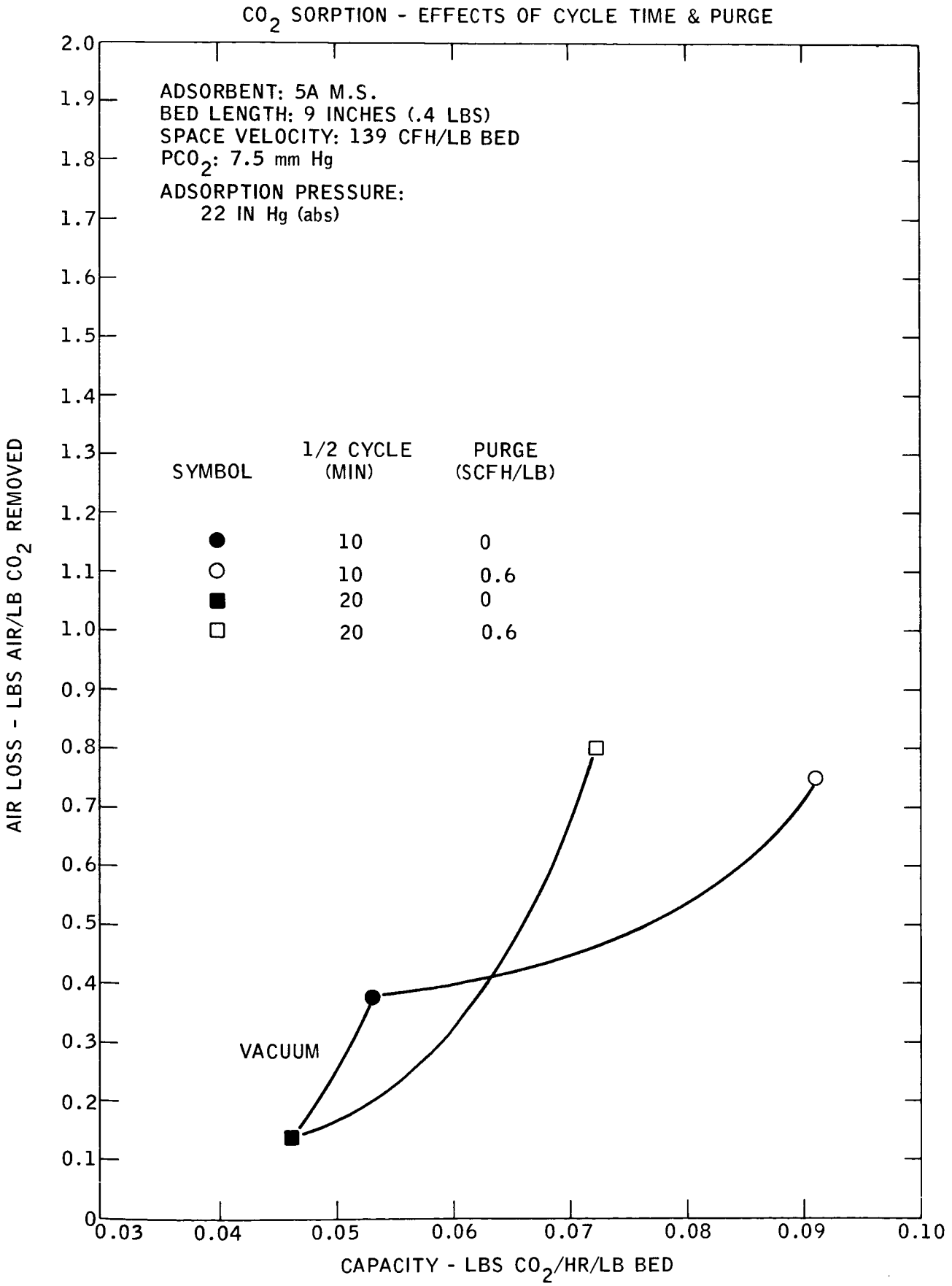
CO_2 SORPTION - EFFECTS OF CYCLE TIME & PURGE
ADSORBENT: 5A M.S.
BED LENGTH: 9 INCHES (.4 LBS)
SPACE VELOCITY: 139 CFH/LB BED
PCO_2: 7.5 mm Hg
ADSORPTION PRESSURE:
22 IN Hg (abs)
SYMBOL
1/2 CYCLE (MIN)
PURGE (SCFH/LB)
10 0
10 0.6
20 0
20 0.6
VACUUM
AIR LOSS - LBS AIR/LB CO_2 REMOVED
CAPACITY - LBS CO_2/HR/LB BED
2.0
1.9
1.8
1.7
1.6
1.5
1.4
1.3
1.2
1.1
1.0
0.9
0.8
0.7
0.6
0.5
0.4
0.3
0.2
0.1
0
0.03
0.04
0.05
0.06
0.07
0.08
0.09
0.10

5.4.2. Effect of PED Purge

The effects of using a PED purge to improve vacuum desorption can be seen from the data presented in Figure 33. The solid symbols represent capacities and air loss for a vacuum system while the open symbols are the corresponding data with PED purge.

In general, the increase in capacity obtained with PED purge was greater than that obtained with product purge below air loss ratio of about .6 lbs air/lb CO_2. The most significant difference between the two purge techniques, however, showed up at the very low air loss ratios most important for long space missions. Thus, at the higher carbon dioxide concentration, PED provided a capacity increase of over 40% compared to conventional vacuum desorption (i.e., .065 W/Hr/W versus .045 W/Hr/W) at an air loss ratio of 0.15 lbs air/lb CO_2. From the shapes of the curves, it would appear that similar increases in capacity would be obtained at longer cycle times where even less air would be lost. Additional improvements might also be made by increasing the size of the purge cylinders. The limiting factor in doing this, is that increasing the PED cylinder size adds fixed weight and volume to the system. In a final design this would have to be measured against the accompanying reduction in bed size which could result from the improved capacity accompanying PED purge. Data now available, however, are not sufficient to predict what this relationship is on a quantitative basis.

5.4.3. Effect of Bed Length

The effect of changing the bed length on the value of purge desorption was determined by reducing the length of the adsorbent cannisters from nine to five inches at constant conditions of cycle time, space velocity, and carbon dioxide partial pressure. The results obtained are shown in Figures 34 and 35 for the two carbon dioxide partial pressures.

In all cases, both with and without purge, the results obtained with the shorter bed were better than with the longer bed. Capacities were as much as fifty percent higher with the 5-inch bed, and this was true for both the cases with and without purge.

Although it was known that shorter beds were preferred for conventional vacuum desorption, there was a question of whether or not this would be the case for purge aided regeneration. In vacuum desorption, the result of decreasing bed length is to reduce bed pressure drop and thus provide a lower, more iniform vacuum for more effective desorption of the bed. This is also true for purge aided desorption except that in this case, larger beds provide a greater opportunity for the purge gas to desorb and equilibrate with the carbon dioxide on the molecular sieve. There are thus two opposing factors in purge aided desorption, but as the data indicate, it is the improved vacuum that is controlling. Therefore, short, low pressure-drop adsorbent beds are preferred regardless of whether sorbent regeneration is accomplished with the aid of a purge, or conventionally by vacuum desorption.

Figure 33

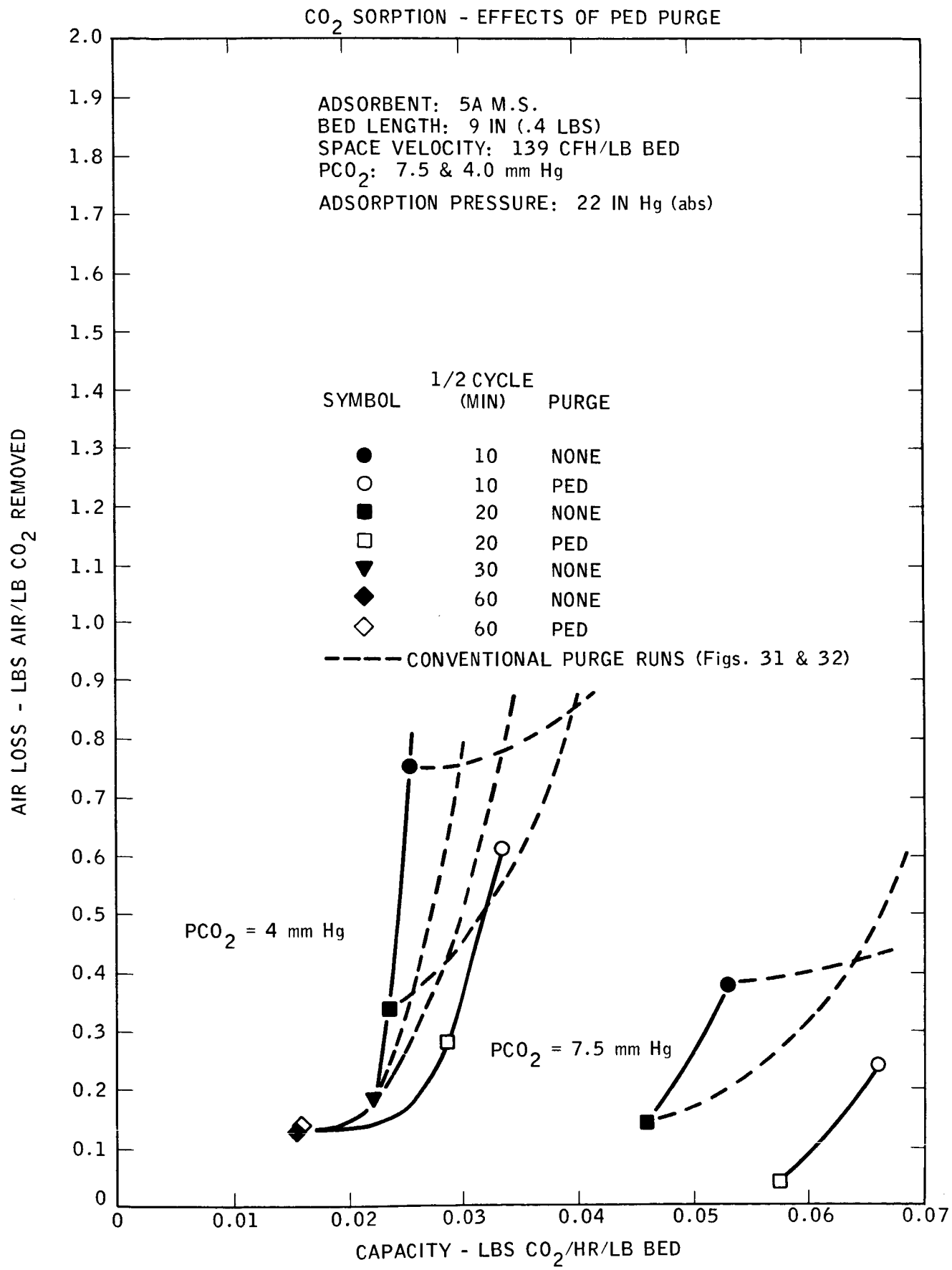
CO_2 SORPTION - EFFECTS OF PED PURGE
ADSORBENT: 5A M.S.
BED LENGTH: 9 IN (.4 LBS)
SPACE VELOCITY: 139 CFH/LB BED
PCO_2: 7.5 & 4.0 mm Hg
ADSORPTION PRESSURE: 22 IN Hg (abs)
SYMBOL
1/2 CYCLE (MIN)
PURGE
10 NONE
10 PED
20 NONE
20 PED
30 NONE
60 NONE
60 PED
CONVENTIONAL PURGE RUNS (Figs. 31 & 32)
PCO_2 = 4 mm Hg
PCO_2 = 7.5 mm Hg
AIR LOSS - LBS AIR/LB CO_2 REMOVED
CAPACITY - LBS CO_2/HR/LB BED
2.0
1.9
1.8
1.7
1.6
1.5
1.4
1.3
1.2
1.1
1.0
0.9
0.8
0.7
0.6
0.5
0.4
0.3
0.2
0.1
0
0.01
0.02
0.03
0.04
0.05
0.06
0.07

Figure 34

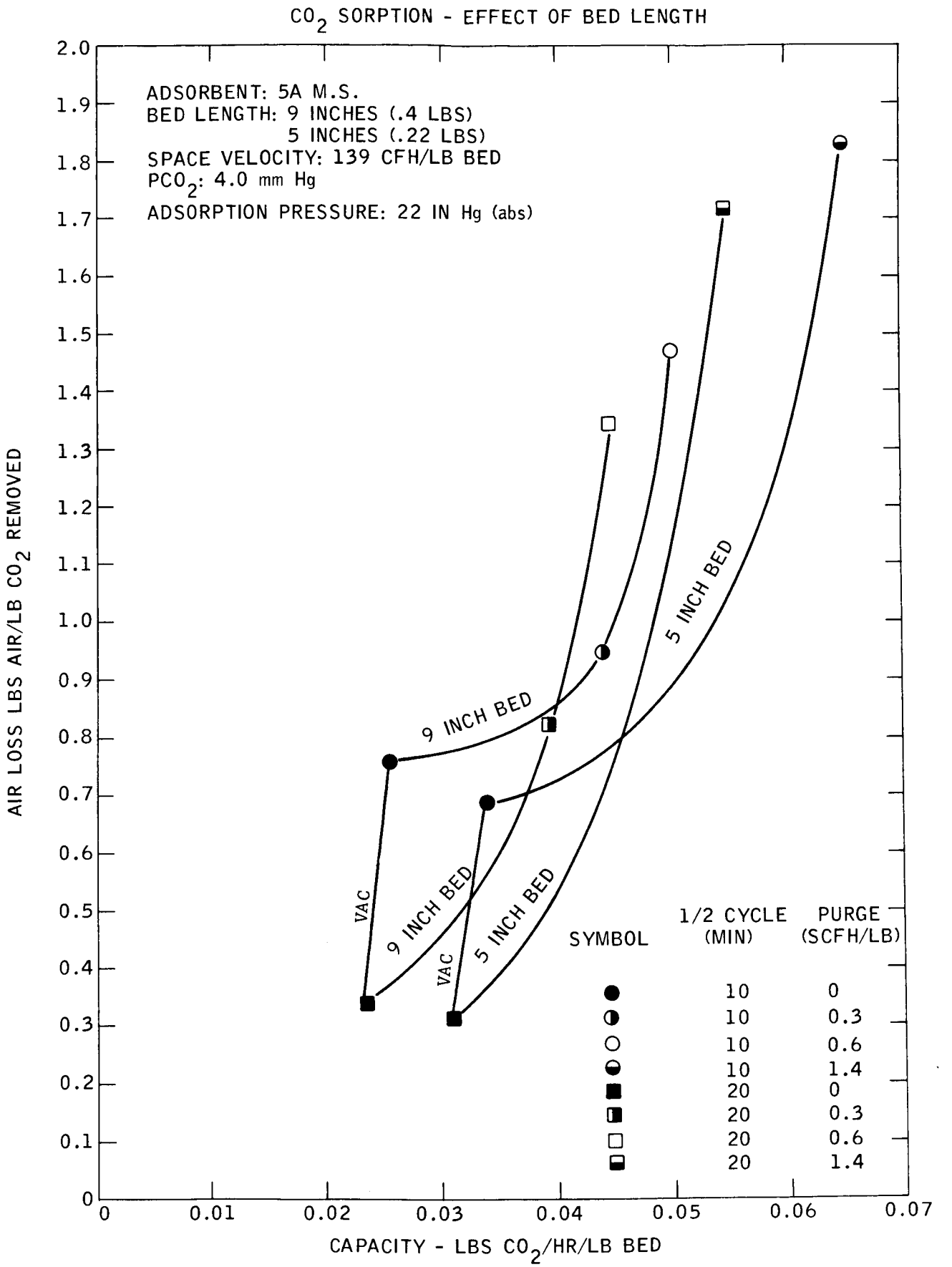
CO_2 SORPTION - EFFECT OF BED LENGTH
ADSORBENT: 5A M.S.
BED LENGTH: 9 INCHES (.4 LBS)
5 INCHES (.22 LBS)
SPACE VELOCITY: 139 CFH/LB BED
PCO_2: 4.0 mm Hg
ADSORPTION PRESSURE: 22 IN Hg (abs)
AIR LOSS LBS AIR/LB CO_2 REMOVED
CAPACITY - LBS CO_2/HR/LB BED
9 INCH BED
5 INCH BED
VAC
SYMBOL
1/2 CYCLE (MIN)
PURGE (SCFH/LB)
10 0
10 0.3
10 0.6
10 1.4
20 0
20 0.3
20 0.6
20 1.4

Figure 35

CO_2 SORPTION - EFFECT OF BED LENGTH

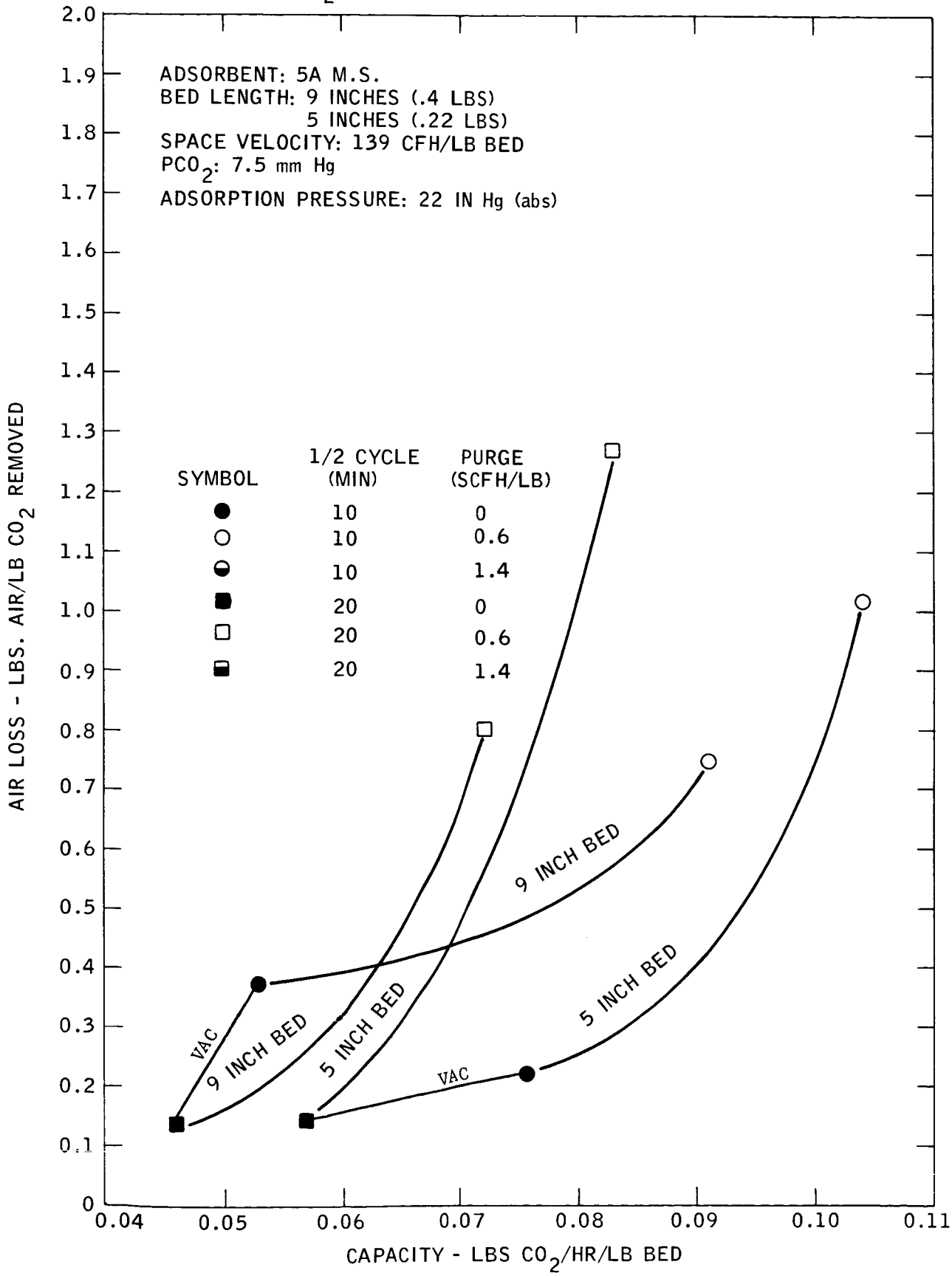

5.4.4. Effect of Changing Space Velocity

Space velocity was studied as the fourth variable in the program to see what effect it would have on the relative value of purge. Three levels of space velocity were investigated 104, 139 and 173 CFH/lb bed for each of two carbon dioxide partial pressures. The results of this part of the program are shown in Figures 36 and 37. As can be noted, the actual effect of changing space velocity on the capacity/air loss relationship wasn't clearly defined in these experiments for either the vacuum or the purge desorbed runs.

It was expected that an increase in space velocity would improve the capacity of the adsorbent up to a point. This improvement would be the result of two factors. First, the increase in gas velocity accompanying an increase in space velocity should improve the mass transfer rate of carbon dioxide from the gas to the adsorbent. Consequently, there should be a closer approach to the maximum capacity possible. Second, an increase in space velocity at constant cycle time means that more carbon dioxide passes through the adsorbing bed each cycle. No part of the bed should thus lack for its full compliment of carbon dioxide. Increasing the adsorption cycle time at constant space velocity should produce the same results. At low space velocities, or cycle times on the other hand, there might not be enough carbon dioxide passing through the bed to saturate all the adsorbent completely. The improvement in capacity resulting from increasing space velocity or cycle time would not be expected to last indefinitely since once the adsorbent had been saturated, any additional carbon dioxide passing over the sieve would have no effect.

Based on the above reasoning, it would be expected that increasing the space velocities would give an improved capacity/air loss relationship up to a point, and that the magnitude of the improvement would decrease with increasing cycle time. In Figure 37, both these effects can clearly be seen. For the forty-minute cycles, there is little effect of increasing space velocity. In contrast, the capacity continues to improve with increasing space velocity in the shorter, twenty-minute cycles. In Figure 36, on the other hand, the results are no longer consistent. For the twenty-minute cycles, the data at the highest space velocity fall between the corresponding data at the low and median value, while for the forty-minute cycles, the low space velocity falls between the other two. What is probably being reflected in Figure 36 are the effects of small differences in the actual carbon dioxide partial pressures at different space velocities since changing space velocity required changing both the air and carbon dioxide flow rates.

Within this mixed picture, one pertinent point still emerges, however. On the average, the effect of changing space velocity in the purge desorbed runs is about the same as changing space velocity in those that were vacuum desorbed in a conventional manner. Thus, there is no more advantage to increasing or decreasing the space velocity in purge desorbed systems than there is in a vacuum regenerated system.

Figure 36

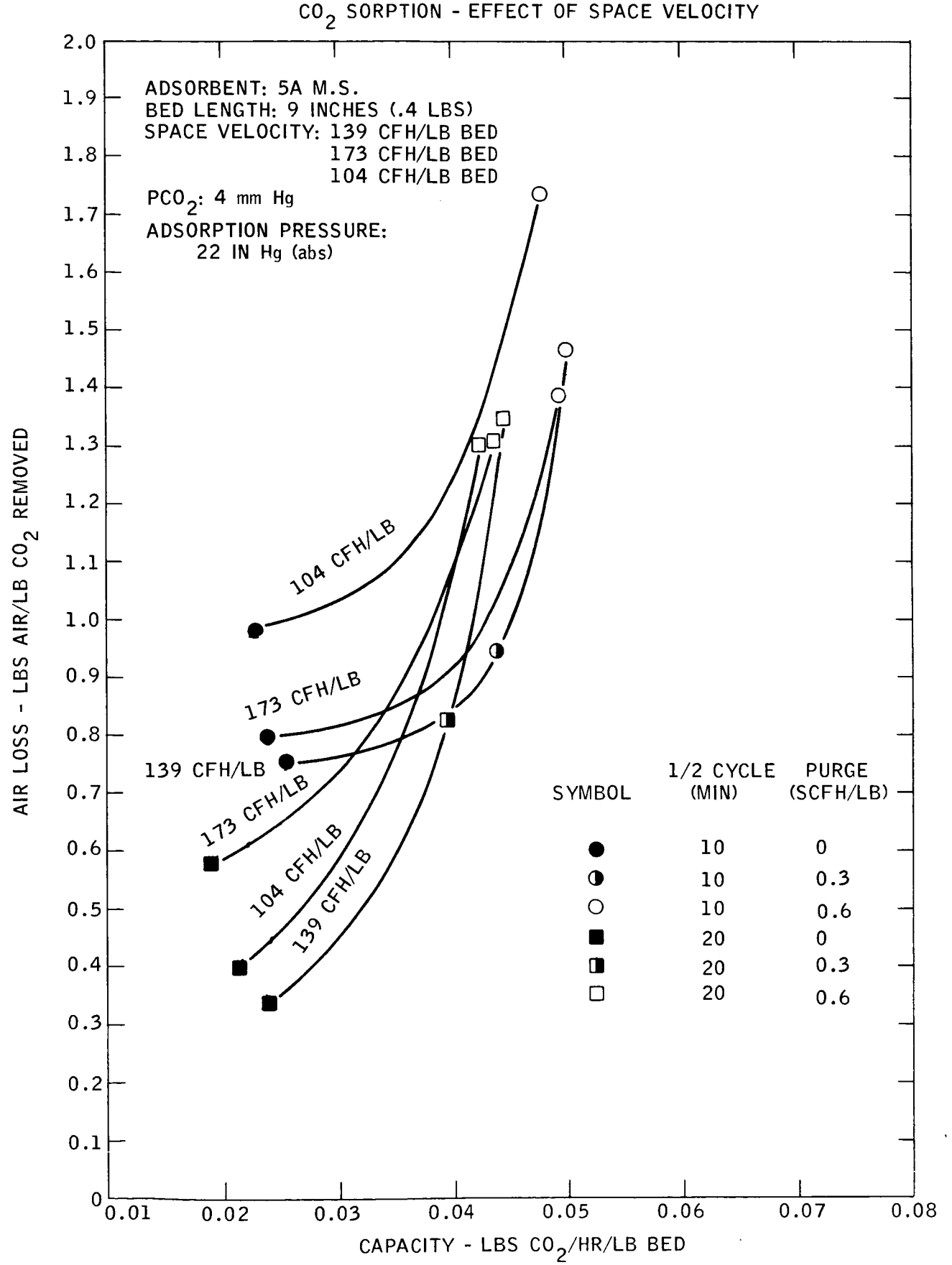
CO_2 SORPTION - EFFECT OF SPACE VELOCITY
ADSORBENT: 5A M.S.
BED LENGTH: 9 INCHES (.4 LBS)
SPACE VELOCITY: 139 CFH/LB BED
173 CFH/LB BED
104 CFH/LB BED
PCO_2: 4 mm Hg
ADSORPTION PRESSURE:
22 IN Hg (abs)
104 CFH/LB
173 CFH/LB
139 CFH/LB
173 CFH/LB
104 CFH/LB
139 CFH/LB
SYMBOL
1/2 CYCLE (MIN)
PURGE (SCFH/LB)
10 0
10 0.3
10 0.6
20 0
20 0.3
20 0.6
AIR LOSS - LBS AIR/LB CO_2 REMOVED
CAPACITY - LBS CO_2/HR/LB BED
2.0
1.9
1.8
1.7
1.6
1.5
1.4
1.3
1.2
1.1
1.0
0.9
0.8
0.7
0.6
0.5
0.4
0.3
0.2
0.1
0
0.01
0.02
0.03
0.04
0.05
0.06
0.07
0.08

Figure 37

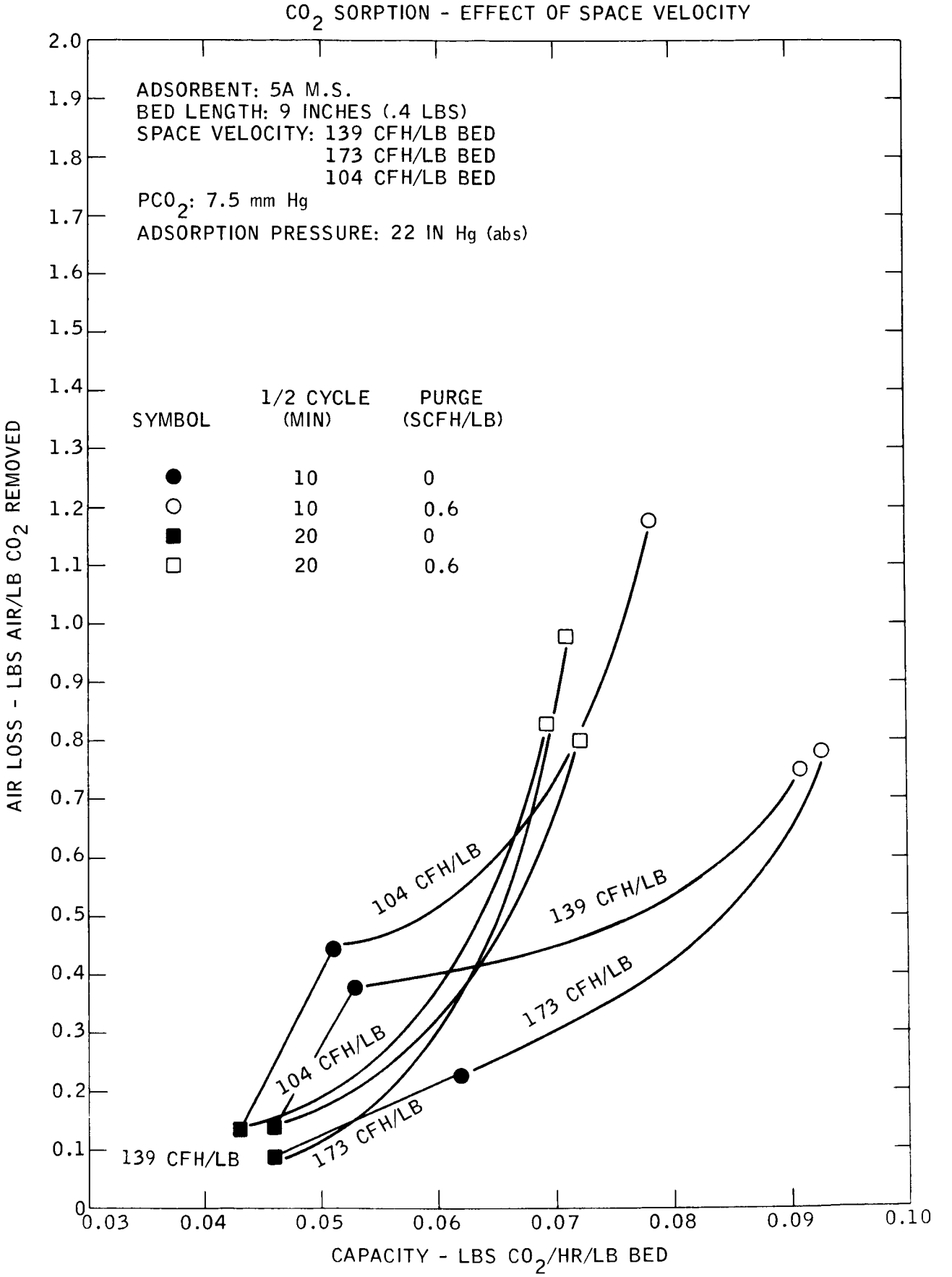
CO_2 SORPTION - EFFECT OF SPACE VELOCITY
ADSORBENT: 5A M.S.
BED LENGTH: 9 INCHES (.4 LBS)
SPACE VELOCITY: 139 CFH/LB BED
173 CFH/LB BED
104 CFH/LB BED
PCO_2: 7.5 mm Hg
ADSORPTION PRESSURE: 22 IN Hg (abs)
SYMBOL
1/2 CYCLE (MIN)
PURGE (SCFH/LB)
10 0
10 0.6
20 0
20 0.6
104 CFH/LB
139 CFH/LB
173 CFH/LB
104 CFH/LB
139 CFH/LB
173 CFH/LB
AIR LOSS - LBS AIR/LB CO_2 REMOVED
CAPACITY - LBS CO_2/HR/LB BED
0
0.1
0.2
0.3
0.4
0.5
0.6
0.7
0.8
0.9
1.0
1.1
1.2
1.3
1.4
1.5
1.6
1.7
1.8
1.9
2.0
0.03
0.04
0.05
0.06
0.07
0.08
0.09
0.10

5.4.5. Comparison of 4A and 5A Molecular Sieves

A comparison of 4A and 5A molecular sieves concluded this phase of the experimental program on the use of purge in the carbon dioxide sorption system. This comparison was prompted by a desire to decrease the amount of air lost when regenerating the sieve (i.e., improve the capacity/air loss relationship). Apart from purge, such air loss results from air contained in the voids of the sorbent bed and from oxygen and nitrogen adsorbed by the sieve. Experimental data indicated that it was the adsorbed air which contributed most to the total loss of air in vacuum desorbed runs.(a) The 4A sieve was chosen because its capacity for oxygen and nitrogen is less than that of the 5A sieve. Reference to Figure 38 shows that in the region of interest (5-10 psia), the 4A sieve has about 25% less equilibrium capacity for oxygen and about 35% less capacity for nitrogen than does 5A sieve. On the other hand, the capacities of the two sieves for carbon dioxide are about the same. (At a carbon dioxide partial pressure of 4 mm Hg, both sieves have an equilibrium capacity of about 7 wt.%. At a partial pressure of 7.5 mm, the carbon dioxide capacity of the 4A sieve is 8.2 wt.% while that of the 5A sieve is 8.7 wt.%).

To determine if the difference in the oxygen/nitrogen capacities would be reflected in a cyclic operation, the desorbates from comparable 4A and 5A vacuum desorbed runs were analyzed by mass spectroscopy. The results of these analyses are shown in Table 14.

Table 14

Analysis of Desorbates by Mass Spectroscopy

Half Cycle Time, Min.	Adsorbent	Mole Ratio N_2/O_2 in Desorbate
10	5A MS	8.3
10	4A MS	6.7
20	5A MS	7.3
20	4A MS	6.3
		3.8 in air

Although the data shows that 4A sieve adsorbs less air than 5A sieve and should therefore be preferred in the cyclic process, the actual capacity/air loss results did not always substantiate this. Based on the data shown in Figures 39 and 40, the following mixed picture emerges.

- At low CO_2 partial pressures, Figure 39, the 4A sieve is preferred. Less air will be lost at equivalent capacities with this adsorbent.

(a) This can be verified using the desorbate (void gas and adsorbed gas) compositions shown in Table 14 for the 5A sieve.

Figure 38

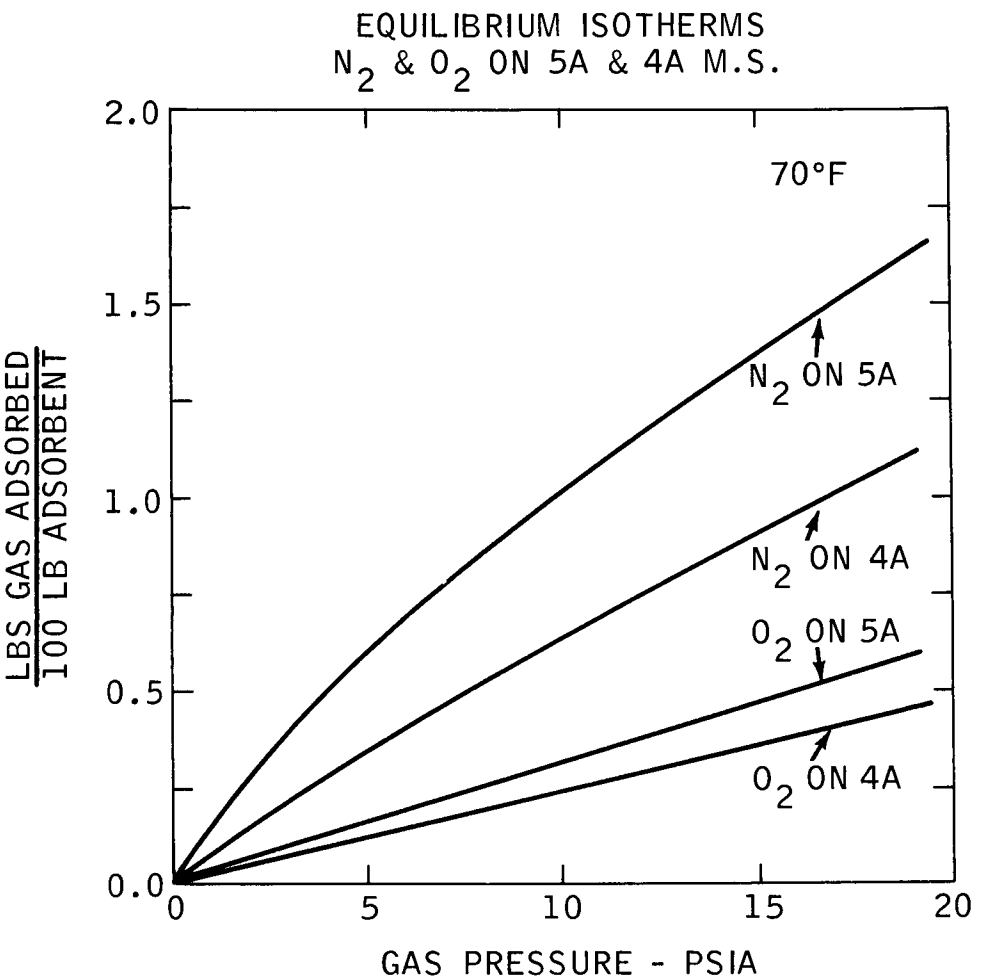
EQUILIBRIUM ISOTHERMS
N2 & O2 ON 5A & 4A M.S.
LBS GAS ADSORBED / 100 LB ADSORBENT
2.0
1.5
1.0
0.5
0.0
0
5
10
15
20
GAS PRESSURE - PSIA
70°F
N2 ON 5A
N2 ON 4A
O2 ON 5A
O2 ON 4A

Figure 39

CO_2 SORPTION - EFFECT OF ADSORBENT

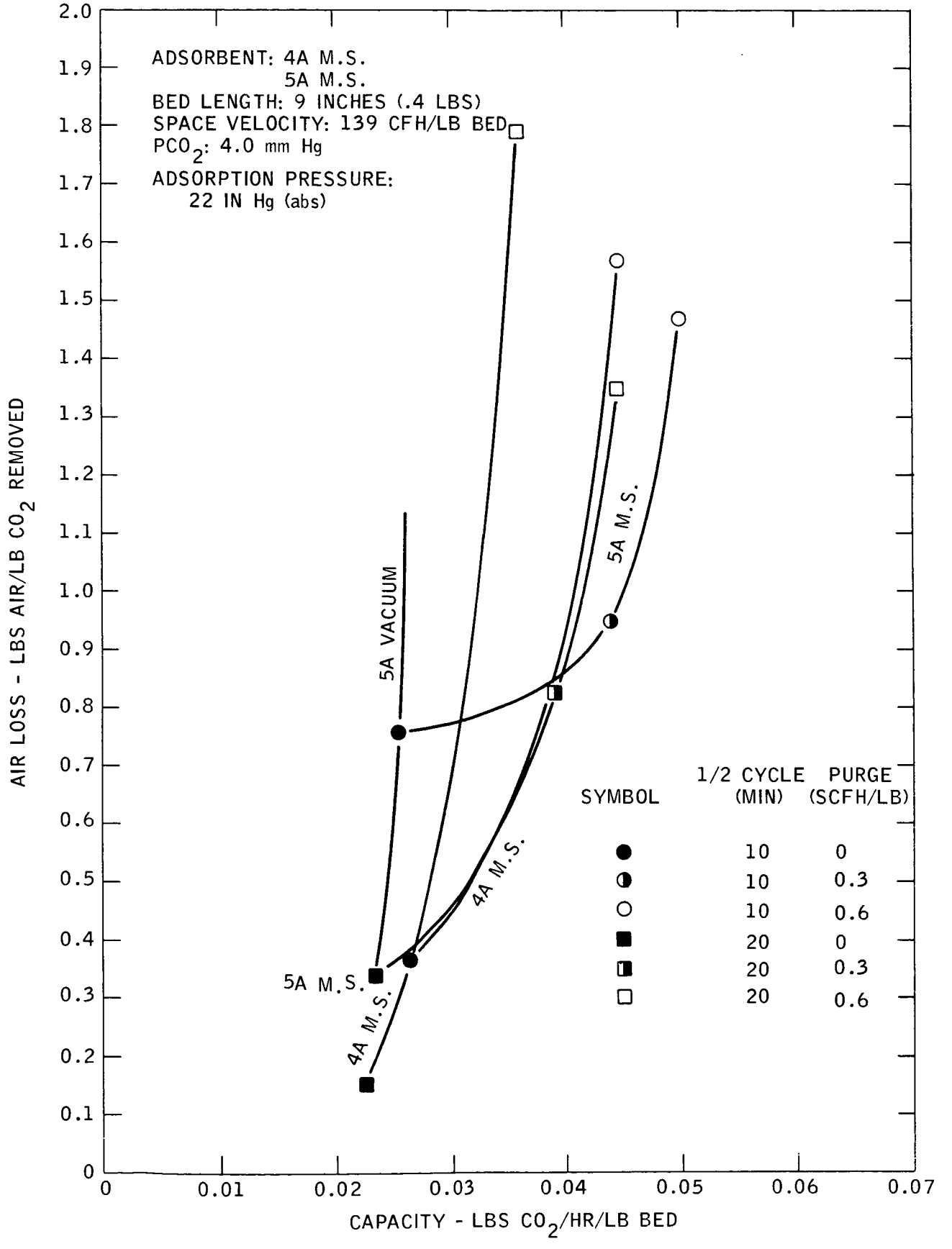

Figure 40

CO_2 SORPTION - EFFECT OF ADSORBENT

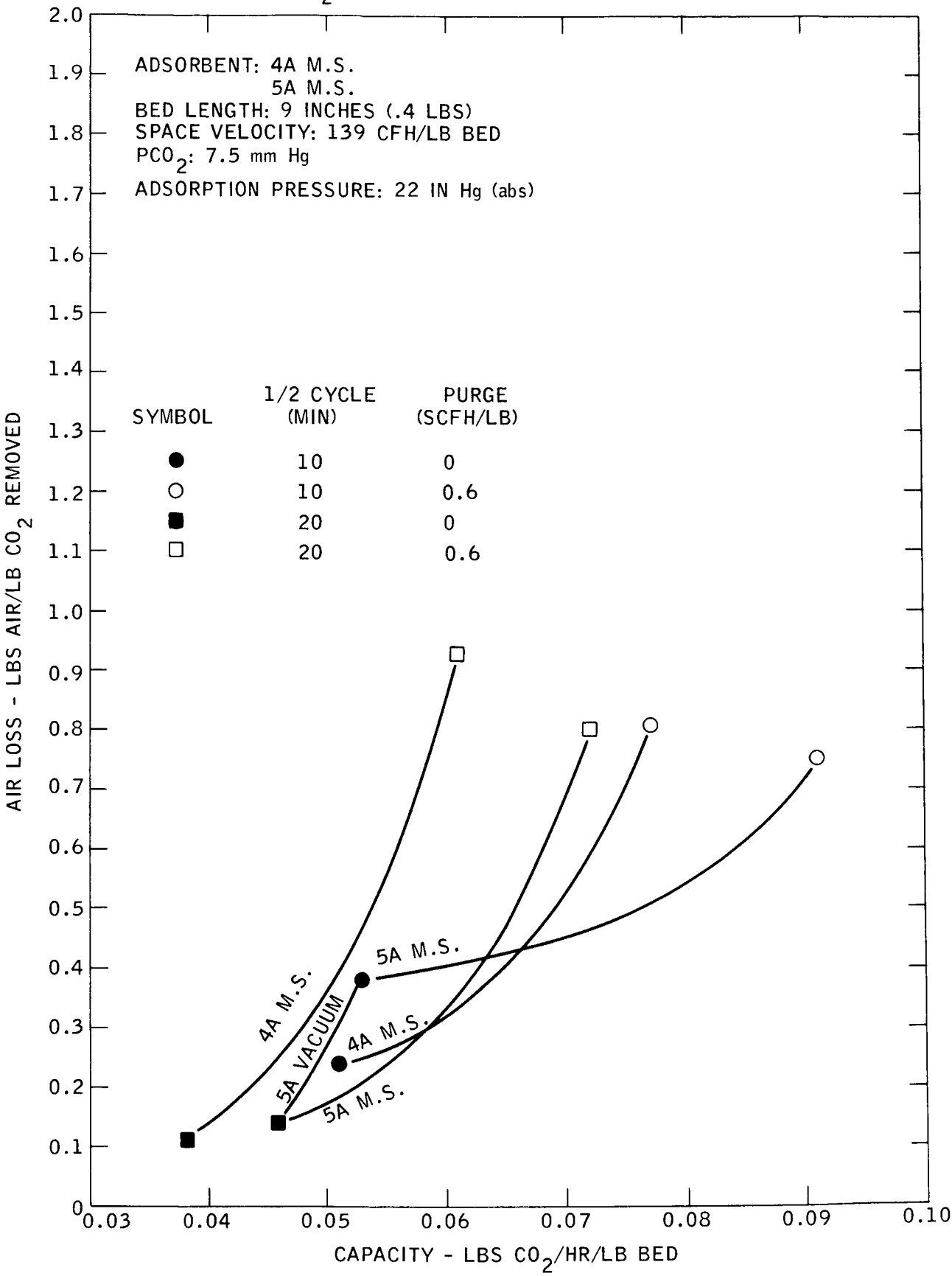

- At high CO_2 partial pressures, Figure 40, the somewhat higher CO_2 capacity of the 5A sieve provides a more favorable capacity/air-loss relationship for long cycle (i.e., 20 minutes or more half cycle times).

- For short cycles, there are more desorptions/hour. Consequently, the reduction in the amount of adsorbed air which is lost during the desorption becomes more important than the increase in capacity obtained with the 5A sieve. Therefore, 4A sieve is preferred in this situation.

- Purge tends to improve the capacity/air-loss relationship for both the 4A and 5A sieves.

On the basis of these results, it can be concluded that the preferred adsorbent depends primarily on the carbon dioxide pressure, and cycle time. Since long cycle times will be preferred for reducing air loss, 4A adsorbent appears best when operating at low carbon dioxide pressures ($\backsim$4 mm Hg or less), while 5A sieve will be preferred when operating at the higher carbon dioxide pressures.

5.5. Use of Experimental Data For Designing CO_2 Sorption Systems

The data presented in Figures 31 through 39 of section 5.5. provide all the information required to specify a system design. The examples shown below serve to indicate how the data would be used to design specific systems for 3 man missions. The valve of product and PED purge should become clear from these examples. However, it is important to again emphasize that because of equipment limitations, these results may not appear attractive on an absolute basis.

3 Man CO_2 Sorption System

CO_2 production rate	2.4 lbs. CO_2/man/day
CO_2 partial pressure	7.5 mm Hg in pre-dried air
Adsorbent	5A molecular sieve

Case I: Maximum air loss rate set at .5 lbs air/man/day

$$\frac{.5 \text{ lbs. air/man/day}}{2.4 \text{ lbs. } CO_2\text{/man/day}} = \frac{.208 \text{ lbs. air lost}}{\text{lb. } CO_2}$$

2.4 lbs. CO_2/man day x 3 men/24 hrs/day = .3 lbs CO_2/hr

Based on data from Figures 32 and 33 for a 9" long bed, a 139 CFH/lb space velocity, and a CO_2 partial pressure of 7.5 mm Hg., the following table can be constructed.

Type of Cycle	Capacity @ .208 lbs air lost / lb CO_2	Half Cycle Time, Min
Vacuum Desorption (Fig. 32)	.048 W/Hr/W	~ 18
Product Purge (Fig. 32)	.054 "	20
PED Purge (Fig. 33)	.065 "	12

Type of Cycle	lbs. adsorbent / bed	Required Gas Flow Rate CFM
Vacuum Desorption	.3/.048 = 6.25	x 139/60 = 14.5
Product Purge	.3/.054 = 5.55	" = 12.9
PED Purge	.3/.065 = 4.61	" = 10.7

For the product purge run (Figure 32) required purge $>$ 0 SCFH/lb but $<$ .60 SCFH/lb. At a capacity of .055 W/Hr/W, we are about 1/6th of the way between 0 and .60 SCFH/lb or about .1 SCFH/lb.

Required Purge is .1 x 5.55 = .555 SCFH

For the PED purge, cylinder size was .065 ft^3/lb x 4.61 lbs = .3 ft^3

Case II: lbs. adsorbent/bed specified at 5 lbs.

Gas Flow Rate: $5 \times \frac{139}{60} = 11.6$ CFM

Required Capacity = $\frac{.3 \text{ lbs } CO_2/\text{hr}}{5 \text{ lbs.}} = .06$ W/Hr/W

Type of Cycle	Air Loss Rate lbs. air/lb. CO_2		Lb. Air Lost / Day	Half Cycle Time, Min.
Vacuum Desorption (Fig. 32)	$>$ .4	x 7.2	$>$ 2.9	$<$ 10
Product Purge (Fig. 32)	.4		2.9	20
PED Purge (Fig. 33)	.09		.65	18

For the product purge run, purge is about 20% of the way between 0 and .6 SCFH/lb or about .2 SCFH/lb

Required purge is therefore .2 x 5 lbs. = 1.0 SCFH

For the PED purge, cylinder size will be .065 ft^3/lb x 5 lbs = .33 ft^3

5.6. CONCLUSIONS AND RECOMMENDATIONS

The results obtained in this part of the program confirm that purge techniques improve the capacity (i.e., capacity/air loss relationship) of the carbon dioxide control system relative to that obtained with conventional vacuum desorption. For long space missions, PED would be the preferred purge method since it provides the lowest air loss rates possible. The full extent of the improvement which PED purge could make in a spacecraft system is yet to be determined. The experiments with PED purge were made with the 9" long sorbent beds. Based on the increased capacity obtained in the 5" beds for the product purge experiments, the corresponding PED results should also be improved through the use of snorter beds. Furthermore, from the results obtained with the product purge technique, it would appear that 4A molecular sieve would be preferred for PED cycles when operating at low carbon dioxide pressures in the range of 4 mm Hg.

Although, a relative improvement was obtained in these tests, it is important to emphasize that the full benefit that may be derived from purge-aided desorption could not be demonstrated because of equipment limitations. It is therefore recommended that additional studies be made with equipment designed to minimize these limitations. In any future program, emphasis should be given to PED purge techniques. A complete evaluation of PED purge should be made with different bed configurations, space velocities, carbon dioxide partial pressures and sorbents. Increase in capacity should be measured against increase in weight (volume) associated with the PED cylinders. When such data have been obtained, the full improvement resulting from purge aided desorption could then be evaluated.

APPENDIX 1

Purge to Feed Requirements in Heatless Adsorption

In any Heatless Adsorption process the use of a volumetric purge to feed ratio of at least 1:1 is a necessary condition for insuring containment of the mass front within the adsorbent beds. Consider the situation shown in the diagram below (Figure A1-1)

Figure A1-1

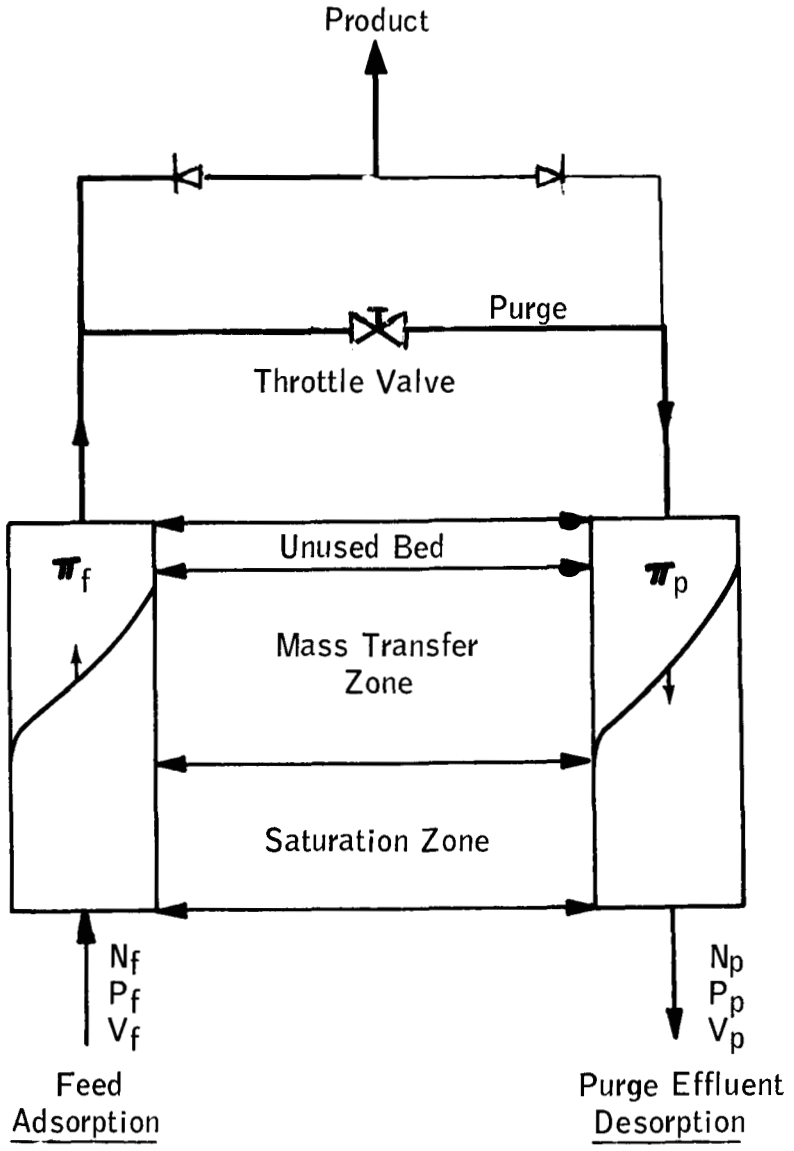

During adsorption, the front end of the bed equilibrates with the adsorbate at its partial pressure, P_f. The product of the adsorbing bed leaves much less concentrated in the adsorbable component and a portion of this lean adsorbate will be transferred from the solid to the gas stream and the partial pressure of the adsorbate in the purge effluent, P_p, will tend to re-equilibrate with the bottom end of the bed. Obviously it would require an infinitely large saturation zone to insure complete re-equilibration but for all practical purposes it can be assumed that some finite length of wet bed exists so that:

$$P_p \lesssim P_f$$

Providing breakthrough does not occur, and assuming the behavior of the gaseous components can be represented by the ideal gas law, an expression can be written which gives the total amount of adsorbate removed per unit cycle:

$$\frac{\text{Moles Adsorbed}}{\text{Cycle}} = \frac{P_f V_f}{RT}$$

Similarly, the amount of adsorbate desorbed by the purge is given by:

$$\frac{\text{Moles Desorbed}}{\text{Cycle}} = \frac{P_p V_p}{RT}$$

At steady state, the moles adsorbed per cycle must equal the moles desorbed per cycle or:

$$\frac{P_p V_p}{RT} = \frac{P_f V_f}{RT}$$

Therefore, if adsorption and desorption temperatures are about the same, $V_p = V_f$ and the required purge to feed ratio, defined as $V_p{:}V_f$ will equal 1:1.

The use of a 1:1 purge to feed ratio is, however, a limiting case. If a purge to feed ratio greater than 1:1 is used (i.e., $V_p > V_f$) then P_p can be less than P_f and still have $\frac{P_p V_p}{RT} = \frac{P_f V_f}{RT}$. This means that at purge to feed ratios above 1:1 complete resaturation of the purge is not required and so a smaller saturation zone can be tolerated and smaller beds can be used.

List of Symbols

P_p, P_f	=	partial pressure in purge effluent and feed respectively
π_p, π_f	=	total desorption and total adsorption pressure respectively
V_p, V_f	=	actual volumes of purge and feed respectively
N_p, N_f	=	moles of purge and moles of feed respectively
R	=	gas constant
T	=	absolute gas temperatures

APPENDIX 2

Reasons For Reporting Moisture Content of Dried Gas In PPM

The amount of moisture remaining in the "dry" effluent from the desiccant beds can be expressed in several different ways. Throughout most of this report, moisture content has beed expressed in terms of PPM (Parts Per Million). This is defined by equation (1):

$$\text{PPM } H_2O \text{ in gas} = (P_{H_2O}\ P_{atm}) \times 10^6 \qquad (1)$$

P_{H2O} = partial pressure H_2O in gas

P_{atm} = atmospheric pressure

To compute the partial pressure of water remaining in the effluent from the drying beds, one then simply multiplies:

$$\text{PPM} \times P_{atm} \times 10^6 = P_{H_2O} \qquad (2)$$

It is this partial pressure that determines the amount of moisture carried into the molecular sieve beds, since:

Moles H_2O/Hr (into molecular sieve beds)

$$= kP_{H_2O}Vp \qquad (3)$$

k = proportionality constant ($\frac{1}{RT}$ for ideal gas)

V_p = actual volumetric flow rate (e.g., CFH) as operating pressure P

P = actual operating system pressure

By rearrangement:

Moles H_2O/Hr (into molecular sieve bed)

$$= k\ (\text{PPM})\ (P_{atm})\ (10^6)\ (V_p) \qquad (4)$$

$$= k'\ (\text{PPM})\ (V_p) \qquad (5)$$

where $k' = k\ (P_{atm})\ (10^6)$

Equation (5) shows that the amount of moisture passing into the zeolite beds depends only on the PPM of H_2O in the gas and the actual gas flow rate at operating pressure. It does not depend on the actual operating pressure. Therefore, the fact that the experiments reported here were all conducted at a total pressure of about 11 psia is not important and the results obtained can be translated directly to other systems operating at different total pressures provided that:

(1) Actual gas flow rates through the system in cubic feet per pound of bed are maintained constant.

(2) Inlet dew points are the same (i.e., H_2O partial pressures are equal)

(3) Bed length, purge to feed ratios and adsorbent are the same.

APPENDIX 3

Results of Heatless Drying Runs

Desiccant: Davison's Grade 40 Silica Gel, 6-12 Mesh

Run No.	Space Velocity (CFH/Lb Bed)	P/F (Vol/Vol)	1/2 Cycle Time (Seconds)	Temp (°F)	Bed Length (Inches)	Date Run Started	Cycle No.	Effluent H_2O Conc. (PPM)	Cycle No.	Effluent H_2O Conc. (PPM)
1	156	1.1	30	77	4.5	3-30-67	240	1.50	2264	74.90
							360	1.87	2384	74.90
							475	1.50	2504	71.16
							1440	6.37	2624	71.16
							1680	9.74	2744	63.67
							1800	23.97	3824	74.90
							1910	27.71	4044	72.65
							1911	74.90	4164	67.41
							2031	74.90	4284	59.92
							2051	37.45	5144	56.18
							2171	37.45	5564	52.43
							2262	35.20		
2	156	1.2	30	77	4.5	4-10-65	240	3.00	3120	7.87
							360	2.25	3240	8.01
							480	3.00	3630	7.87
							1560	3.37	4440	6.97
							1680	3.60	4560	6.74
							1800	3.67	4680	6.97
							1920	3.75	4800	6.44
							2300	5.39	5760	6.14
							2880	6.74	5880	6.14
							3000	8.24		
3	93.8	1.1	30	77	4.5	4-24-67	180	2.55	4622	20.97
							300	2.77	4742	22.47
							420	2.62	5702	27.71
							1380	3.15	5822	30.71
							1740	3.67	5942	35.95
							1860	4.72	6062	36.70
							2820	11.54	6182	31.46
							2940	11.76	7232	28.46
							3060	13.63	7277	28.46
							3180	15.35	7382	28.46
							3300	16.18	7562	37.45
							4262	20.97	7818	29.21
							4382	20.60	8582	23.22
							4502	19.85		

Run No.	Space Velocity (CFH/Lb Bed)	P/F (Vol/Vol)	1/2 Cycle Time (Seconds)	Temp (°F)	Bed Length (Inches)	Date Run Started	Cycle No.	Effluent H_2O Conc. (PPM)	Cycle No.	Effluent H_2O Conc. (PPM)
4	93.8	1.1	60	77	4.5	5-1-67	60	2.47	1650	3.0
							120	1.50	2130	11.24
							180	2.25	2190	11.24
							210	2.25	2250	8.99
							690	1.12	2310	10.49
							750	1.50	2370	11.24
							810	1.87	2850	17.23
							870	1.87	2910	22.47
							930	1.87	2970	29.96
							1410	2.02	3030	29.96
							1470	2.02	3090	30.71
							1530	2.62	3623	26.96
							1590	2.62	4343	32.96
5	93.8	1.2	60	77	415	5-8-67	60	.749	1710	.749
							120	.749	2160	.90
							180	.90	2280	.82
							240	.749	2340	.97
							720	.749	2400	.90
							780	.90	2880	.97
							840	.97	2940	1.05
							900	.749	3000	1.12
							960	.82	3060	1.12
							1470	.749	3120	1.12
							1530	.749	3720	1.20
							1590	.749	4410	1.50
							1650	.749		
6	156	1.2	60	77	4.5	5-15-67	1	.749	1680	7.12
							60	.749	2160	8.01
							120	.749	2220	8.39
							180	.749	2280	8.31
							240	.749	2340	8.84
							720	.749	2400	9.74
							780	.749	2880	7.49
							840	.749	2940	8.39
							900		3000	9.14
							960	1.50	3060	
							1440	6.14	3120	
							1500	6.52	3700	7.19
							1560	6.67	4400	8.99
							1620	6.89		

Run No.	Space Velocity (CFH/Lb Bed)	P/F Vol/Vol)	1/2 Cycle Time (Seconds)	Temp (°F)	Bed Inches (Inches)	Date Run Started	Cycle No.	Effluent H_2O Conc. (PPM)	Cycle No.	Effluent H_2O Conc. (PPM)
6-R1	156	1.2	60	77	4.5	5-15-67	90	4.0	1770	13.5
							600	2.5	2010	15.5
							660	3.0	2280	16.0
							750	3.3	2400	16.0
							1290	10.5	4200	15.0
							1350	11.0	4470	15.0
							1440	11.5	4830	16.5
							1500	13.0	4950	17.5
									5100	17.0
									5400	17.0
6-R2	156	1.2	60	77	4.5	5-15-67	0	5.3	840	9.6
							120	5.3	900	10.9
							180	5.6	960	12.4
							300	4.9	1020	13.5
							480	5.3	1050	15.0
							600	6.4	1200	16.2
							660	7.1	1260	18.0
							720	7.5	1320	18.7
6-R3	156	1.2	60	77	4.5	9-21-67	0	15.9		
							40	14.4		
							900	8.4	2950	6.6
							1020	10.4	3040	8.1
							1060	10.6	3130	10.4
							1480	7.5	3190	12.2
							1510	14.9	3670	8.9
							2230	9.8	3790	9.0
7	156	1.1	60	77		5-22-67	0	1.5		
							600	3.0		
							720	8.6		
							840	16.2		
							930	30		
							1470	76.5		
							1590	.91		
							1710	100		
							2190	119		
							2340	108		
							2430	131		
							2910	141		
							3030	185		
							3150	162		

Run No.	Space Velocity (CFH/Lb Bed)	P/F (Vol/Vol)	1/2 Cycle Time (Seconds)	Temp (°F)	Bed Length (Inches)	Date Run Started	Cycle No.	Effluent H_2O Conc. (PPM)	Cycle No.	Effluent H_2O Conc. (PPM)
7-R1	156	1.1	60	77	4.5	9-11-67	0	8.54	2310	423.19
							60	11.24	2820	430.68
							105	6.59	2850	471.87
							120	6.44	2880	464.38
							150	6.14	2910	449.40
							630	53.35	2940	464.38
							690	101.12	2970	462.51
							720	143.06	3000	464.38
							780	187.25	3030	434.42
							810	220.96	3840	363.27
							840	213.47	4950	329.56
							1350	239.68	4980	333.31
							1380	307.09	5010	329.56
							1410	355.78	5040	310.84
							1440	415.70	5088	299.60
							1465	419.44	5130	288.37
							1500	423.19	5160	290.24
							1548	411.95	5190	286.87
							1590	408.21	5670	273.39
							2070	348.29	5700	325.82
							2100	374.50	5730	348.29
							2138	400.72	5780	352.03
							2160	411.95	5820	378.25
							2190	426.93	5850	378.25
							2220	426.93	5880	395.10
							2250	426.93	6390	745.26
							2280	419.44		
10	93.8	1.2	30	77	4.5	11-15-67	0	1.6	2940	1.6
							60	1.05	3000	1.9
							120	.95	3060	1.9
							180	1.1	3120	1.6
							240	1.3	3180	1.1
							360	1.1	3240	1.05
							1320	.8	4560	1.8
							1380	.9	7080	1.05
							1440	.9	7140	
							1500		7200	1.05
							1560	1.3	7260	1.1
							1680	1.3	7320	1.2
							1740	1.4	7440	1.2
							1800	1.6	7500	1.3
							2760	1.0	7560	1.3
							2820	1.3	8580	1.3
							2880	1.5		1.2

Run No.	Space Velocity (CFH/Lb Bed)	P/F (Vol/Vol)	1/2 Cycle Time (Seconds)	Temp (°F)	Bed Length (Inches)	Date Run Started	Cycle No.	Effluent H_2O Conc. (PPM)	Cycle No.	Effluent H_2O Conc. (PPM)
8	93.8	1.1	60	60	4.5	6-19-67	60	3.22	2898	4.72
							120	3.26	2958	5.02
							180	3.07	3018	5.47
							225	3.0	3078	6.59
							690	2.25	3565	7.72
							750	2.40	3588	
							810	2.47	4278	13.41
							858	2.70	4308	14.08
							918	2.47	4998	19.85
							1398	2.40	5058	21.72
							1458	"	5118	"
							1518	2.70	5178	22.85
							1638	3.37	5718	24.72
							2118	3.67	5748	27.71
							2178	2.25		
							2238	3.37		
							2298	4.12		
							2358	4.87		
8-R1	93.8	1.1	60	60	4.5	7-3-67	1	134.82	1665	65.16
							705	74.9	2145	57.67
							765	77.15	2205	59.92
							825	74.15	2265	62.17
							885	"	2325	59.17
							945	77.90	2385	58.80
							1425	68.91	2820	56.18
							1485	67.41	2835	52.93
							1545	69.28	2850	58.18
							1605	63.67	2865	54.68
9	93.8	1.2	30	60	4.5	6-27-67	1	27.34	4170	4.93
							30	26.59	4290	5.17
							90	24.34	4470	4.64
							210	26.22	4590	4.68
							330	22.85	4650	4.64
							1290	14.98	5610	3.52
							1410	12.73	5670	3.37
							2730	5.17	7080	3.0
							2850	5.24	8460	2.77
							2970		8490	2.92
							3080	5.69	8550	"

Run No.	Space Velocity (CFH/Lb Bed)	P/F (Vol/Vol)	1/2 Cycle Time (Seconds)	Temp (°F)	Bed Length (Inches)	Date Run Started	Cycle No.	Effluent H_2O Conc. (PPM)	Cycle No.	Effluent H_2O Conc. (PPM)
11	156	1.1	30	60	4.5	7-11-67	60	39.70	3000	52.43
							120	38.95	3090	59.17
							205	43.07	3120	58.42
							240	42.69	3180	57.67
							310	31.83	3240	51.68
							360	42.69	3300	53.18
							420	43.82	3630	44.19
							1380	48.31	4280	61.42
							1500	53.18	4320	65.91
							1580	58.05	4405	"
							1640	52.43	4440	68.91
							1680	58.05	4520	69.28
							1740	50.94	4560	70.41
							1800	61.79	4620	69.66
							1860	59.17	4680	65.54
							2820	56.92	4740	64.79
							2880	61.42	5700	66.66
							2940	62.17		
12	156	1.2	60	60	4.5	7-17-67	0	12.73	1899	5.24
							492	2.92	1929	5.54
							522	2.88	1959	5.47
							552	3.11	1989	6.14
							582	3.26	20.32	6.25
							624	4.27	2049	6.44
							639	4.23	2079	6.52
							669	4.19	2109	6.59
							729	4.08	2619	6.37
							1209	4.49	2649	6.67
							1239	4.72	2679	7.04
							1269	4.94	2724	7.64
							1299	5.09	2739	7.87
							1336	5.39	2769	8.16
							1366	6.29	2799	8.24
							1389	6.89	2829	8.54
							1419	6.74	3624	7.87
									4749	7.64

Run No	Space Velocity (CFH/Lb Bed)	P/F (Vol/Vol)	1/2 Cycle Time (Seconds)	Temp (°F)	Bed Length (Inches)	Date Run Started	Cycle No.	Effluent H_2O Conc. (PPM)	Cycle No.	Effluent H_2O Conc. (PPM)
13	93.8	1.1	60	77	6.3	11-3-67	0	2.1	3750	5.8
							60	2.25	3780	6.1
							90	2.25	3810	5.7
							120	"	4290	4.9
							150	2.3	4320	6.3
							180	"	4350	6.7
							210	2.2	4380	6.8
							990	1.75	4410	7.6
							2130	.71	4440	9.0
							2160	1.1	4500	11.0
							2190	1.3	4530	"
							2220	1.4	4965	16.0
							2250	1.6	5010	
							2280	2.0	5040	15.5
							2340	2.5	5070	
							2370	2.2	5130	15.5
							3030	3.75	5160	
							3570	4.5	5250	16.0
							3600		5730	"
							3630	3.75	5760	16.3
							3660	4.3	6180	16.2
							3690	4.9		
14	93.8	1.2	30	77	6.3	10-16-67	0	2.7	3060	1.8
							60	3.3	3180	1.7
							120	3.5	3300	1.8
							240	2.4	4260	1.4
							300	2.5	4320	1.5
							360	2.7	4380	1.8
							420	2.4	4440	2.1
							1380	2.1	4500	2.0
							1440	2.0	4620	"
							1500	2.3	4680	1.8
							1560	2.5	4740	"
							1620	2.6	5700	1.1
							1680	2.8	5760	"
							1740	2.9	5820	1.2
							1800	2.0	5940	1.4
							1860	1.9	6000	1.6
							2820	1.5	6060	1.2
							2880	1.8	6120	1.1
							3000	2.0		

Run No	Space Velocity (CFH/Lb Bed)	P/F (Vol/Vol)	1/2 Cycle Time (Seconds)	Temp (°F)	Bed Length (Inches)	Date Run Started	Cycle No.	Effluent H_2O Conc. (PPM)	Cycle No.	Effluent H_2O Conc. (PPM)
15	156	1.1	60	77	6.3	10-23-67	0		1470	69
							30	.90	1500	73
							60	0.97	1560	72
							90	1.3	1590	75
							120	"	1620	76
							180	"	1650	77
							210	1.4	2130	69.0
							690	2.1	2160	77
							720	2.5	2190	84
							750	3.6	2220	94
							780	4.6	2250	103
							810	6.2	2310	100
							840	6.5	2340	"
							870	7.6	2370	"
							900	8.6	2850	68
							930	9.7	2880	72
							1410	68.0	2910	78
16	156	1.2	30	77	6.3	10-30-67	0		2820	2.74
							60	2.25	2880	3.04
							120	2.7	2940	3.1
							180	2.85	3000	"
							240	"	3120	2.85
							300	2.77	3180	"
							360	"	3240	"
							1320	2.4	4140	3.82
							1380	"	4200	3.95
							1440	2.3	4260	"
							1500	"	4320	4.15
							1560	2.4	4380	4.4
							1620	"	4440	"
							1680	"	4500	4.3
							1740	2.3	4560	4.45
							1800	"	4620	4.3
							2760	3.1		

APPENDIX 4

Sample Calculation For CO_2 Sorption Experiments

Data

Feed rate to adsorbing bed: 30.5 SCFH
Bed weight: 0.4 lbs.
Half cycle time: 20 min.
Desorbate wet test meter reading: 0.1838 CF at 71°F in 20 min.

Figure A4-1

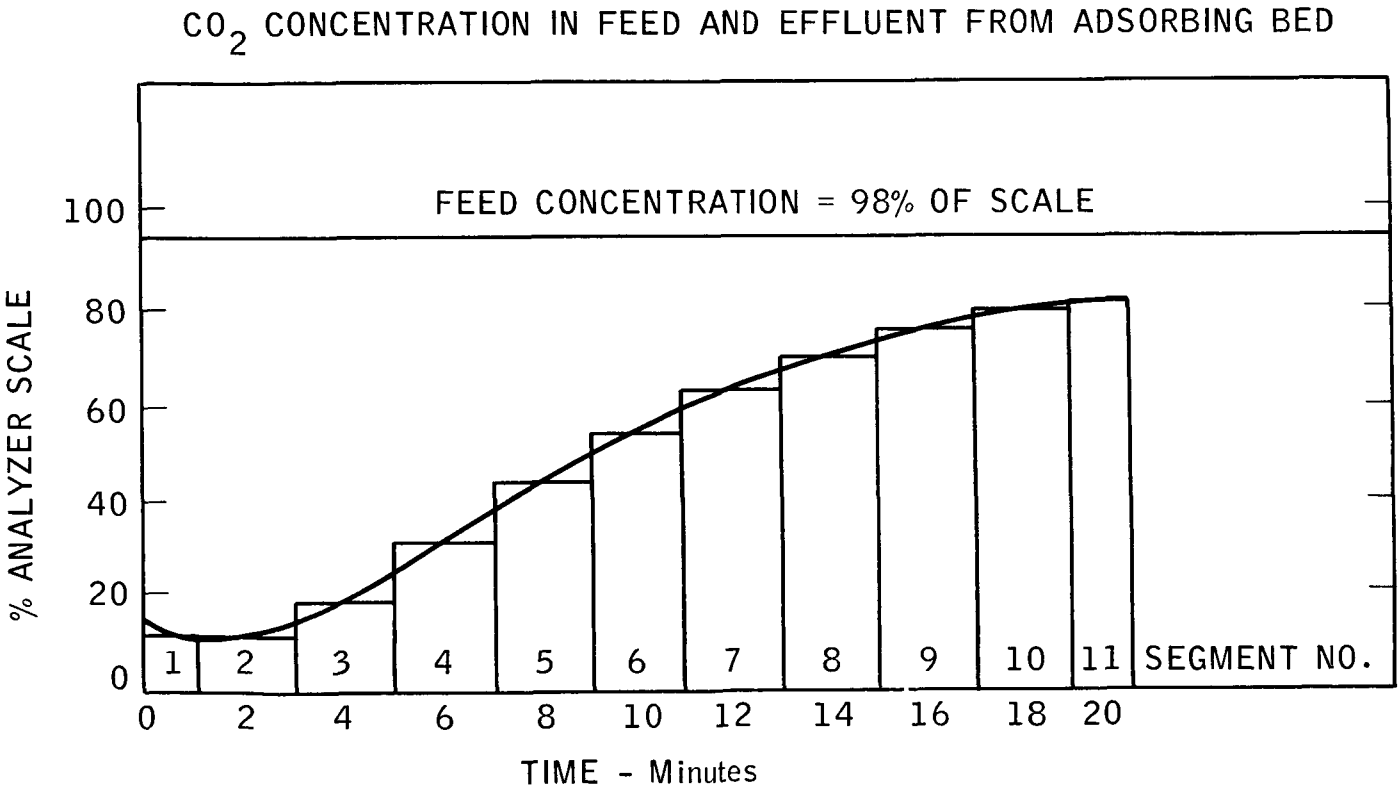

(1) The fraction of CO_2 adsorbed from the feed is calculated by graphical integration. The values of CO_2 partial pressure (psi) in Table A6-1 were obtained by converting CO_2 analyzer scale readings with a calibration curve provided by the manufacturer.

Table A4-1

Segment	Median (% of Scale)	Psi	Seg. Width	Psi x Seg. Width
1	9.5	.015	1.1	.0165
2	11.5	.018	2.0	.036
3	17	.027	"	.054
4	29.5	.029	"	.098
5	42.25	.0745	"	.149
6	52.5	.095	"	.190
7	60.5	.113	"	.226
8	67	.127	"	.254
9	72	.138	"	.276
10	76.25	.1475	"	.295
11	78.75	.1535	1.2	.184
Totals			20.3	1.7785

Average product CO_2 concentration in psia is given by

$$\frac{\sum \text{psi x seg. width}}{\sum \text{seg. width}} = \frac{1.7785}{20.3} = .0876 \text{ psia}$$

$$\text{Vol. Fraction } CO_2 \text{ removed} = \frac{\text{Feed conc. - Prod. conc.}}{\text{Feed conc}} =$$

$$\frac{.198 - .0986}{.198} = \boxed{.5576}$$

(2) $\text{Volume of Desorbate} = .1838 \frac{ft^3}{\text{cycle}} \times \frac{460 + 32}{460 + 71} \frac{SCF}{ft^3} \times 3 \frac{\text{Cycles}}{hr}$

$= \boxed{.510 \text{ SCFH}}$

(3) Vol. CO_2 in Desorbate (hourly rate)

= Vol. Feed Rate (SCFH) x Vol. Fraction CO_2 in Feed x Vol Fraction CO_2 Removed

$= 30.5 \text{ SCFH} \times \frac{.198}{14.7} \frac{PCO_2}{Patm} \times .5576 = \boxed{.2291 \text{ SCFH}}$

(4) Vol. Fraction CO_2 in Desorbate

$= \frac{\text{Vol. } CO_2 \text{ in Desorbate}}{\text{Total Desorbate Vol}} = \frac{.2291 \text{ SCFH}}{.5576 \text{ SCFH}} = \boxed{.4492}$

Vol. Fraction Air in Desorbate

= 1.0 - Vol. Fraction CO_2 in Desorbate

= 1.0 - .4492 = .5508

(5) $\frac{\text{SCF Air Lost}}{\text{SCF } CO_2 \text{ Removed}} = \frac{.5598}{.4492} = \boxed{1.23 \longrightarrow \frac{\text{lb. Moles Air}}{\text{lb. Mole } CO_2}}$

(6) $\frac{\text{Lbs Air Lost}}{\text{Lb } CO_2 \text{ Removed}} = 1.23 \times \frac{28.97 \text{ Lbs, Air/Lb Mole}}{44.0 \text{ Lbs, } CO_2\text{/Lb Mole}}$

$= \boxed{.81 \frac{\text{Lbs Air Lost}}{\text{Lb } CO_2 \text{ Removed}}}$

(7) CO_2 Capacity (Lb CO_2/Hr/Lb Bed)

$= .2291 \frac{\text{SCF } CO_2 \text{ Removed}}{\text{Hr}} \times \frac{1}{359} \frac{\text{Lb Moles}}{\text{SCF}} \times 44 \frac{\text{Lbs } CO_2}{\text{Lb Mole}} \times \frac{1}{.4 \text{ Lb Bed}}$

$= \boxed{\frac{.0720 \text{ Lbs } CO_2\text{/Hr}}{\text{Lb Bed}}}$

APPENDIX 5

CO_2 Sorption Results

Adsorption Pressure: 22 in Hg (abs)

Run Number	Purge Rate (SCFH/lb. Bed)	1/2 Cycle (Min.)	PCO_2 in Feed (mm Hg)	Space Velocity (CFH/lb. Bed)	Bed Length (Inches)	Adsorbent	Minimum Desorption Pressure (mm Hg)	Bed Capacity ($\frac{lb.\ CO_2/Hr.}{lb.\ Bed}$)	Air Loss ($\frac{lb.\ Air}{lb.\ CO_2}$)
1-1	None	10	4.0	139	9	5A M.S.	0.858	0.0260	0.756
1-2	0.3	10	4.0	139	9	5A M.S.	1.877	0.0441	0.945
1-3	0.6	10	4.0	139	9	5A M.S.	2.910	0.0500	1.468
1-4	None	20	4.0	139	9	5A M.S.	0.726	0.0237	0.335
1-5	0.3	20	4.0	139	9	5A M.S.	1.780	0.0392	0.822
1-6	0.6	20	4.0	139	9	5A M.S.	2.690	0.0445	1.343
1-7	None	30	4.0	139	9	5A M.S.	0.644	0.0221	0.179
1-8	0.3	30	4.0	139	9	5A M.S.	1.710	010360	1.116
1-9	0.6	30	4.0	139	9	5A M.S.	2.400	0.0390	1.696
1-10	None	60	4.0	139	9	5A M.S.	0.506	0.0155	0.129
1-11	0.3	60	4.0	139	9	5A M.S.	1.620	0.0303	0.826
1-12	0.6	60	4.0	139	9	5A M.S.		Not Completed	
2-1	None	10	7.5	139	9	5A M.S.	1.254	0.0531	0.378
2-2	0.6	10	7.5	139	9	5A M.S.	3.201	0.0916	0.747
2-3	None	20	7.5	139	9	5A M.S.	-	0.0460	0.140
2-4	0.6	20	7.5	139	9	5A M.S.	2.830	0.073	0.797
3-1	None	10	4.0	173	9	5A M.S.	0.842	0.0239	0.796
3-2	0.6	10	4.0	173	9	5A M.S.	2.830	0.0494	1.384
3-3	None	20	4.0	173	9	5A M.S.	0.715	0.0191	0.568
3-4	0.6	20	4.0	173	9	5A M.S.	2.615	0.0438	1.308
3-5	None	10	4.0	104	9	5A M.S.	0.842	0.0230	0.981
3-6	0.6	10	4.0	104	9	5A M.S.	3.234	0.0478	1.736
3-7	None	20	4.0	104	9	5A M.S.	0.726	0.0214	0.399
3-8	0.6	20	4.0	104	9	5A M.S.	2.558	0.0425	1.300
4-1	None	10	7.5	173	9	5A M.S.	1.271	0.0620	0.225
4-2	0.6	10	7.5	173	9	5A M.S.	3.366	0.0927	0.780
4-3	None	20	7.5	173	9	5A M.S.	0.932	0.0460	0.086
4-4	0.6	20	7.5	173	9	5A M.S.	3.036	0.0710	0.980
4-5	None	10	7.5	104	9	5A M.S.	1.205	0.0510	0.442
4-6	0.6	10	7.5	104	9	5A M.S.	3.515	0.0782	1.178
4-7	None	20	7.5	104	9	5A M.S.	0.941	0.0432	0.132
4-8	0.6	20	7.5	104	9	5A M.S.	2.871	0.0696	0.827
5-1	None	10	4.0	139	5	5A M.S.	0.743	0.0339	0.688
5-2	1.4	10	4.0	139	5	5A M.S.	2.657	0.0656	1.831
5-3	None	20	4.0	139	5	5A M.S.	0.627	0.0311	0.313
5-4	1.4	20	4.0	139	5	5A M.S.	2.558	0.0574	1.719
6-1	None	10	7.5	139	5	5A M.S.	1.007	0.0758	0.222
6-2	1.4	10	7.5	139	5	5A M.S.	2.888	0.1080	1.015
6-3	None	20	7.5	139	5	5A M.S.	0.759	0.0570	0.142
6-4	1.4	20	7.5	139	5	5A M.S.	2.632	0.0830	1.271
7-1	None	10	4.0	139	9	4A M.S.	0.817	0.0264	0.364
7-2	0.6	10	4.0	139	9	4A M.S.	2.945	0.0446	1.574
7-3	None	20	4.0	139	9	4A M.S.	0.677	0.0226	0.151
7-4	0.6	20	4.0	139	9	4A M.S.	2.827	0.0360	1.793
8-1	None	10	7.5	139	9	4A M.S.	1.139	0.0511	0.475
8-2	0.6	10	7.5	139	9	4A M.S.	3.152	0.0772	0.809
8-3	None	20	7.5	139	9	4A M.S.	0.949	0.0384	0.112
8-4	0.6	20	7.5	139	9	4A M.S.	2.872	0.0610	0.926

APPENDIX 5 (Contd)

CO_2 Sorption Results

Run Number	Purge Rate (SCFH/lb. Bed)	1/2 Cycle (Min.)	PCO_2 in Feed (mm Hg)	Space Velocity (CFH/lb. Bed)	Bed Length (Inches)	Adsorbent	Minimum Desorption Pressure (mm Hg)	Bed Capacity ($\frac{lb.\ CO_2/Hr.}{lb.\ Bed}$)	Air Loss ($\frac{lb.\ Air}{lb.\ CO_2}$)
				PED Results					
PED-10	1	10	4.0	139	9	5A M.S.	1.031	0.0334	0.612
PED-13	1	20	4.0	139	9	5A M.S.	0.770	0.0284	0.279
PED-70	1	60	4.0	139	9	5A M.S.	0.528	0.0160	0.134
PED-1	1	10	7.5	139	9	5A M.S.	1.361	0.0659	0.238
PED-7	1	20	7.5	139	9	5A M.S.	1.023	0.0574	0.040
PED-100	1	10	4.0	173	9	5A M.S.	1.010	0.0282	0.800
PED-101	1	20	4.0	173	9	5A M.S.	0.770	0.0234	0.418
PED-110	1	10	7.5	173	9	5A M.S.	1.298	0.0758	0.170
PED-111	1	20	7.5	173	9	5A M.S.	1.023	0.0492	0.202

BIBLIOGRAPHY

1. C. W. Skarstrom - U.S. 2,889,701, "Apparatus for Analyzing Mixtures of Gaseous Materials by Composition Modulation."

2. C. W. Skarstrom - U.S. 2,944,627, "Method and Apparatus for Fractionating Gaseous Mixtures by Adsorption."

3. C. W. Skarstrom, et al - U.S. 3,069,830, "Improved Heatless Fractionator*."

4. C. W. Skarstrom - U.S. 3,082,166, "Process for the Drying of Volatile Liquids."

5. C. W. Skarstrom, et al - U.S. 3,086,339, "Technique with the Fractionation* or Separation of Components in a Gaseous Feed Stream."

6. C. W. Skarstrom - U.S. 3,101,261, "Process for the Recovery of Hydrogen from Hydrocarbon Gas Streams."

7. C. W. Skarstrom - U.S. 3,102,013, "Heatless Fractionation* Utilizing Zones in Series and Parallel."

8. C. W. Skarstrom, et al - U.S. 3,102,853, "Desulfurizing Fluids Utilizing Pressure Cycling Techniques."

9. C. W. Skarstrom - U.S. 3,104,162, "Timing Cycle for Improved Heatless Fractionation* of Gaseous Materials."

10. C. W. Skarstrom - U.S. 3,122,486, "Improved Combination Process Comprising Distillation Operation in Conjunction with a Heatless Fractionator."

11. C. W. Skarstrom - U.S. 3,138,439, "Apparatus and Process for Heatless Fractionation* of Gaseous Constituents."

12. R. C. Hoke, et al - U.S. 3,141,740, "Hydrogen Purification Process."

13. C. W. Skarstrom, et al - U.S. 3,142,547, "Pressure Equalization Depressuring in Heatless Adsorption."

14. H. Z. Martin - U.S. 3,149,934, "Improved Cyclic Adsorption Process."

15. C. W. Skarstrom - U.S. 3,155,741, "Chemical Reactions in a Heatless Fractionation* Apparatus."

16. C. W. Skarstrom - U.S. 3,237,377, "Oxygen Concentration Process."

17. F. H. Kant, et al - U.S. 3,237,379, "Adsorption Systems in Heatless Fractionation*."

18. C. W. Skarstrom - British 965,565, "Apparatus and Process for Heatless Fractionation* of Gaseous Constituents."

* Note: Heatless Fractionation is another name used for Heatless Adsorption.

19. G. F. Feldbauer, Jr. - British 975,371, "Improved Depressuring Technique for ΔP Adsorption Process."

20. C. W. Skarstrom - British 976,023, "Improved Oxygen Concentration Process."

21. C. W. Skarstrom, et al - French 1,292,423, "Improved Process for the Recovery of a Desired Component from Gas Streams."

22. C. W. Skarstrom, et al - French 1,354,351, "Improved Adsorption Systems in Heatless Fractionation* Processes."

23. C. W. Skarstrom - French 1,397,630, "Processing of Gases."

24. N. H. Berlin, et al - French 1,403,229, "Process and Apparatus for Controlled Environment."

25. Theodore Vermeulen- Advances in Chemical Engineering Vol. II, pg. 175, Thomas B. Drew and John W. Hoopes, Jr. - Editors.

26. John Lovell and Frederick Morris - "Development in the State of the Art of Regenerable Solid Adsorbent CO_2 Removal Systems, reprint #63-AH-6T-66 American Society of Mechanical Engineers.